THE DESIGN, SYNTHESIS, AND CHARACTERIZATION OF POLY(CARBONATE-ESTER)S BASED ON DIHYDROXYACETONE FOR USE AS POTENTIAL BIOMATERIALS

A Dissertation

Presented to the Faculty of the Graduate School

of Cornell University

In Partial Fulfillment of the Requirements for the Degree of

Doctor of Philosophy

by

Jennifer Rose Weiser

January 2013

ABSTRACT

THE DESIGN, SYNTHESIS, AND CHARACTERIZATION OF POLY(CARBONATE-ESTER)S BASED ON DIHYDROXYACETONE FOR USE AS POTENTIAL BIOMATERIALS

Jennifer Rose Weiser, Ph.D.

Cornell University 2013

The creation of new devices and materials with desirable biomedical characteristics, such as biocompatibility and easily tunable physico-chemical parameters, has played a key role in the advancement of the biomedical industry. In recent years, the combination of classical engineering principles with polymer chemistry has led to a wide range of materials that influence the manner in which drugs are delivered, tissues are engineered, and surgery is performed. The work presented in this thesis is focused on the design, synthesis, and characterization of a poly(carbonate-ester) biomaterial based on lactic acid (LA) and a carbonate form of dihydroxyacetone (DHAC) as vehicles for controlled release.

The goal of this work was to synthesize a variety of pLA_x-*co*-$DHAC_y$ copolymers and characterize their behavior to better understand their structure/function relationships. The results show that random copolymers based on dihydroxyacetone and lactic acid are easily and reliably producible, with unique characteristics. In vitro degradation studies showed that the poly(carbonate-ester)s had an unexpected degradation pattern, in that the carbonate bond was more labile to hydrolysis than that of the ester bond. The resulting degradation pattern made from these biomaterials did not appear to have an acidic interior environment, due to a lack of

visible viscous core commonly seen with bulk degrading lactic acid based polymers. Due to the insolubility of the poly(carbonate-ester)s, exploration of copolymer degradation was determined by the development of a newly discovered technique to quantify dihydroxyacetone release from the matrix using the bicinchoninic acid assay.

Finally, the release kinetics and mechanism from these poly(carbonate-ester)s was studied following the incorporation of two different model proteins, bovine serum albumin and lysozyme. Their release behaviors and activities were analyzed to explore the controlled release capabilities of these materials and to identify their potential for the effective release of proteins.

BIOGRAPHICAL SKETCH

Jennifer Rose Weiser was born in New York City on April 18th, 1984 to Dr. Stephen and Dr. Ellen Weiser. She was raised in Pleasantville, New York with her older brother, Dr. Mitchell Weiser. An avid musician and emergency medical service volunteer, she graduated from Pleasantville High School in June of 2002. She entered Rensselaer Polytechnic Institute later that year and graduated cum laude with a degree in Chemical Engineering and a minor in Chemistry in May of 2006. In the fall of 2006 she began work at Wyeth Pharmaceuticals as an exploratory medicinal chemist, before joining the Biomedical Engineering Department at Cornell University in 2007. She received her Master of Science degree in Biomedical Engineering in the winter of 2011, before receiving her doctorate in the fall of 2012.

"If you're not part of the solution, you're part of the precipitate."

-Barry Braebender

ACKNOWLEDGEMENTS

I would like to first and foremost thank my advisor, Professor David Putnam, whose dedication and enthusiasm for science has fundamentally shaped the scientific world that I cherish.

I would also like to thank my other committee members, Professor Lara Estroff and Professor Geoffrey Coates, whose classes and advice were always forthcoming, informative, and greatly appreciated.

I am equally grateful to Laura Austen, Professor Christopher Schaffer, Dr. Shivaun Archer, and Nev Singhota for their work with me as I tackled Cornell's GK-12 program.

I would like to recognize Dr. Jason Spector and his students, whose guidance in the clinical world and the opportunity to work in his laboratory greatly benefited my own scientific career.

I would also like to thank our collaborator, Dr. Ellen Weiser, whose endless scientific knowledge and willingness to be on call 24 hours a day made a good portion of this work possible.

I would also like to acknowledge all of the other students and staff who have helped make this dissertation possible: Dr. Peter Zawaneh, who took the time out of his busy PhD to train me and give me the start I needed into the world of polymers. Dr. Jeisa Pelet, Dr. Anne Doody, and Dr. Sara Yazdi, for teaching me new laboratory techniques and welcoming me into the Putnam lab. Anthony Condo, Ivan Keresztes, and John Hunt from the Cornell Center for Materials Research, who trained me on various polymer characterization techniques. Alice Yueh, Nicole Ricapito, Lindsey Crawford, Bennett Wechsler, and Jessica Schmidt, who all agreed to work with me and offered me unending help throughout my graduate school experience. The

entire Putnam lab, past and present, who are too numerous to name, but each one was always willing to lend a hand or give advice when I needed it the most.

I would like to thank Angela Casolaro, Jennifer Sumner, Lindsay Blackwell, and Jessica Young for their help, loyalty, and nonstop adventures throughout the years. I would also like to thank everyone at AOE (especially PB-M) for making my time at RPI worth it.

Finally, I'd like to dedicate this PhD to my mom, for her infinite wisdom and guidance, my dad, for his unending support, Mitch, for his trailblazing, Rich for his ineffable patience, and my Aunt Sue, for her laugh.

TABLE OF CONTENTS

LIST OF SCHEMATICS

LIST OF FIGURES

LIST OF TABLES

LIST OF ABBREVIATIONS

ANOVA:	Analysis of Variance
BCA:	Bicinchoninic Acid Assay
BSA:	Bovine Serum Albumin
CH_2CL_2:	Dichloromethane
CO_2:	Carbon Dioxide
DA:	Diacid Alkane
DAST:	Draw a Scientist Test
DC:	Diacid Chloride
DHA:	1,3-Dihydroxyacetone
DHAC:	1,3-Dihydroxyacetone Carbonate
DHAP:	Dihydroxyacetone Phosphate
DI H_2O:	Deionized Water
DMAP:	4-dimethylaminopyridine
DMSO:	Dimethyl Sulfoxide
DSC:	Differential Scanning Calorimetry
CLIMB:	Cornell Learning Initiative in Medicine and Bioengineering
CIBT:	Cornell Institute of Biology Teachers
EU:	Enzyme Units
FDA:	Food and Drug Administration
GK-12:	Graduate STEM Fellows in K-12 Education
GLY:	Glycerol
GPC:	Gel Permeation Chromatography
HPLC:	High-Performance Liquid Chromatography
I_2:	Iodine
LA:	Lactic acid
MPEG:	Monomethoxy-polyethylene glycol
M_n:	Number average molecular weight
M_w:	Weight average molecular weight
Na_2CO_3:	Sodium Carbonate
NaOH:	Sodium Hydroxide
NMR:	Nuclear Magnetic Resonance
NSF:	National Science Foundation
PBS:	Phosphate Buffered Saline
PDI:	Polydispersity Index
pI:	Isoelectric Point
PLGA:	Poly(lactic-*co*-glycolic) acid
pMMA:	Poly(methyl methacrylate)
SDS-PAGE:	Sodium Dodecyl Sulfate Polyacrylamide Gel Electrophoresis
SE:	Standard Error
SEM:	Scanning Electron Micrograph
$Sn(OCT)_2$	Stannous Octoate
STEM:	Science, Technology, Engineering, and Math
TGA:	Thermal Gravimetric Analysis

T_d:	Degradation Temperature
TFA:	Trifluoroacetic Acid
T_g:	Glass Transition Temperature
THF:	Tetrahydrofuran
T_m:	Melting temperature
TMC:	1,3-Trimethylene Carbonate

poly(DL-lactide-*co*-2,2-dimethoxy-1,3-propylene carbonate): protected pLA_x-*co*-$DHAC_y$
poly(DL-lactide-*co*-2-oxopropylene carbonate): pLA_x-*co*-$DHAC_y$
poly(2-oxopropylene carbonate): $pDHAC_{100}$

CHAPTER 1 - BACKGROUND

1.1 Introduction

Biomaterials are defined as any natural or synthetic substance, other than drugs, that treat, augment, or replace any tissue, organ or body function.[1] A biomaterial's chemical structure governs its properties and functions. Biomaterials are commonly found in the pharmaceutical industry. Examples include coatings for tablets or transdermal patches. They are also common in the biomedical device industry, acting as materials for vision correction, kidney dialysis, stents, pacemakers and thousands of other applications.[2-5] As of the 1990s, there are numerous functions for biomaterials found in about 2,700 different kinds of medical devices, 2,500 separate diagnostic products, and 39,000 different pharmaceutical preparations, with more than half of biomaterial applications made of or containing some polymeric component.[3] The estimated annual sales of biomaterials as medical devices or diagnostic products equates to over 100 billion US dollars.[3] More currently, medical devices comprised solely of polymeric materials is a $1 billion dollar industry that has a growth rate of 10-20% each year.[6]

Physicians often seek to cure ailments or improve a patient's quality of life by replacing a defective body part with a substitute. However, up until this past century, the limitations on doctors was to use materials only found in nature, whose design may not necessarily be for the specific purpose the patient requires. Throughout the late 19th and 20th centuries, the creation of new biomedical materials has undergone a renaissance, driven by advances in polymer chemistry. Basic discoveries, like the process of vulcanization, were the impetus for renewed interest in creating semi-synthetic materials. In the early 20th century, the advances in the field of polymer chemistry led to the introduction of polymers as they are thought of today. Yet, it was not until the mid 20th century that polymeric materials began to be included in medical applications. Numerous planned and unplanned events led to the creation of new synthetic

polymers, and with those new ideas came potential biomaterial applications for use by the medical field.

From its fledgling start in the 20th century, synthetic polymers began appearing in hundreds of other biomedical applications such as dialysis tubing, drug eluting heart stents and joint replacement. Physicians, motivated by a need for custom-made materials for specific medical applications, turned to chemists, materials scientists, chemical engineers, and researchers in other disciplines to help create biocompatible, polymeric biomaterials.[7-10] Over the past quarter century, there has been extensive research studying the biological interactions between the human body and each biomaterial. This better understanding of the tissue-biomaterial interactions helped to revolutionize how researchers create new biomaterials, especially biodegradable polymers. This insight led to the modification of natural substances specifically designed for use in a wide range of implantable applications including orthopedic and dental devices, drug-delivery systems, and tissue engineering scaffolds.[4]

The field of polymer chemistry encompasses the synthesis and characterization of newly developed polymers. A polymer's structure is manipulated to fit the need for the material or create certain properties that are desired from the material. Something as simple as a homopolymer, a polymer made from a single type of monomer, already may fit a need, however, it is often found that copolymerizing two or more types of monomers offers the ability to fine tune the intrinsic properties of the material. The ability to tune the ratio of the different monomers within the copolymer backbone help to create a valuable new material. Another important parameter of copolymers that is often manipulated is the architecture of the backbone. Copolymers are found in numerous configurations, such as a block copolymer, where two or more homopolymers are linked covalently, alternating copolymers, where the monomer subunits

are alternating, statically random copolymers, where the monomer subunits follow a statistical rule as to how they are arranged in the backbone, or graft copolymers, where side chains of a different structure emanate from the main backbone. By manipulating the architecture of the copolymer, different properties are made that can meet the need of the material, such as crystallinity, strength of the material, flexibility, etc.

Along with the type of synthesis used to create new polymer biomaterials comes the characterization of the materials. Understanding the intrinsic properties of new polymers is important to produce a material reliably. One example is nuclear magnetic resonance (NMR), which creates a profile of the material based on the principle that particular chemical groups and arrangement of atoms resonant at known radio frequencies in an applied magnetic field. NMR can help to verify the polymer chemical structure synthesized, elucidate the arrangement of monomers in the backbone of copolymers, and in certain cases, quantitatively determine the molecular weight of a polymer. In most cases a polymer's molecular weight is qualitatively assessed by size exclusion chromatography, or gel permeation chromatography (GPC). GPC separates polymers based on hydrodynamic volume and the process creates a profile to determine the number average molecular weight (M_n), weight average molecular weight (M_w), and polydispersity index (PDI) of the polymer. All of these parameters are intrinsic to the type of polymer synthesized and are important in accurately characterizing the polymeric material.

Other intrinsic properties of the polymer are important to help understand how a polymer will behave under different environmental conditions. How a polymer responds to temperature is determined by thermogravimetric analysis (TGA) and differential scanning calorimetry (DSC). TGA determines a polymer samples change in weight, or degradation, in response to an increase in temperature. The polymer degradation profile offers insight into the thermal stability of a

polymer and is often represented by the degradation temperature (T_d). DSC is used to determine a sample's melting temperature (if present) and glass transition temperature. A polymer's melting temperature (T_m) represents the change from a crystalline or semi-crystalline state to an amorphous state. This property helps determine the type of polymer created, either a thermoplastic, or a material that may be heated, molded, and cooled again, or a thermoset, or material that is irreversibly cured and decomposes when heated. Thermoplastic materials are the only materials that have a T_m. DSC is also used to determine the glass transition temperature (T_g), which is the point where a polymer undergoes a transition from atomistic chain movement to segmental chain movement. Knowing this temperature is important to determine long-term stability of the polymer, as well as to understand how the material will behave at any given temperature.

1.2 Classic approach to biomaterial synthesis

Classically, the process of biomedical device innovation is driven by clinical demand in which a patient or physician defines a need, which then initiates an invention. Yet, it is here that the development of new polymeric biomaterials diverges. The first path to synthesizing a new polymer-derived biomaterial involves having a medical need clearly defined and then rationally designing the material based on the need. The second path involves rationally designing unique materials that are biocompatible and don't enlist an immune response; however, these materials often do not have specific medical applications clearly defined. From this latter path, it is the material characterization and understanding of its inherent properties that allow for the exploration of potential therapeutic biomaterial applications. This approach also includes the exploration of previously synthesized materials for new medical purposes for which they were

not originally intended.

The archetypal rational design of polymeric biomaterials includes the creation of materials such as the first biodegradable surgical sutures derived from polyesters of glycolic acid. Though the first poly(glycolic acid) polymer was developed by Dupont in 1954, it wasn't until the 1960s that researchers Dr. Schmitt and Dr. Polistina, and later on Dr. Frazza, of the American Cyanamide Corporation, were able to create Dexon, the first synthetic bioresorbable suture.[9, 11] This discovery began an entire field of work devoted to improving this vital and most basic surgical device. Further examples of significant polymeric biomaterials that have been rationally designed include the drug delivery device, GLIADEL®. Invented by Dr. Langer and Dr. Brem, the creation of this device used rational design to synthesize a specific polymer to address the problem of prolonged drug delivery to glioblastoma multilamela form of brain cancer patients. The invention is one of the first of its kind to be a directly implantable, surface eroding, drug eluting device.[12-14] GLIADEL® was intentionally designed to have a hydrophobic polyanhydride backbone, which exhibits surface eroding characteristics, which is necessary to maintain a constant, extended, zero order release of a drug. This polymeric drug delivery system revolutionized the treatment of gliomas, by allowing release of the drug directly into the resected tumor region of the brain, thereby avoiding the blood brain barrier.

1.3 Alternate approaches to biomaterial synthesis

The counter approach to this method of creating new biomaterials is to either create a completely unique, biocompatible material and explore its structure function relationships or take an already known material and explore new applications. The ability to be open-minded and flexible with old and new biomaterials has led to numerous advances in medicine. An example of

one of the first polymeric materials created in this manner was polymethylmethacrylate (pMMA). Originally, pMMA was used in the cockpit windshield of World War II fighter planes. Its presence in the eyes of injured pilots drew the attention of the physician, Sir Harold Ridley. Sir Ridley noticed these plastic pieces of shrapnel did not enlist an immune response even years after the ocular trauma occured.[5] This eventually led to the development of other pMMA-based materials for such applications as contact lenses. The example of pMMA finding a niche in ocular repair and altering the corrective vision industry is just one of these discoveries that helped improve medical care by using a material not originally designed for this new medical purpose.[5] Other examples include the repurposing of the rationally designed surgical sutures to be the starting point for all of modern day tissue engineering. Dr. Charles Vacanti, an anesthesiologist by training, took extra polymeric suture materials from the operating room and began to grow chondrocytes on these structures. This early attempt at tissue engineering was in response to the need for synthetic cartilage which could be made from naturally occurring materials and shaped into the desired form to mimic native tissue. These materials, already known to be biocompatible with cells and FDA approved, were one of the first rudimentary tissue engineering scaffolds.[7, 15]

In modern medicine, polymeric biomaterials play an important role in the progression of health care. The advancement of polymer synthesis techniques and the discovery of new, biocompatible building blocks alter the way through which new biomaterials are created. On one hand, inventing a new material with specific properties for a specific application is vital in addressing a need for certain patients or physicians. However, as polymeric chemistry evolves and the number of unique biocompatible polymeric materials synthesized continues to grow, the ability to understand a material's characteristics and to find a useable function for these materials

is just as crucial to transforming the medical industry.

1.4 Goals of this study

The ability to successfully create functional polymer-based biomedical devices has been a significant challenge in recent years. The need to create materials that are biocompatible and do not enlist immune responses or unfavorable side effects, while still performing their intended purpose, is the key to creating successful biomaterials. Biomaterials comprised of biologically-derived monomers are of particular interest because each building block has the ability to impart unique characteristics that may improve processability, the mechanical properties, and overall effectiveness of the material for its intended application.[3, 7, 14, 16-22] By adjusting the ratio of monomers, the molecular weight, and type of monomers, a copolymer's intrinsic properties may be altered and optimized. The specific goal of this thesis project was to create various copolymers based on the glycolytic intermediate, dihydroxyacetone, and analyze their characteristics for potential biomaterial.

Dihydroxyacetone (DHA) is a glycolytic metabolite that, in its natural form, is an intermediate in the conversion of glucose to pyruvate in the human body. DHA is used as the active ingredient in sunless tanners, and is naturally derived from sugar beets, sugar cane, and by the fermentation of glycerin. In recent years DHA and a carbonate form of DHA, DHAC, have been used as a building block for a number of different types of polymers.[20, 22-25] Early work aimed at creating an adhesive biomaterial saw the creation of homopolymers based on the dimer form of DHA due to DHA being in equilibrium with its dimer in solution.[25] Linear hompolymers based on DHAC were made possible by protecting the ketone group of DHA and creating a cyclic form of the monomer before polymer synthesis.[26] However, upon deprotection, these

materials were insoluble in most common solvents and did not possess the desired adhesive properties. The next generation of this biomaterial saw the creation of a block copolymer based on monomethoxy polyethylene glycol (MPEG) and DHAC.[21] This material was found to be very effective for the treatment of seroma and for hemostasis.[20, 22, 27] This success has guided the next generation of DHAC based copolymers.

For this thesis project, random poly(carbonate-ester)s based on DL-lactic acid (LA) and a protected carbonate form of dihydroxyacetone were synthesized for use as a potential biomaterial (Figure 1.1). Characterization of the protected and deprotected form of these copolymers was conducted using standard techniques such as ^{1}H and ^{13}C nuclear magnetic resonance spectrometry (NMR), gel permeation chromatography (GPC), thermogravimetric analysis (TGA), and differential scanning calorimetry (DSC). The copolymers were then deprotected by a different technique than previously explored for this class of polymers by using iodine and acetone, to produce various, random, poly(carbonate-ester) backbone materials of DHAC and LA. All copolymer compositions are defined according to the following abbreviations: LA_x = mol % lactic acid; $DHAC_y$ = mol % dihydroxyacetone carbonate. (pLA_x-*co*-$DHAC_y$).[20-22] The poly(carbonate-ester) backbone allowed for a long term degradation studies to be conducted as well as model protein release studies.

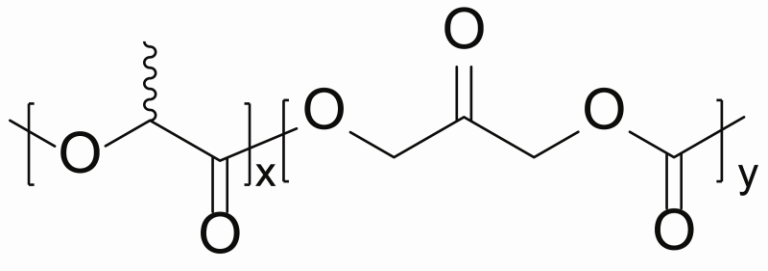

Figure 1.1. Structure of LA-DHAC based copolymers (pLA_x-*co*-$DHAC_y$)

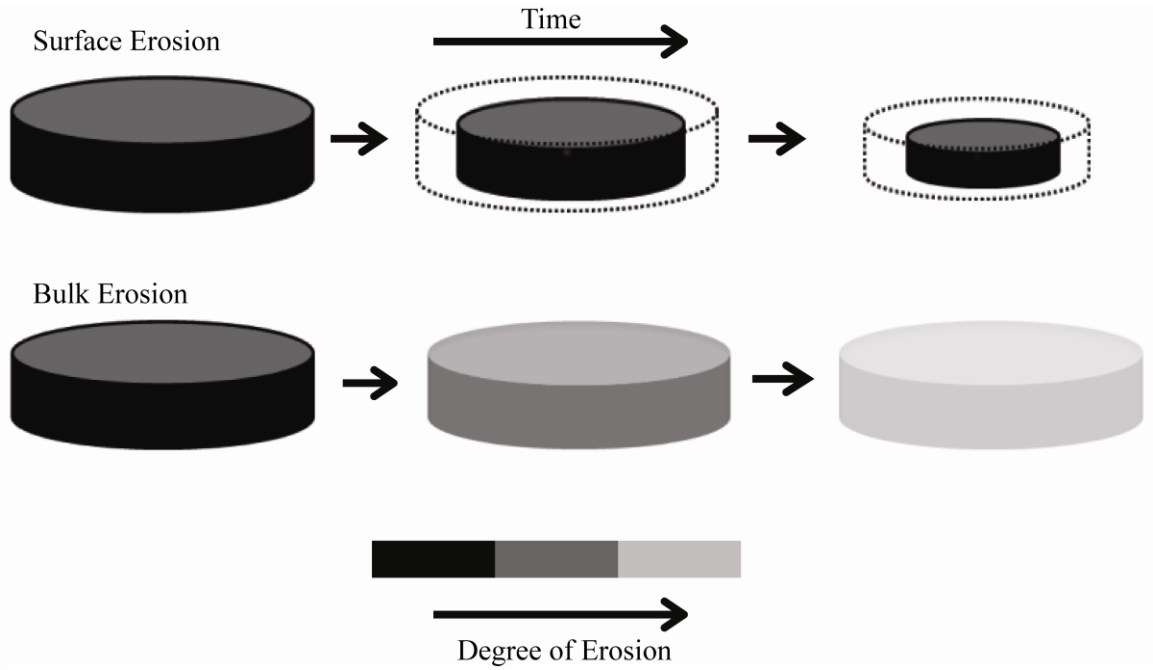

Figure 1.2. Illustration of surface erosion vs. bulk erosion during polymer degradation. (Adapted from Von Burkersoda and Göpferich, et al.)[28]

Polymer erosion, defined as the loss of mass from a polymer system, proceeds via two main pathways, surface erosion or bulk erosion, as shown in Figure 1.2. The manner in which a polymer degrades, defined as the chain scission of the polymer backbone, determines the unique erosion profile of each polymer system. Surface eroding polymers proceed at a constant velocity, where only material from the surface of the polymer is lost. Thus these materials will get smaller, but will keep their original geometric shape. The advantage to this type of erosion is that the process is predictable, which is desirable for controlled drug delivery. In contrast, bulk erosion is a much more complex process. Bulk eroding polymers do not have their degradation and erosion confined to the surface of the device. This may lead to the geometric shape and size of the device remaining constant, while the matrix interior is already degrading. The bulk erosion process will then proceed at a variable velocity that is more complex to predict than surface eroding

materials. However, both pathways of erosion depend on a number of parameters such as polymer degradation, copolymer composition, swelling, the dissolution and diffusion of oligiomers and monomers, autocatalysis by acidic degradation products trapped in the matrix, etc.[28-30]

A two month in vitro degradation study was conducted on pLA_x-*co*-$DHAC_y$ tablets formed via direct compression and each sample's degradation kinetics were characterized via mass loss and changes in tablet dimension. The trends seen in the mass loss data suggests a more surface eroding-like material rather than bulk erosion-like material. Visualization of the degradation was conducted using scanning electron microscopy (SEM) to characterize the internal degradation pattern of this class of biomaterial. The results show that increasing the DHAC content, and therefore the carbonate content in the copolymer backbone, increases the rate at which the copolymers degrade. The SEM data correlates with this result, as it too shows the increased degradation of copolymers richer in carbonate bonds. The SEM data also shows that the degradation profile does not fully align with either a bulk eroding or surface eroding matrix. There is no presence of a liquid core that would indicate a significant decrease in pH at the center of the tablet due to excess acid production from the LA in the degrading copolymer backbone.

Due to the insoluble nature of deprotected pLA_x-*co*-$DHAC_y$ in most common solvents, the molecular weight change of the degrading copolymer was unable to be monitored using tradiational methods, such as GPC. To address this issue, a new method to assay the degrading samples was developed via the repurposing of the bicinchoninic acid assay. This assay, generally used for protein quanitification, was seen to reliably quantify α-hydroxy ketones, such as DHA, in solution. Under alkaline conditions, the BCA assay determines the total concentration of an

analyte via the reduction of Cu^{2+} ions.[31, 32] The reduced Cu^{2+} to Cu^{1+} reacts with bicinchoninic acid which forms a complex that absorbs light strongly at 562 nm. The absorbance of this complex is then used to quantify an analyte's concentration either using a standard curve or Beer's law ($A=\varepsilon*b*c$).

By employing this assay, the degrading, directly compressed tablets made of deprotected pLA_x-*co*-$DHAC_y$ were able to be monitored and an accurate release profile of DHA, a degradation product of DHAC, created. A zero-order release pattern was observed for pLA_{15}-*co*-$DHAC_{85}$ while a first order release of DHA was observed for pLA_{25}-*co*-$DHAC_{75}$ and pLA_{50}-*co*-$DHAC_{50}$.

Finally, a more detailed profile of the intrinsic characteristics of pLA_x-*co*-$DHAC_y$ was obtained by the implementation of two protein release studies. Two model proteins, bovine serum albumin (BSA) and lysozyme, were incorporated into the copolymer matrix prior to direct compression and the tablets were placed in physiologically simulated in vitro conditions. The release profiles for both model proteins show that increasing DHAC content in the backbone increases the rate at which the protein releases. The trend for all of the ratios follows a first order release for both proteins, with the BSA generally releasing faster. This study also provided information about the interior environment of the degrading copolymer matrix via the assessment of lysozyme activity throughout the study. It was observed that lysozyme remained highly active throughout the faster release from pLA-*co*-$DHAC_{85}$ and pLA_{25}-*co*-$DHAC_{75}$, while it retained at least 50% of its activity for well over the first month of release from the slower releasing pLA_{50}-*co*-$DHAC_{50}$ copolymer matrix.

Due to the complexity of the degradation and erosion pattern, mathematical modeling was employed to garner a better understanding of how these materials behave. The use of

mathematical models helps predict the release kinetics of a drug before the release systems are completely understood. One way to model drug release is to use mathematical functions to describe the dissolution process. The most basic model is the zero-order release model that is used to model drug dissolution from dosage forms that do not disaggregate and release drugs slowly over time. This model is used to describe the drug dissolution from some transdermal systems, as well as matrix tablets with poorly soluble drugs, or certain polyanhydride systems.[33, 34] A more complex system is the first order model and is often used to describe adsorption or elimination of drugs and is useful in modeling pharmaceutical dosage forms such as those containing water-soluble drugs in a porous matrix.[33]

One of the earliest mathematical models used to describe drug release from a matrix system was the Higuchi model. Originally created for planar systems, it has since been expanded to other geometries. The Higuchi model is based on six principles: drug diffusion takes place only in one dimension, drug particles are smaller than the pore size of the matrix, initial drug concentration in the polymer matrix is higher than the drug solubility, drug diffusivity is constant, near perfect sink conditions are maintained and the matrix swelling and dissolution are negligible. This model is used to describe drug release from matrix tablets with water soluble drugs and transdermal systems.[33, 35]

Hixson and Crowell recognized that a particle's area is proportional to the cube root of its volume and created the Hixson-Crowell model that describes drug release from systems when there is a change in surface area or diameter of the particle or tablet. This model applies to tablets, where dissolution occurs in planes that are parallel to the drug surface and the tablet's dimensions diminish proportionally.[33, 36]

Korsmeyer and Peppas derived a simple relationship to deduce the mechanism of drug release from cylindrical shaped matrices. By fitting drug release data to the model, parameters are calculated that describe the release mechanism of the drug. The release mechanisms may correspond to a Fickian diffusion mechanism, a non-Fickian transport, a Case II (relaxational) transport, pseudo-Fickian transport, or to super case II transport, which are detailed in Table 1.1.[37-40]

Modeling the mechanism of release from the pLA_x-*co*-$DHAC_y$ copolymer matrix suggests that the release mechanism is quite complex, and may depend on numerous other factors such as drug diffusion, porosity, the crystallinity, polymeric swelling, and polymer erosion.

Release exponent (n)	Drug transport mechanism	Rate as a function of time	Mechanism
n<0.45	Psuedo-Fickian	t^{n-1}	Complex and depends on drug diffusion, porosity, the crystallinity, polymeric swelling, and polymer erosion
0.5	Fickian diffusion	$t^{-0.5}$	Penetrant mobility is slower than polymer segmental relaxation rate
n > 0.45 n < 0.89	Non-Fickian (Anomalous) transport	t^{n-1}	Contains characteristics of Fickian diffusion and Case II transport - glassy polymers
0.89	Case II transport	Zero-order relase	Penetrant mobility is faster than polymer segmental relaxation rate - swelling
n > 0.89	Super case II transport	t^{n-1}	Like Case II, however there is rapid increase in rate at a certain time

Table 1.1. Korsmeyer-Peppas drug transport mechanism from cylindrical polymer matrices.

CHAPTER 2 – INITIAL CHARACTERIZATION OF POLY(CARBONATE-ESTER)S

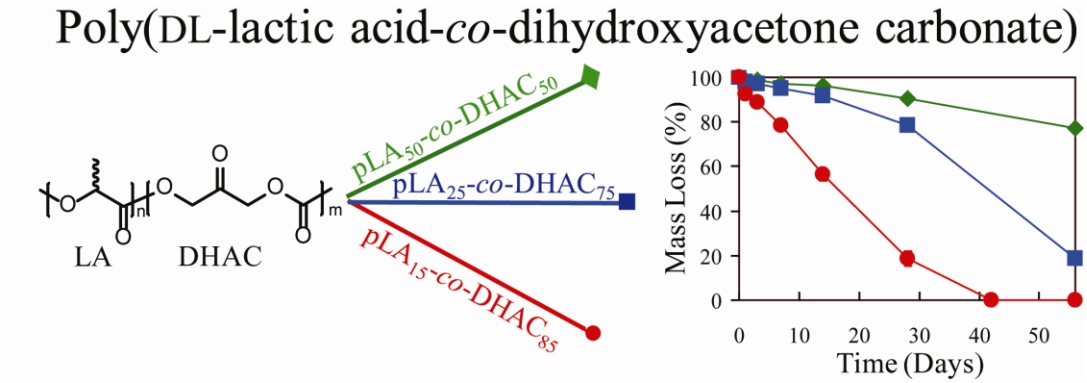

2.1 Introduction

The creation of new devices and materials with desirable biomedical characteristics, such as biocompatibility and easily tunable physico-chemical parameters, has played a key role in the advancement of the biomedical industry. In recent years, the combination of classical engineering principles with polymer chemistry has led to a wide range of materials that influence the manner in which drugs are delivered, tissues are engineered, and surgery is performed.[7, 8, 11, 17, 41-43] The combination of engineering and chemistry, aided by the use of naturally occurring biocompatible monomeric building blocks, has yielded a number of advances in the field of biomedical engineering.

Examples of two naturally occurring monomeric building blocks that have shown to be valuable in the area of polymeric biomaterials are dihydroxyacetone and lactic acid. Dihydroxyacetone (DHA), a glycolytic metabolite, has only in recent years been explored for its use as a polymeric biomaterial. In its natural form, DHA is an intermediate in the conversion of glucose to pyruvate, is used as the active ingredient in sunless tanners, and has been used as a building block for a number of different types of polymers in a carbonate form (DHAC).[20, 22, 24, 25, 44]

In contrast to the more recently developed dihydroxyacetone monomer, lactide, a cyclic di-lactone of lactic acid (LA), has been used for decades as a robust building block for the creation of a variety of tunable lactic acid containing polymers via a coordination-insertion controlled ring-opening polymerization.[9, 45, 46] One traditional example, poly(lactic acid-*co*-glycolic acid) (PLGA) copolymers, is one of the most well characterized and widely used biomaterials because of its low toxicity, easily controllable degradation rates, and its ability to be cleared via normal metabolic pathways.[16, 47-50] Previous work by Grinstaff, *et al,* shows the value

of polymerizing lactic acid with other cyclic carbonates, such as glycerol derived monomers, to increase the hydrolytic degradation rate. The characteristics of these new lactic acid based copolymers for use as scaffolds for delivering drugs has been reported.[51] From this initial work, other poly(carbonate-ester)s have been explored and developed as new biomaterials for various medical applications.[52-54]

The properties imparted to the copolymer from each monomer are the main driving force in exploring the creation of random copolymers formed via ring opening polymerization of DL-lactide and a protected cyclic carbonate of dihydroxyacetone. Previous studies show that the degradation characteristics enable both LA- and DHAC-based polymers to hydrolyze into safe products and are a central motivation to maximize the biocompatibility of the materials.[10, 22]

It is the intent of this work to report the creation of poly(carbonate-ester)s derived from DHA and LA and to demonstrate the ease of synthesis for various molar ratios of the two monomers. Additionally, we report a new method through which to deprotect the DHAC in a way that is more compatible with polyesters. Previous work using DHA for the synthesis of copolymers exemplified the need to create a protected monomer due to DHA's vulnerability toward nucelophilic addition at the C2 carbonyl and its capacity for forming a dimer in solution.[25, 26] However, we considered that the previously reported method of acetal deprotection via acid catalyzed cleavage in the presence of water, while proven to be efficacious for the case of diblock copolymers based on a polycarbonate of DHA and ethylene glycol, may be unsuitable for copolymers containing the more hydrolytically susceptible ester-based copolymer backbone.[21] This motivation led to an alternative deprotection method for the polymeric DHAC's protecting group (a dimethoxy acetal) using elemental iodine in the presence of acetone and heat.[55] Additionally, the in vitro degradation characteristics of this new material are reported.

Contrary to the behavior normally seen in compressed polyester tablets, specifically those comprised of poly(lactic acid), the copolymers of DHAC and LA appear to have a primarily surface erosion pattern of degradation rather than a bulk erosion pattern. The tablets also show no sign of a liquid core that would be the result of a faster degradation inside the copolymer than outside, which is the case for tablets comprised of poly(lactic acid).[10, 56, 57] Lastly, contrary to most polycarbonate degradation studies, increasing the carbonate group content in the copolymer backbone increases the rate of degradation.[58-60]

2.2 Experimental

2.2.1 Materials

Dihydroxyacetone dimer, *p*-toluene sulfonic acid, stannous octoate ($Sn(Oct)_2$), ethyl chloroformate, iodine, and acetone (CHROMASOLV®, for HPLC, ≥99.9%) were purchased from Sigma-Aldrich (St. Louis, MO) and used as received. Triethylamine, tetrahydrofuran (THF), sodium carbonate (Na_2CO_3), dichloromethane (CH_2Cl_2), diethyl ether, and methanol were purchased from VWR (West Chester, PA) and used as received. Trimethyl orthoformate was purchased from Alfa Aesar (Ward Hill, MA) and used as received. DL-Lactide was purchased from VWR (West Chester, PA) and recrystallized in methanol. Phosphate buffered saline (PBS) without calcium or magnesium was purchased from BioWhittaker® (Lancaster, MA).

2.2.2 Characterization methods

^1H and ^{13}C NMR spectra were recorded on Mercury 300 MHz and Inova 400 MHz spectrometers, respectively. ^1H NMR traces were normalized to the residual DMSO-d_6 solvent

peak at $\delta = 2.50$ and ^{13}C NMR normalized to the DMSO-d_6 residual peak at $\delta = 39.52$. Gel permeation chromatography (GPC) was carried out using SDV columns (Polymer Standard Service) 500A, 50A, and linear M (in series) with a THF mobile phase (1 ml/min), and 20 polystyrene standards ranging from 1,000 to 1,000,000 Daltons (Polymer Standard Service Win GPC software fit to a 5^{th} order polynomial equation) as a reference for the number average and weight average molecular weight calculations, UV (Waters 486) and RI (Waters 2410) detection. Thermal gravimetric analysis (TGA) experiments were conducted on a TGA Q500 (TA Instruments) with a heating rate of 10 ºC/min and nitrogen flow rate of 50 mL/min. Differential scanning calorimetry (DSC) measurements were performed on a DSC Q1000 (TA Instruments) equipment at a heating/cooling rate of 10 ºC/min and nitrogen flow rate of 50 mL/min. SEM images were taken with a Leica 440 (5kV, 600 pA, Leica Microsystems) on samples sputter coated with gold-palladium (60-40) using a Denton Vacuum Sputter Coater Desk II. Static contact angle measurements were performed under ambient conditions with a Ramé-Hart contact angle goniometer equipped with a syringe and flat-tipped needle allowing for a minimum droplet size of 10 µl. The probe fluid use was purified water and applied directly to the surface of dry copolymer tablets.

2.2.3 Synthesis of 2,2-dimethoxypropylene carbonate (III)

This compound was synthesized following a previously published method.[21, 26] In brief, DHA dimer (62.5g, 0.348 mol), trimethylorthoformate (76.1 mL, 0.695 mol), and *p*-toluenesulfonic acid (250 mg) were dissolved with magnetic stirring in methanol (700 mL). After 12 hours, sodium carbonate (750 mg) was added and the reaction mixture allowed to stir for an additional 12 hours after which the mixture was filtered, the solvent removed *in vacuo*, and the

remaining viscous, brown liquid recrystallized repeatedly from diethyl ether to afford 2,2-dimethoxy-propane-1,3-diol (II) as a white, crystalline material. This compound was then cyclized by a 15 minute dropwise addition of triethylamine (27.8 mL, 0.2 mol) in THF (50 mL) into a stirring flask of 2,2-dimethoxy-propane-1,3-diol (14.3 g, 105 mmol) and ethylchloroformate (19 mL, 0.2 mol) in THF (200 mL) at 0 ºC. After the addition of triethylamine was complete, the reaction was allowed to stir at room temperature for an additional 3 hours after which the mixture was filtered and the THF removed *in vacuo*. The viscous, yellow product was recrystallized from ethyl ether three times to yield, 2,2-dimethoxypropylene carbonate (III), a white, crystalline powder. Yield and characterization are reported in the aforementioned references.

2.2.4 Synthesis of poly(DL-lactide-*co*-2,2-dimethoxy-1,3-propylene carbonate) (IV) (protected pLA_x-*co*-$DHAC_y$)

Prior to each reaction, a 5 mL pear shaped flask with magnetic stir bar was flame dried and evacuated for 10 minutes. Varying feed mole ratios of LA and 2,2-dimethoxypropylene carbonate (III), for a combined total of 3 mmol (pLA_{100}, protected pLA_{85}-*co*-$DHAC_{15}$, protected pLA_{75}-*co*-$DHAC_{25}$, protected pLA_{50}-*co*-$DHAC_{50}$, protected pLA_{25}-*co*-$DHAC_{75}$, protected pLA_{15}-*co*-$DHAC_{85}$, $pDHAC_{100}$), were added to the reaction vessel and allowed to evacuate for an additional 5 minutes. The reaction vessel was then sealed and partially immersed in a 130 ºC paraffin oil bath for approximately 1-3 minutes until a melt had formed at which time the reaction was allowed to stir magnetically. Following this step, $Sn(Oct)_2$ was added immediately using a 20 μL micropipette and the vessel evacuated for 10 seconds to 50 mmHg exactly, then immediately sealed under vacuum. The reaction was allowed to proceed at 130 ºC for one hour

with stirring after which the reaction was cooled to room temperature. The solid, semi-transparent copolymer was dissolved in 1 mL dichloromethane and precipitated by dropwise addition into 60 mL of stirring methanol before isolation by filtration and dried under vacuum. Reprecipitation was performed twice in the same manner and each time yielded a solid, white copolymer. The yield for each feed ratio ranged from 50-80% and each ratio was synthesized in triplicate. For the in vitro degradation study, the amount of initiator was altered to create consistent molecular weights (M_w ~70 kDa). For the degradation study, the amount varied from 5.1 μL, 6.4 μL, or 12 μL of $Sn(Oct)_2$ for the protected pLA_{50}-*co*-$DHAC_{50}$, protected pLA_{25}-*co*-$DHAC_{75}$, protected pLA_{15}-*co*-$DHAC_{85}$, reactions, respectively. These three ratios were chosen due to their physical characteristics during deprotection. Upon deprotection the ratios containing ≥50% DHAC precipitated out of solution as a fine white powder and thereby were amenable to direct compression into uniform discs. Those with less that 50% DHAC in the backbone remained in solution until precipitation into cold diethyl ether whereby they became a very tough, solid white mass. Molecular weights obtained by GPC and thermal data are provided in Table 2.1 and Table 2.2. The ^1H and ^{13}C NMR spectra are similar for each copolymer and are exemplified by the spectrum found for protected pLA_{50}-*co*-$DHAC_{50}$ copolymer in Figures 2.1 and 2.2, respectively. ^1H NMR (DMSO-d_6) δ: 5.05-5.21 (broad m; LA 1H), 4.12 (s; DHAC 2H), 3.18 (s; DHAC 3H), 1.43-1.48 (broad; LA 3H). ^{13}C NMR (DMSO-d_6): δ 169 (LA, CO, multiplet), 153 (DHAC, O-CO-O, multiplet), 99 (DHAC, C), 68-69 and 71 (LA, CH, multiplet) 62 and 60 (DHAC, CH2, multiplet), 49 (DHAC, OCH3), 16 (LA, CH3). Multiplets and ranges were designated as shown in Figure 2.

2.2.5 Synthesis of poly(DL-lactide-*co*-2-oxopropylene carbonate) (V) (pLA_x-*co*-$DHAC_y$)

V was prepared via conversion of the dimethoxy acetal to a carbonyl using molecular iodine in acetone. Deacetalization of IV with molecular iodine (1:1 w:w) was carried out in acetone (CHROMASOLV®, for HPLC, ≥99.9%). A 25 mL round bottom flask was flamed under vacuum before being charged with IV (250 mg) and iodine (250 mg) in acetone (7 mL) and allowed to stir for 2 hours partially submerged in a 52 ^{o}C paraffin oil bath. For the copolymers containing 50% DHAC or more, the deprotected copolymer was too insoluble to remain in solution for the entirety of the set time period. For these copolymers, the insoluble, partially deprotected copolymer was allowed to settle to the bottom of the flask after the two hour reaction whereupon the acetone was decanted. The fine powder product was then washed repeatedly with fresh diethyl ether to remove any visible signs of residual iodine before being transferred to a 20 mL scintillation vial. Fresh ether (15 mL) was added, the vial capped and the suspension allowed to stir for an additional 3 days. During this time the ether was decanted twice daily and fresh ether was added as needed to remove excess iodine before being dried under vacuum. For the copolymers containing less than 50% DHAC, the deprotected copolymer remained in solution for the set time period. For these copolymers, all but 2 ml of solvent was removed *in vacuo* and the copolymer was precipitated by the slow dropwise addition of cold ether into the vigorously swirling flask containing the copolymer/iodine solution. The precipitated copolymer was washed with diethyl ether before dissolution in a minimal amount of dichloromethane and precipitated into stirring methanol (60 mL) three times. The copolymers were washed a final time with diethyl ether, isolated by filtration, and dried under vacuum. The yield for each deprotected copolymer was approximately 75%. Thermal data are shown in Tables 2.1 and 2.2. Elemental analysis (Intertek QTI Laboratory©) of the material show minimal

residual iodine (<0.1%). The ^{1}H NMR spectra are similar for each copolymer and are represented by Figure 2.4 for the pLA_{50}-*co*-$DHAC_{50}$ copolymer. Due to low solubility, a ^{13}C NMR analysis of the deprotected copolymer was not possible. ^{1}H NMR (DMSO-d_6) δ: 5.05-5.21 (broad m; LA 1H), 4.99 (broad; DHAC 2H), 1.43-1.48 (broad; LA 3H).

2.2.6 Monomer distribution analysis

^{13}C NMR was performed on the protected copolymers using an Inova 400 MHz spectrometer in DMSO-d_6 for a period of 12 hours and the results are provided in Figure 2.3.

2.2.7 In vitro degradation analysis

The in vitro degradation study was designed to run for 56 days and followed three copolymer monomer ratios, pLA_{50}-*co*-$DHAC_{50}$, pLA_{25}-*co*-$DHAC_{75}$, pLA_{15}-*co*-$DHAC_{85}$ all with M_w ~70,000 g/mol. Each ratio was synthesized at least five times and the fine, white powders combined before being sizing through a 250 μm sieve. Tablets were formed using direct mechanical compression to 1000 psi for 10 seconds on 20 mg of copolymer at room temperature. The final cylindrical tablets had dimensions of approximately 5.32 ± 0.02 mm x 0.84 ± 0.02 mm (diameter x thickness) as measured by digital calipers. Each tablet was placed in 1X PBS buffer solution (1.5 mL, pH 7.4) and incubated with rotation (N=3) at 37 ºC. Every three days the buffer solutions were exchanged and a control was used to ensure a constant pH. At predetermined time points, the samples were removed from the buffer solution, rinsed with DI water, dried by KimWipe© and lyophilized for three days. The mass loss and new tablet geometry were then recorded. The percent mass loss was calculated using the following expression:

$$M_{loss}(\%) = \left(\frac{m_0 - m_f}{m_0} \right) \times 100 \quad (1)$$

where m_0 refers to the initial mass and m_f refers to the final mass at a specific time point.

2.2.8 Morphological characterization

Scanning electron microscopy (SEM) was used to determine the morphology of the surface and the cross-section of each tablet at each time point (Leica 440). In brief, each tablet was placed on a small metal stub and sputter coated with gold-palladium (60-40) to a thickness of 10 nm using a Denton Vacuum Sputter Coater Desk II. For the cross-sectional view, each pellet was cut in half with a razor blade, immersed in liquid nitrogen and fractured in half again by hand before sputter coating.

2.2.9 Surface characterization

Static contact angle measurements were used to explore the surface of the three copolymer ratios used in the hydrolytic degradation study. Manual addition of a droplet of water to the top surface of each copolymer tablet allowed the contact angle to be measured. This experiment was repeated for each ratio to confirm the validity of the reading.

2.3 Results and Discussion

2.3.1 Synthesis of poly(DL-lactide-*co*-2-oxopropylene carbonate)

The synthetic strategy employed to create copolymers of lactide and dihydroxyacetone is shown in Scheme 2.1. The DHAC monomer was prepared based on earlier work using a dimethoxy acetal protecting group to prevent the DHA from forming a dihemiacetal dimer.[21, 26] The protected DHA was then converted into a six-membered, cyclic carbonate ring to be used for

ring-opening polymerization (III).[26] Stannous octoate ($Sn(Oct)_2$) was used as the coordination catalyst due to its efficacy to promote ring opening polymerizations of both the cyclic lactide and DHAC monomers.[9, 21, 22, 26]

Five monomer ratios of the pLA_x-*co*-$DHAC_y$, (pLA_{85}-*co*-$DHAC_{15}$, pLA_{75}-*co*-$DHAC_{25}$, pLA_{50}-*co*-$DHAC_{50}$, pLA_{25}-*co*-$DHAC_{75}$, pLA_{15}-*co*-$DHAC_{85}$), were synthesized by adjusting the feed ratio of the two monomers while maintaining a constant $Sn(Oct)_2$/monomer ratio. As a basis for head-to-head comparisons, LA and DHAC homopolymers (pLA_{100} and $pDHAC_{100}$) were also synthesized. For the three ratios of copolymers that were investigated in the in vitro degradation study (pLA_{50}-*co*-$DHAC_{50}$, pLA_{25}-*co*-$DHAC_{75}$, pLA_{15}-*co*-$DHAC_{85}$), a constant molecular weight was maintained by varying the amount of $Sn(Oct)_2$ as described in the methods section. Due to the higher melting temperature of the LA monomer as compared to the protected DHAC monomer, all molar ratios were synthesized by a melt injection of the $Sn(Oct)_2$ at 130 ^{o}C to ensure the creation of a homogenous monomer mixture. The mole fractions of each monomer in the copolymers were confirmed via ^{1}H NMR analysis of the -CH_3 species present in the LA (δ = 1.43-1.48) and the protected DHAC (δ =3.18), which is shown in Figure 2.1 and the average values reported in Table 2.1. GPC analysis of the protected copolymers with different feed ratios was performed and the relative molecular weight, shown in Table 2.1, shows a direct relationship exists between increasing DHAC content and M_w for each copolymer. In addition, the GPC traces, which show a single peak, helped to substantiate the creation of the copolymers, rather than two populations of homopolymers.

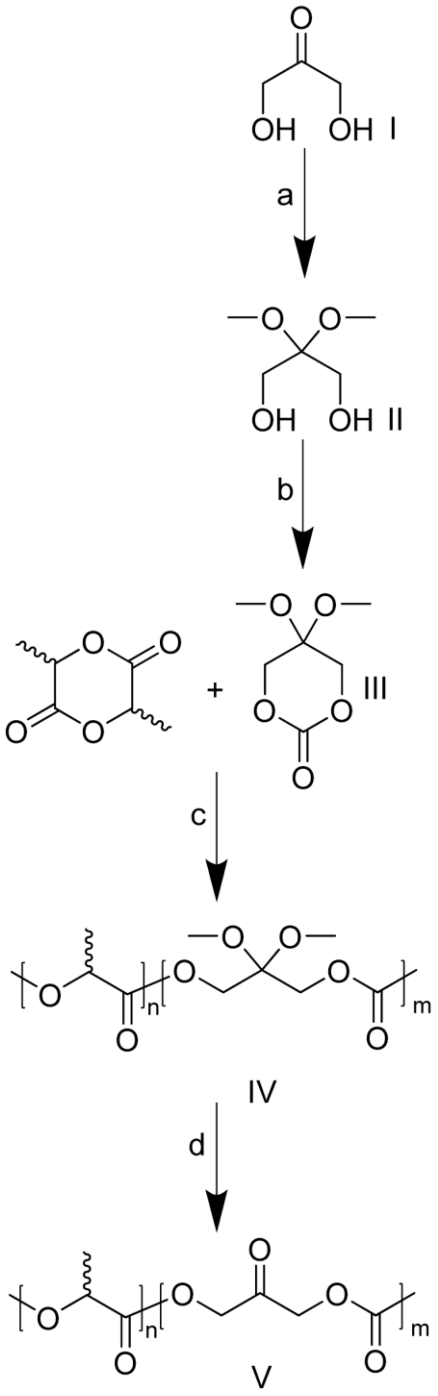

Scheme 2.1. Synthetic route to poly(DL-lactide-co-2-oxopropylene carbonate) (V) a) trimethyl orthoformate, p-toluene sulfonic acid, methanol, 24 h; sodium carbonate, 24 h. b) ethylchloroformate, triethylamine, tetrahydrofuran, 3 h c) stannous octoate, vacuum, 130ºC, 1 h. d) iodine, acetone, reflux, 2 h.

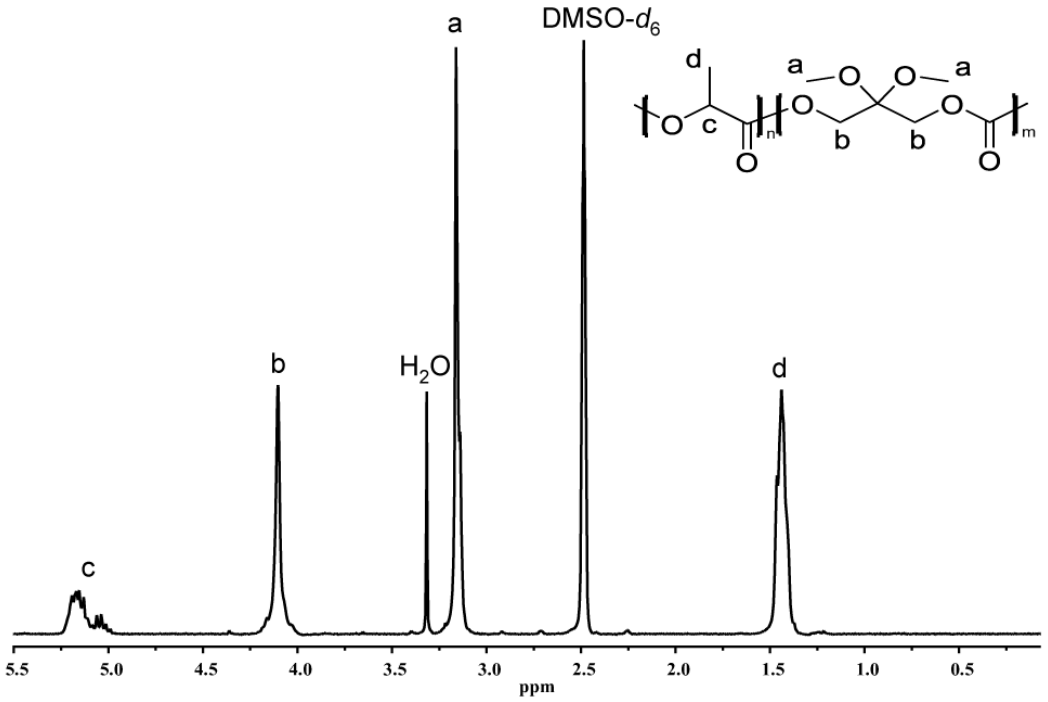

Figure 2.1. ^{1}H NMR spectrum of protected poly(lactic acid-*co*-2,2-dimethoxy-1,3-propylene carbonate) (IV) (pLA_{50}-*co*-$DHAC_{50}$) in DMSO-d_6.

		Molecular Weight (GPC)			Protected pLA_x-*co*-$DHAC_y$		Deprotected pLA_x-*co*-$DHAC_y$		
Mole Feed LA:DHAC	Confirmed Ratio LA:DHAC	M_w (g/mol)	M_n (g/mol)	M_w/M_n	T_d (ºC) 50 wt%	T_g (ºC)	% Deprotected	T_d (ºC) 50 wt%	T_g (ºC)
0:100	0:100	81 000	56 400	1.44	246	45	80	273	68
15:85	16:84	75 100 ± 700	52 500 ± 1 000	1.43 ± 0.05	240 ± 11	51 ± 1	86	252 ± 1	65 ± 1
25:75	27:73	62 400 ± 900	45 500 ± 1 900	1.37 ± 0.04	239 ± 1	50 ± 1	90	246 ± 4	64 ± 2
50:50	52:48	51 400 ± 4 100	35 700 ± 7 200	1.47 ± 0.20	240 ± 4	51 ± 1	>95	261 ± 6	58 ± 1
75:25	78:22	50 400 ± 3 800	37 800 ± 3 200	1.33 ± 0.03	236 ± 2	53 ± 1	>95	330 ± 3	55 ± 1
85:15	89:11	47 500 ± 7 100	35 400 ± 6 900	1.35 ± 0.07	228 ± 5	52 ± 1	>95	316 ± 27	54 ± 1
100:0	100:0	37 900 ± 1 200	26 800 ± 2 700	1.42 ± 0.15	236 ± 5	53 ± 1	-	-	-
100:0[a]	100:0	-	-	-	-	-	-	309 ± 37	53

[a] This value is based on a pLA_{100} sample subjected to the acetone/I_2 deprotection conditions.

Table 2.1. Molecular weight and thermal data of pLA_x-*co*-$DHAC_y$ copolymers.

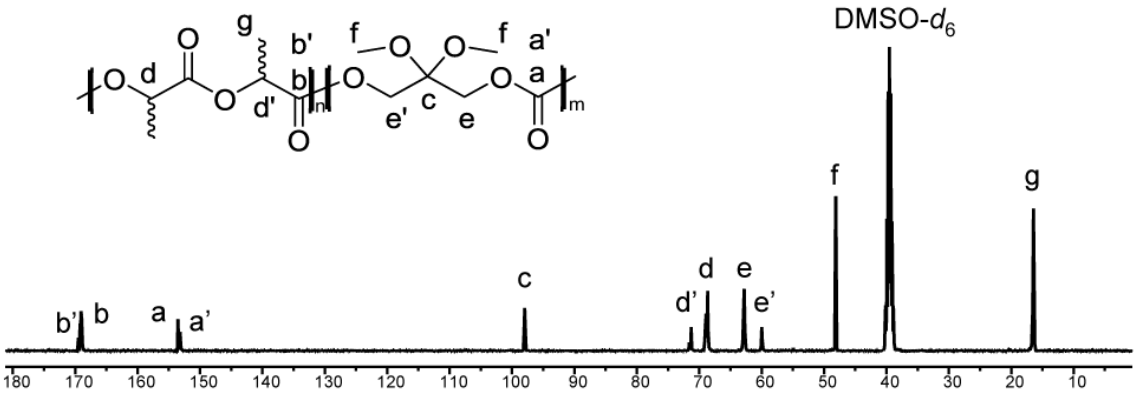

Figure 2.2. ^{13}C NMR spectrum of protected poly(lactic acid-*co*-2,2-dimethoxy-1,3-propylene carbonate) (IV) (pLA$_{50}$-*co*-DHAC$_{50}$) in DMSO-d_6. The peaks assigned to a', b', c', and d' are peak shifts due to the heterogeneous placement of monomers throughout the backbone, i.e. a DHAC next to a LA, or a DHAC next to another DHAC.

2.3.2 Monomer distribution analysis

To further elucidate the distribution of the monomers in the copolymers, ^{13}C NMR was employed to first verify the structure, seen in Figure 2.2, and then to determine the monomer sequence based on the carbon resonances, which can be seen in Figure 2.3. ^{13}C NMR spectra provided the means to determine whether the copolymer is random, block, or alternating depending on how each monomer interacts with its neighboring species.[51, 61-64] In the case of a statistically random copolymer, 2^3 triads can be theoretically formed and these can be used to understand the molecular architecture of the copolymer. For the DL-lactide (L) and the protected DHAC (D) copolymers, the 8 possible triads that can be formed are as follows: LLL, LLD, DLL, DLD, LDL, LDD, DDL, and DDD. ^{13}C spectra of the homopolymers provided the basis for the LLL and DDD homopolymer resonances and thus the position of the subunits throughout the backbone. The pLA$_{100}$ spectrum indicated that the resonance for the central carbonyl carbon in

LLL is a trio of peaks that lie between 169.0 ppm and 169.21 ppm. The multiple resonances seen for pLA_{100} were attributed to the creation of a mixture of atactic and isotactic regions along the polymer backbone and are due to a number of influencing factors. These factors include, but are not limited to, the polymerization kinetics, lactide feed composition, the favoring of *meso* dyads in L,L or D,D dimeric repeat units, extent of conversion, and the possibility of transesterification when the reaction conditions have a temperature set point higher than 120 ^{o}C.[62-65] The protected $pDHAC_{100}$ spectrum showed the DDD resonance at 153.52 ppm for the carbon associated with its carbonate bond. The determination of the two extra shifts associated with the carbonate bond's carbon seen in the copolymer spectra was determined by the gradual superposition of the spectra toward the homopolymers as the molar feed ratios changed as shown in Figure 2.3. Using this information and preliminary predictive ^{13}C NMR modeling software, the new peaks observed were assigned to the two XLD triads (LLD, DLD) and two XDL triads (DDL, LDL) with signals located at 169.47 ppm and 153.18 ppm, respectively.[66] This information supports the conclusion that the synthesized polymers are random copolymers of the LA and DHAC monomers.

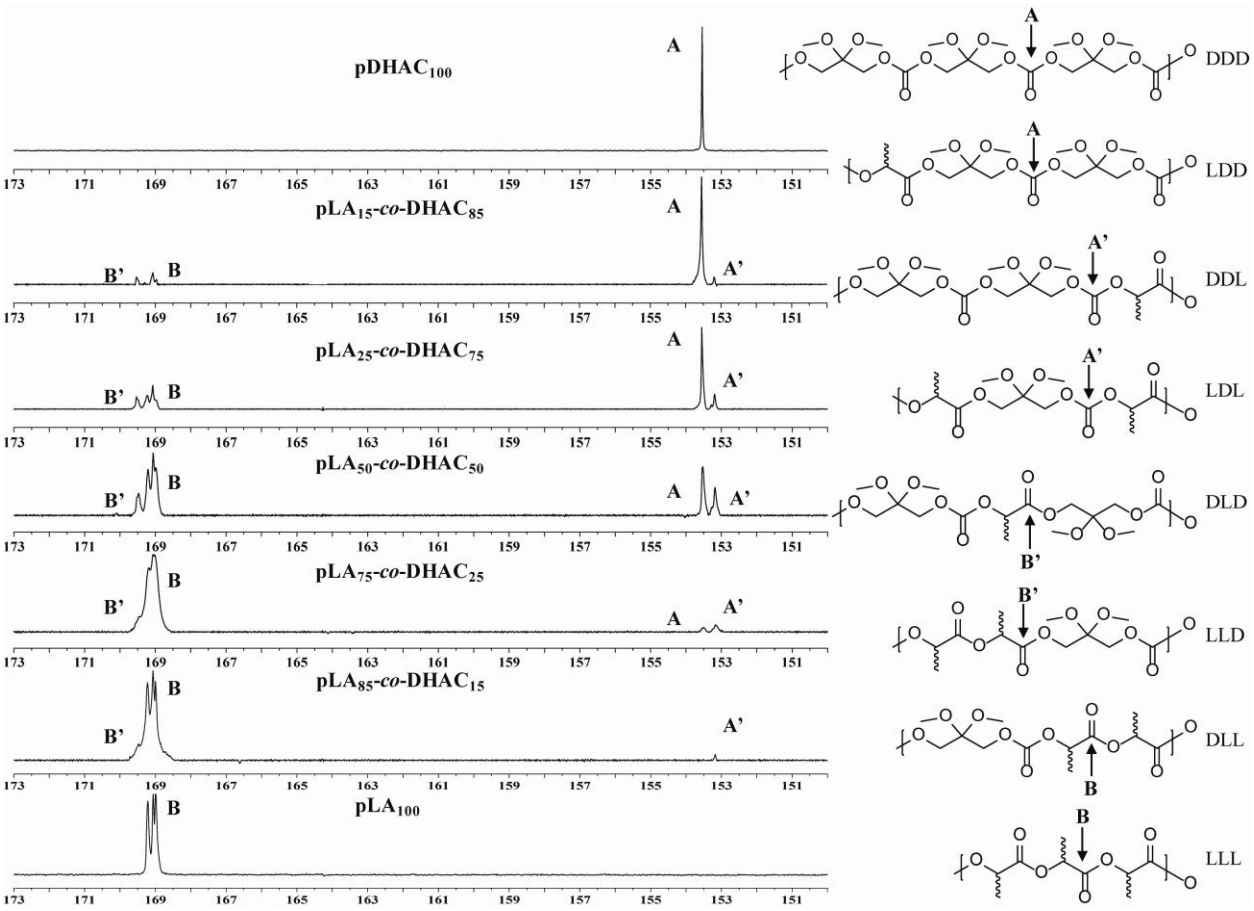

Figure 2.3. ^{13}C NMR spectra of $pDHAC_{100}$, pLA_{15}-*co*-$DHAC_{85}$, pLA_{25}-*co*-$DHAC_{75}$, pLA_{50}-*co*-$DHAC_{50}$, pLA_{75}-*co*-$DHAC_{25}$, pLA_{85}-*co*-$DHAC_{15}$, and pLA_{100} in DMSO-d_6. The chemical structures of the eight possible triads along with their respective carbonyls noted have been included.

2.3.3 Copolymer deprotection

The removal of the dimethoxy acetal group to obtain the final copolymer, (V), was conducted utilizing a method different from the one previously reported by our group for the protected DHAC derived monomer.[21, 22, 25] To eliminate the possibility of ester hydrolysis from the reaction conditions present in a trifluoroacetic acid:water deprotection, a deprotection

catalyzed by molecular iodine in acetone was investigated.[55] With this method the degree of deprotection was directly correlated to the molar ratio of LA and DHAC within the copolymer. This relationship was found to be caused by the poor solubility of the deprotected DHAC monomer in acetone. At higher concentrations of DHAC in the copolymer (≥50%), the deprotection reached a solubility limit prior to complete deprotection. When a significant amount of the protected DHAC within the copolymer backbone had been deprotected, the LA and remaining protected DHAC were no longer able to keep the copolymer soluble in solution leading to its precipitation. The degree of deprotection for these ratios, including $pDHAC_{100}$, ranged from 80% to greater than 95% and was determined via ^1H NMR. An example of the deprotected copolymer ^1H NMR spectrum is shown in Figure 2.4. Interestingly, it was noticed that even though the pLA_{50}-*co*-$DHAC_{50}$ ratio copolymers came out of solution prior to the two hour time point, their degrees of deprotection were all greater than 95%. In contrast, at lower concentrations of DHAC (<50%), all of the copolymers remained soluble in the acetone and the degrees of deprotection were all found to be greater than 95%. We anticipate that total deprotection was not achieved over this two hour time scale due to the presence of trace amounts of water in the acetone which has been reported to affect the rate and degree of deprotection.[55]

2.3.4 Thermal analysis

Thermal analysis of the materials was conducted to characterize the influence of each ratio of monomers on the copolymer characteristics. Thermal gravimetric analysis (TGA) revealed that protected $pDHAC_{100}$ had a T_d of ~246 ^oC, while LA_{100} showed a T_d of ~237 ^oC. The T_d for all of the protected copolymers was consistent within this temperature range and the data are presented in Table 1. Also shown in Table 2.1 are the T_d values for the deprotected copolymers. Upon

deprotection, the T_d of $pDHAC_{100}$ was elevated to 273 ^oC and a new trend was observed. As the ratio of LA increased within the deprotected copolymers, the observed T_d also increased to values greater than pLA_{100}. This phenomenon may be attributed to the solubility difference of the copolymers with varying pLA_x-*co*-$DHAC_y$ ratios. Due to the insolubility of the copolymer with greater than or equal to 50% DHAC, these copolymers precipitate out of solution upon deprotection as a fine powder. In contrast, the copolymers that contain more LA remain soluble throughout the deprotection and precipitate in cold ether as a sticky mass. Using pLA_{100} as a control under the same deprotection conditions, elemental analysis found a very small residual amount of iodine in all of the deprotected copolymers (<0.1%), which may be the cause for the increased T_d.

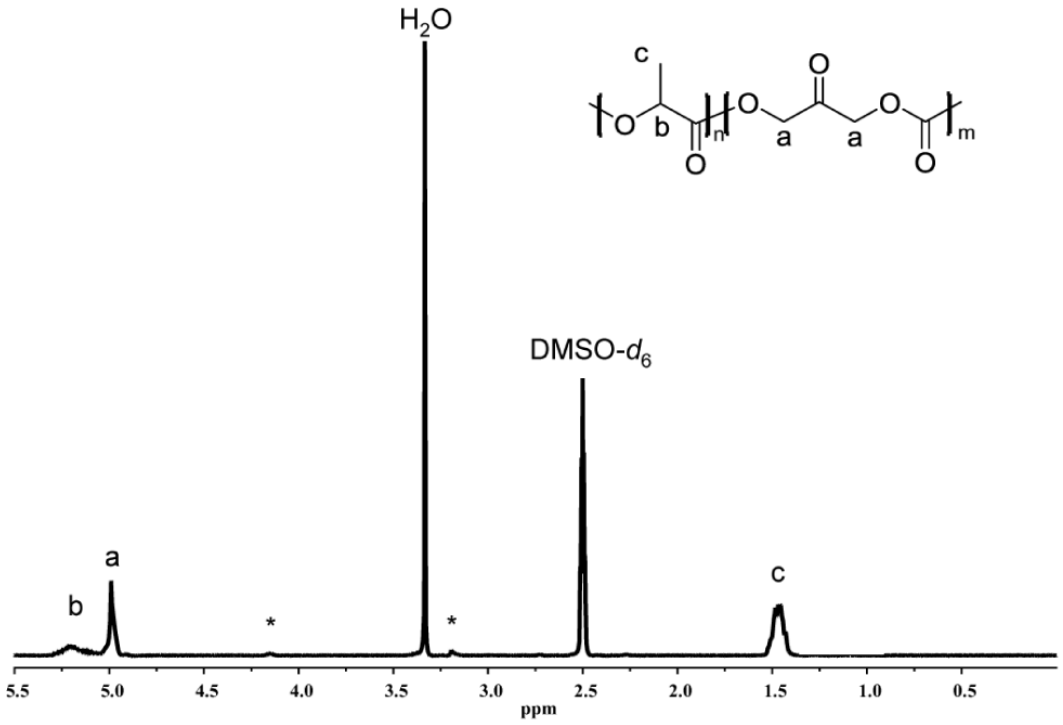

Figure 2.4. ^1H NMR spectrum of deprotected poly(lactic acid-*co*-2-oxopropylene carbonate) (V) (pLA_{50}-*co*-$DHAC_{50}$) in DMSO-d_6. (*) denotes residual protected DHAC peaks.

Differential scanning calorimetry was conducted to further distinguish the thermal characteristics of each copolymer. A glass transition temperature, T_g, was observed for each copolymer while a melting temperature, T_m, was not observed for any of the copolymers within the set temperature range of -60 ºC to 140 ºC. The lack of a T_m also supports the conclusion that the LA in the copolymer backbone has little stereospecificity due to the random distribution of the D- and L- chiral carbons from the DL-lactide monomer and the inclusion of DHAC in the backbone that may disrupt the configuration of chain segments needed to form the crystalline lattice.[67] As seen in Figure 2.5, the T_g of the protected $pDHAC_{100}$ was ~45 ^oC, while the T_g of pLA_{100} was ~53 ^oC. All of the T_g values for the protected copolymers were between 49 ^oC and 53 ^oC. However, deprotected $pDHAC_{100}$ showed an increased T_g at ~68 ^oC. The increase in T_g observed for the deprotected DHAC homopolymer was also observed for each deprotected copolymer (Figure 2.6). A trend was observed toward an increasing T_g as the DHAC content within the copolymers increased as shown in Table 2.1. The trend of an increased T_g as the molecular weight increased was expected because of the reported relationship that exists between T_g and molecular weight.[68]

An interesting feature of the pLA_x-*co*-$DHAC_y$ copolymers is their variable solubility as the DHAC content within the copolymers change. Earlier work on DHAC homopolymers showed that characterization was a challenge.[21] The introduction of 50% or more LA monomer within the copolymer allowed more facile characterization of the copolymers. Copolymers with higher LA monomer ratios were soluble in common organic solvents such as acetone, dimethyl sulfoxide, and dichloromethane. This solubility allowed the I_2/acetone deprotection method to be more reliable than the previously reported TFA-based methods because it avoids potential acid catalyzed hydrolysis of the copolymer backbone, which can lead to a reduced molecular weight.

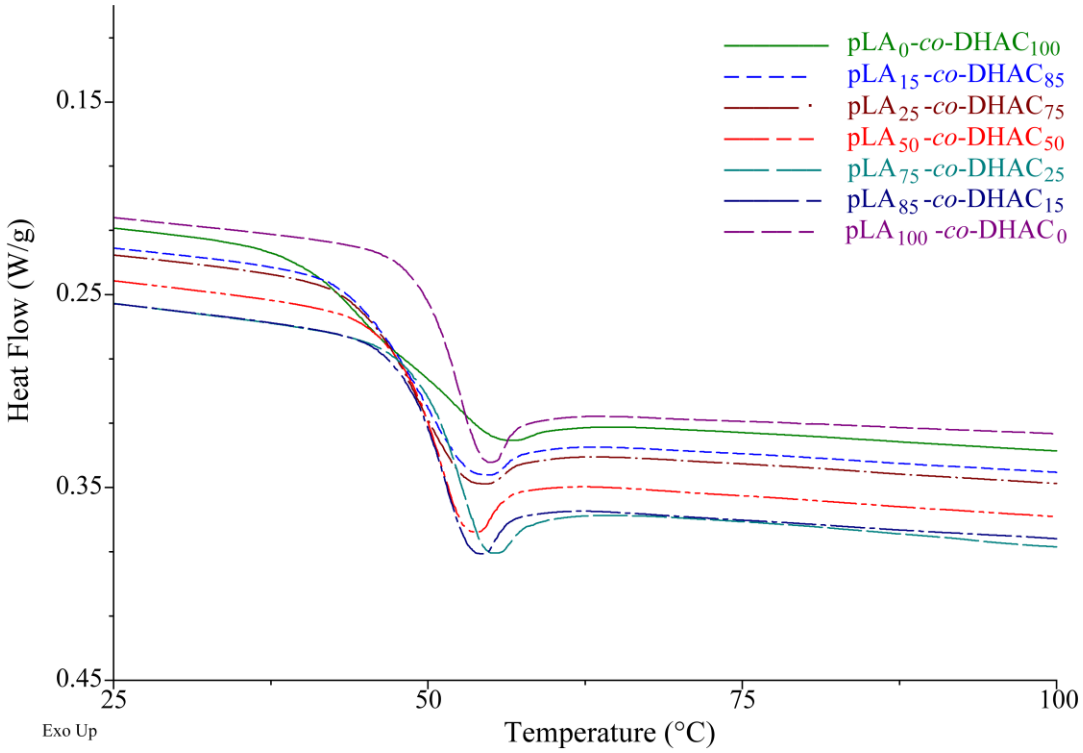

Figure 2.5. DSC traces for all protected copolymer ratios.

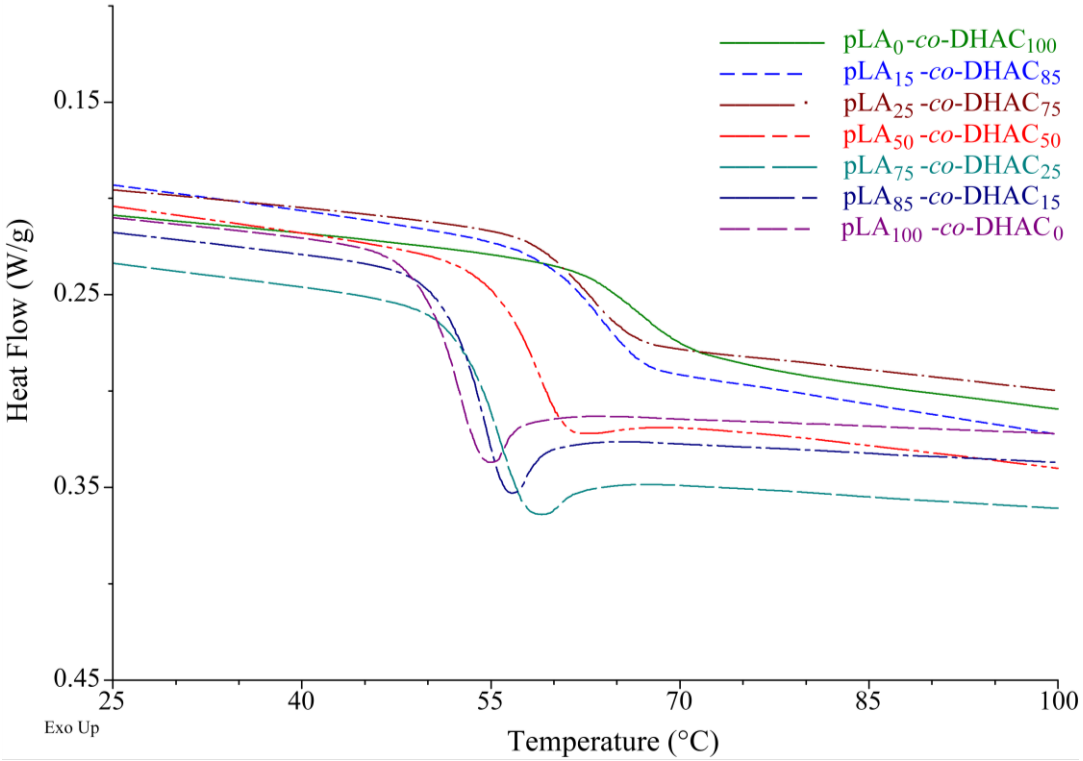

Figure 2.6. DSC traces for all deprotected copolymer ratios.

2.3.5 In vitro degradation of poly(DL-lactide-co-2-oxopropylene carbonate)

To begin to evaluate hydrolysis of the copolymer, an eight week in vitro degradation study was performed. Due to the physical form of the >50% LA deprotected copolymers when precipitated, the pLA_{75}-*co*-$DHAC_{25}$ and the pLA_{85}-*co*-$DHAC_{15}$ copolymers were unsuitable candidates for the degradation study. Following deprotection, the precipitated pLA_{75}-*co*-$DHAC_{25}$ and the pLA_{85}-*co*-$DHAC_{15}$ became very tough, solid materials that were not amenable to grinding into a powder. However, the ratios of pLA_x-*co*-$DHAC_y$ with ≤50% LA had a fine powdery physical form upon deprotection making them much more suitable for a study of this nature. Three copolymers with monomer ratios were synthesized: pLA_{50}-*co*-$DHAC_{50}$, pLA_{25}-*co*-$DHAC_{75}$, pLA_{15}-*co*-$DHAC_{85}$ by varying the amount of initiator to obtain copolymers with a M_w ~70 kDa and slightly higher molecular weight distribution of ~1.7-1.8 than the previous materials (Table 2.2). Due to the insolubility of the deprotected copolymers in common GPC mobile phase solvents, molecular weight values to track the degradation of the copolymer backbone vs. time were unable to be obtained. Thermal characterization of these higher molecular weight copolymers showed slightly altered values for T_d and T_g due to the change in molecular weight and polydispersity. The glass transition temperature data observed for the 70 kDa in vitro degradation copolymers are shown in Table 2.2. The decrease in T_g as compared to the T_g of the copolymers shown in Table 1 is most likely attributed to the increase in the polydispersity, where the molecular weight range increases the number of lower molecular weight polymers in the final material that can act as plasticizers.[69] Static contact angle measurements revealed that the surface of each copolymer ratio, while tending to be more hydrophilic in nature, did not vary significantly among the three different ratios.

	Molecular Weight (GPC)			Deprotected pLA_x-*co*-$DHAC_y$		
Mole Feed LA:DHAC	M_w (g/mol)	M_n (g/mol)	M_w/M_n	contact angle (º)	T_d (ºC)	T_g (ºC)
15:85	69 900 ± 1 200	40 500 ± 3 800	1.77 ± 0.10	60.5 ± 1	233	58
25:75	71 200 ± 2 400	39 800 ± 2 600	1.79 ± 0.10	61.5 ± 1	234	56
50:50	70 000 ± 2 300	43 500 ± 2 000	1.66 ± 0.10	61.5 ± 1	260	56

Table 2.2. Molecular weight and thermal data for the copolymers used in the in vitro degradation study. The T_d is measured at 50 wt%.

Visual inspection of the compressed tablets from each time point, post lyophilization, showed a white exterior and cylindrical shape, with each tablet maintaining its geometry and color over the course of the erosion study. Upon fracture, the interior was the same white color as the exterior and each sample appeared to have uniform structural integrity throughout the tablet. This result is significant because monomeric DHAC degrades to DHA, which can further degrade into a dark brown product, suggesting chemical degradation past DHA does not occur within the pellet. Depending on the copolymer composition, the longer time points of 4 weeks and 8 weeks contained samples that were more brittle. However, comparing the interior and exterior of each sample, there were no visual signs of any large difference in mechanical properties, color changes, or morphology. This result is particularly interesting because a number of studies have tracked the in vitro degradation of lactic acid-derived polymers and copolymers and have found significant morphological changes over the course of the experiment. To directly compare with relevant literature, Li, *et al*, tracked the degradation of DL-lactic acid based

polymer tablets formed using direct compression molding at a temperature below its T_g. They observed that amorphous PLA polymers underwent heterogeneous degradation with the rate of degradation on the inside faster than that of the outside.[70, 71] This "inside-out" degradation pattern leads to the formation of a hard, white outer shell surrounding a viscous, transparent core that could be seen starting at 6 weeks for 100% LA (M_w = 65 000 kDa). Other studies have investigated similar morphological changes and the autocatalytic effect that causes these polyesters to degrade in this particular pattern.[10, 56, 57, 71]

Compared to the in vitro degradation of polyesters, specifically LA homopolymers, the in vitro degradation of polycarbonates and poly(carbonate-ester)s is quite different. Long term in vitro degradation studies using high molecular weight polycarbonate homopolymers derived of 1,3-trimethylene carbonate (TMC) show no sign of degradation after 2 years (M_n = 320 kDa) , while $pTMC_{50}$-*co*-LA_{50} copolymers (M_n = 220 kDa) show mass loss starting around 10 weeks with the onset of degradation occurring later with increasing TMC content.[58] Another study with lower molecular weight homopolymers of TMC (M_n = 114 kDa) showed no mass loss during a 53 week in vitro degradation study, while $pTMC_{67}$-*co*-LA_{33} (M_n = 88 kDa) and $pTMC_{50}$-*co*-LA_{50} (M_n = 104 kDa) displayed mass loss at 9 weeks.[59] Both studies exemplify the trend that TMC and LA based poly(carbonate-ester)s have an increasing degradation rate with increasing ester content in their backbone, opposite of the results with pLA_x-*co*-$DHAC_y$ copolymers seen in Figure 2.7. In general, the poly(carbonate-ester) degradation pattern can be attributed to carbonate bonds being less labile to hydrolysis than ester bonds, but for pLA_x-*co*-$DHAC_y$ copolymers we see the opposite.[60] These results however are consistent with previous reports of DHA based polycarbonates.[21, 26] Also of note is that, unlike copolymers containing only ester bonds, studies using other poly(carbonate-ester)s comprised of glycerol and L-lactic acid showed

no appreciable change in physical appearance throughout a two week study time period even though there was a molecular weight decrease of 35%.[51]

2.3.6 Interior visualization

To further explore the mechanism of degradation, SEM was used to visualize the erosion pattern on a microscopic level. Images were taken from the top, side, and cross-sectional surfaces to get a better understanding of the copolymer erosion mechanism. The images show that those copolymers with more LA in their backbone took longer to erode during the experimental time frame than those richer in DHAC. This visual finding correlates to the mass loss data seen in Figure 2.7 which also shows that copolymers with more LA in the backbone erode at a much slower rate than those with more DHAC in the backbone. The top and side views show a similar erosion pattern for the three ratios, though the erosion was much more accelerated in pLA_{15}-*co*-$DHAC_{85}$ than in pLA_{50}-*co*-$DHAC_{50}$ and can be seen in Figure 2.8. Similar to the top and side views, upon comparison of the cross-sectional views, a different degradation pattern was seen among the three ratios and these results are shown in Figures 2.9 and 2.10. The materials made of pLA_{50}-*co*-$DHAC_{50}$ showed very little morphological change in the center of their cores until 4 weeks, whereupon small pores had begun to form. However, the edges closest to the outside surfaces of the cross-sectional view appear to erode much more rapidly at earlier time points. At the one day time point, subtle morphological changes and small pores seem to form near the edge. This area of erosion increased in size with the length of time the tablets were allowed to rotate in the buffer solution and by day 56 noticeable regions of erosion near the edges can be seen in Figure 2.11, as compared to the relatively unaltered interior. Tablets made of pLA_{25}-*co*-$DHAC_{75}$ showed a similar erosion pattern to those made of

pLA_{50}-*co*-$DHAC_{50}$, where the very center of the material did not show signs of degradation until the 4 week time point. At this time a change in morphology and pores was once again observed. Unlike pLA_{50}-*co*-$DHAC_{50}$, the interior edge of pLA_{25}-*co*-$DHAC_{75}$ showed a larger, more distinct region of erosion and by week 8 the entirety of the material's cross-section showed morphological changes. In comparison, the copolymers comprised of pLA_{15}-*co*-$DHAC_{85}$ began to show morphological changes to the center of the interior by 2 weeks. These copolymers also had the largest eroded region near the edges of the interior as compared to the copolymers containing more LA. Also of note is that the pLA_{15}-*co*-$DHAC_{85}$ copolymers eroded to completion between weeks 6 and 7 and by week 2 the copolymer's cross-section showed morphological changes throughout the tablet.

These findings indicate that these poly(carbonate-ester)s display both surface and bulk erosion patterns that are unlike the erosion patterns seen with other lactic acid or lactic acid derived copolymers. The SEM images show that there is an erosion zone near the edges of the sample, and the area of this zone increases during later time points. However, at later times during the study, the very center of the interior does begin to show morphological changes as well. The erosion rate for all three samples does display some linearity, but there is not a constant value throughout the study that would indicate that this material erodes by only surface erosion. The data also do not indicate that this material erodes only by bulk erosion since the geometry of the materials stays consistent and there is no distinct time at which a drastic change in erosion rate occurs, a phenomenon normally seen with lactic acid or lactic acid copolymers. Li*, et al*, reported previously that pure DL-lactic acid polymers (M_w=65 kDa) showed this extreme rate change at 7 weeks, while for the pLA_{50}-*co*-$DHAC_{50}$ copolymer there is no extreme change of erosion rate throughout the 8 week study.[70, 71] This result is surprising since extensive

work by the Göpferich group to model erosion behavior shows that there is a critical thickness required before a sample can undergo surface erosion.[28, 29] This thickness has been theorized to be 7.4 cm for poly(α-hydroxy-acids). Other studies that track the erosion of TMC and LA poly(carbonate-ester)s reported a shift from surface erosion to bulk erosion with a LA content of more than 30% in the backbone.[60]

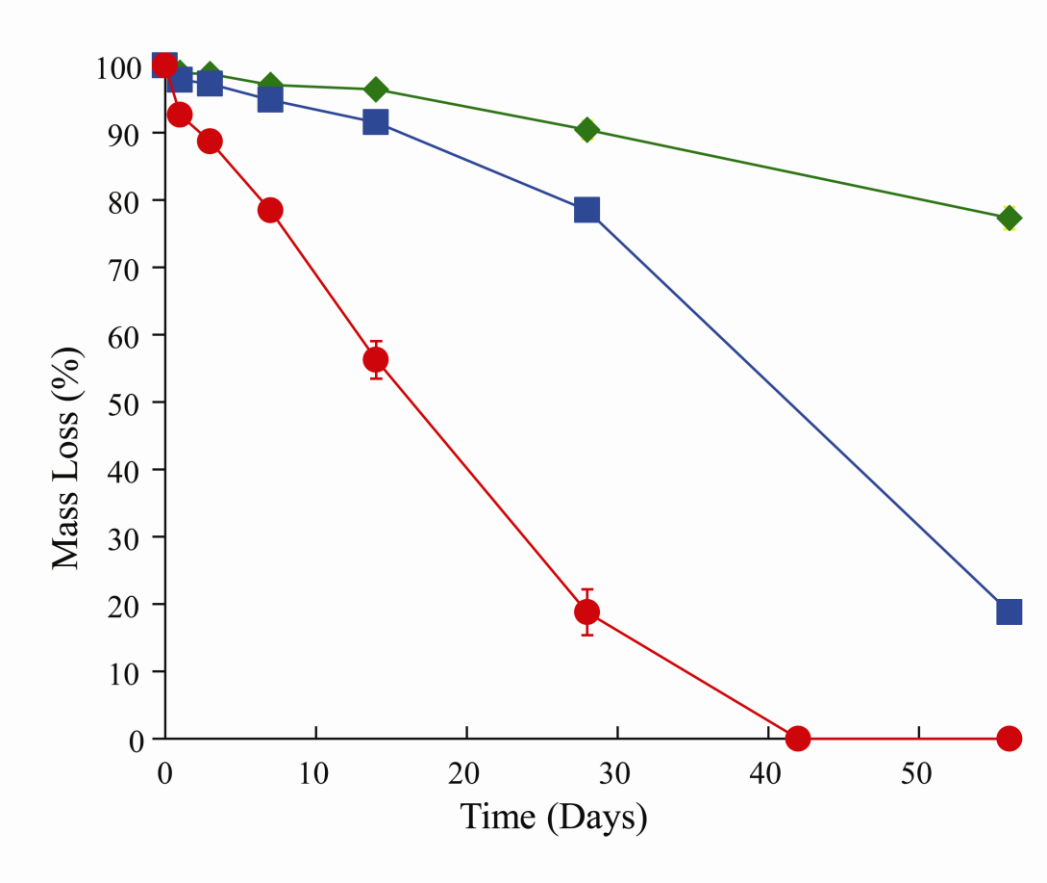

Figure 2.7. Mass loss as a function of degradation time for LA and DHAC copolymers: (♦) pLA_{50}-*co*-$DHAC_{50}$ (■) pLA_{25}-*co*-$DHAC_{75}$ (●) pLA_{15}-*co*-$DHAC_{85}$

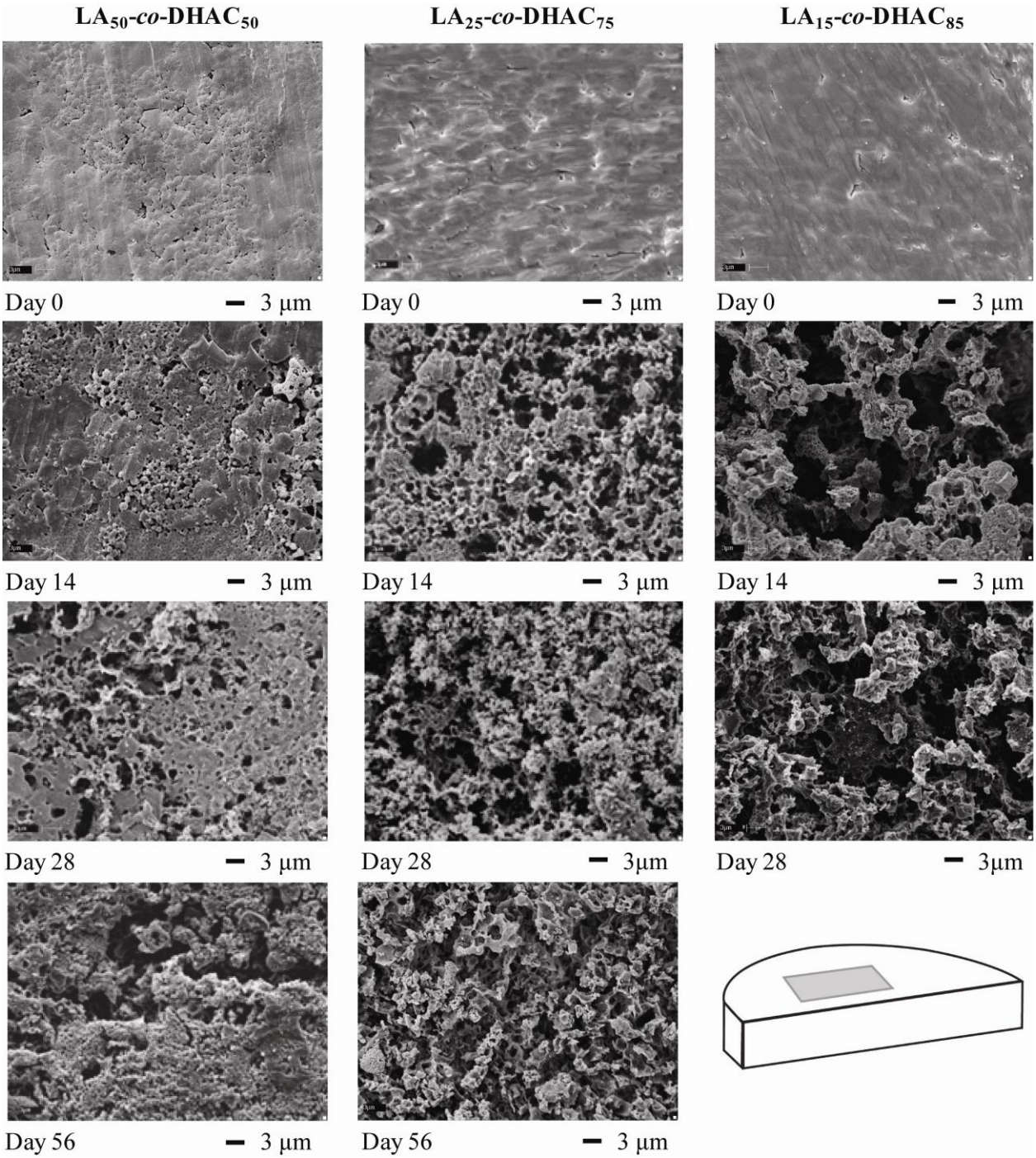

Figure 2.8. SEM of the top surface of pLA_x-*co*-$DHAC_y$ copolymers taken at select time points (magnification = 5000 x). The shaded region of the image in the bottom right depicts the surface that is under magnification. The day 56 image for pLA_{15}-co-$DHAC_{85}$ does not exist due to complete degradation prior to this time point.

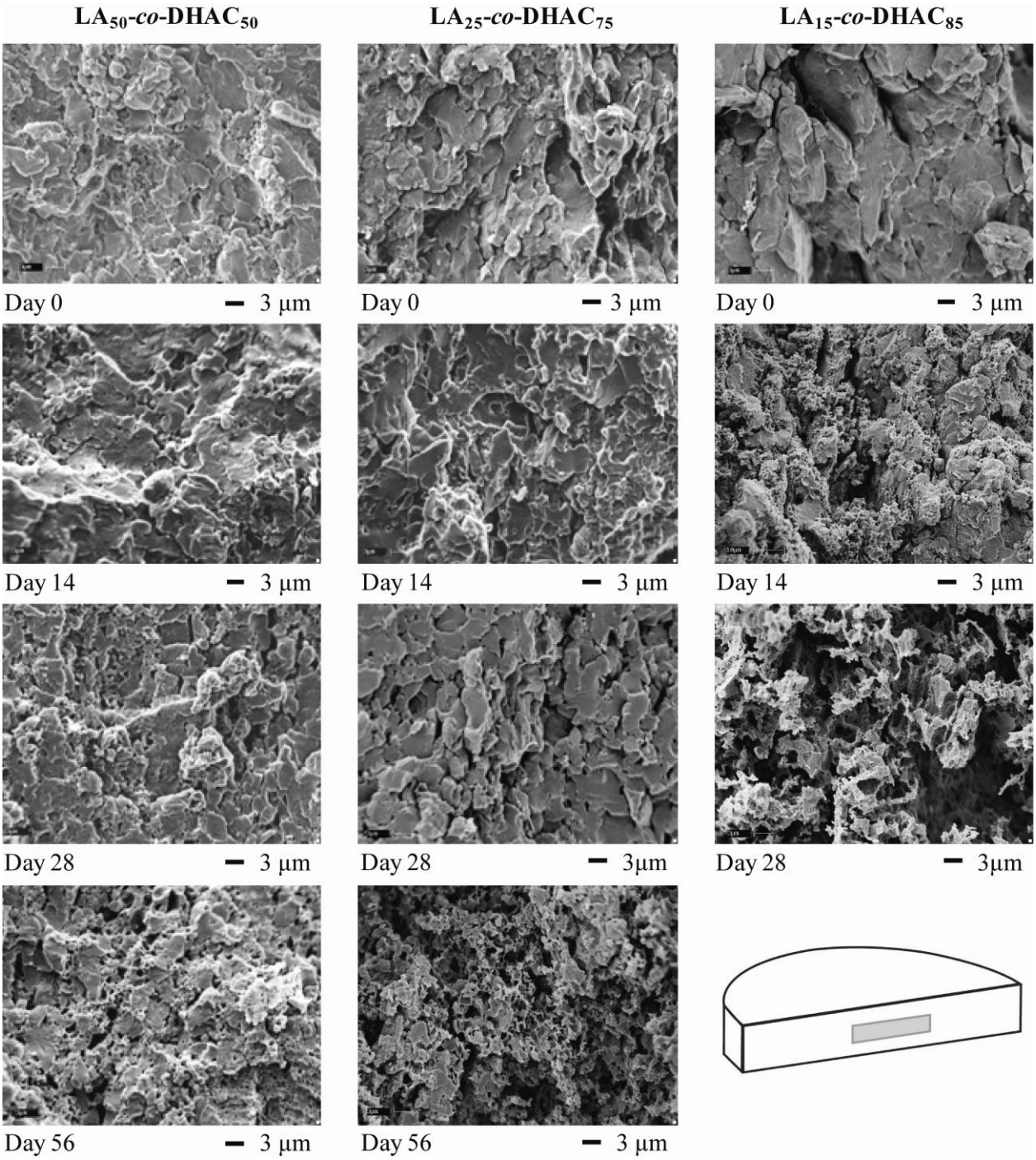

Figure 2.9. SEM of the cross-sectional surface near the interior of LA_x-co-$DHAC_y$ copolymers taken at select time points (magnification = 5000 x). The shaded region of the image in the bottom right depicts the surface that is under magnification. The day 56 image for pLA_{15}-co-$DHAC_{85}$ does not exist due to complete degradation prior to this time point.

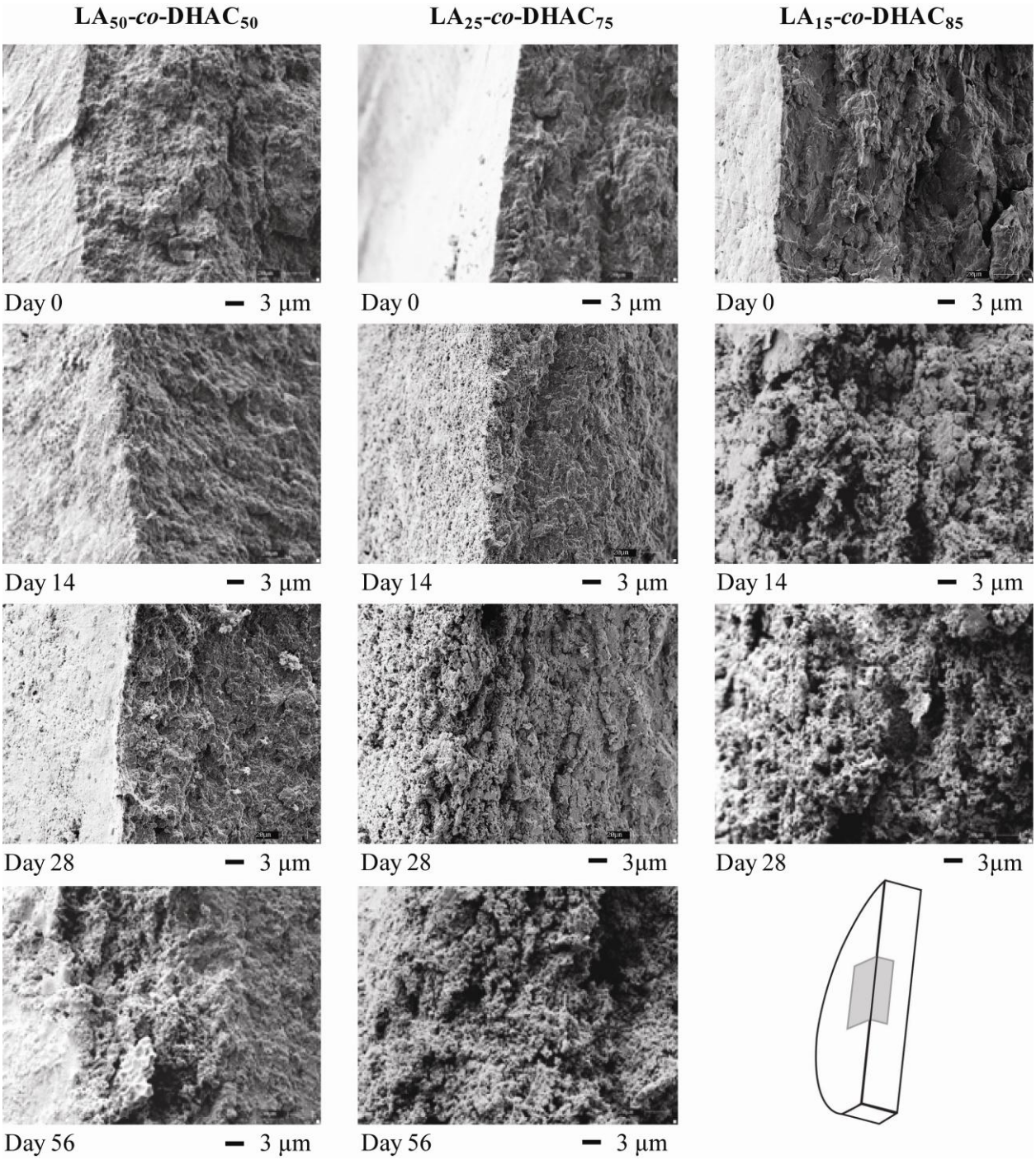

Figure 2.10. SEM of the cross-sectional surface at the edge of pLA_x-co-$DHAC_y$ copolymers taken at select time points (magnification = 1000 x, tilt = 61º). The shaded region of the image in the bottom right depicts the surface that is under magnification. The day 56 image for pLA_{15}-co-$DHAC_{85}$ does not exist due to complete degradation prior to this time point.

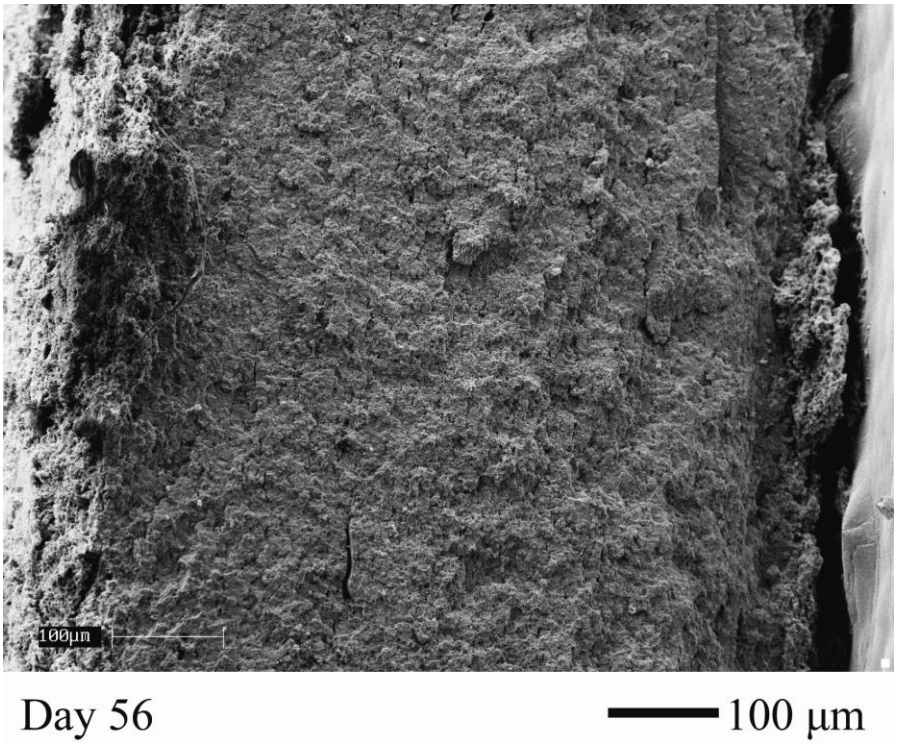

Figure 2.11. SEM of the entire cross-sectional surface of pLA_{50}-*co*-$DHAC_{50}$ copolymer taken at 56 days (magnification = 315 x).

2.4 Conclusion

Random copolymers of cyclic DL-lactide and a 6-membered ring of carbonyl-protected dihydroxyacetone carbonate can be synthesized via a ring-opening polymerization. The chemically protected DHAC subunits of the copolymer were deprotected with a new method using elemental iodine in acetone. By successfully employing this new deprotection scheme, future DHA based polymers can be reliably created in a more favorable environment (i.e less hydrolysis) than previously studied.[21] It was found that by copolymerizing DHAC with a monomer of higher solubility in common solvents, a better degree of deprotection could be achieved. The intrinsic characteristics of each molar ratio of the LA and DHAC copolymers revealed degradation temperatures and glass transition temperatures above physiological temperature. The copolymer also showed unique degradation and erosion characteristics. It was found that even with LA amounts of 50% within the copolymer backbone there appeared to be a more surface like erosion pattern. It was also observed that contrary to previously reported polycarbonate behavior, increasing the amount of polycarbonate content within the copolymer increased the rate of degradation by hydrolysis. These poly(carbonate-ester)s possess very unique and favorable intrinsic characteristics such as the apparent lack of a viscous core formation due to lactic acid build up in the interior of the pellet, or the increased degradation rate with copolymers more rich in carbonate bonds.

CHAPTER 3 – DEVELOPING A NEW METHOD FOR POLY(CARBONATE-ESTER) DEGRADATION ANALYSIS

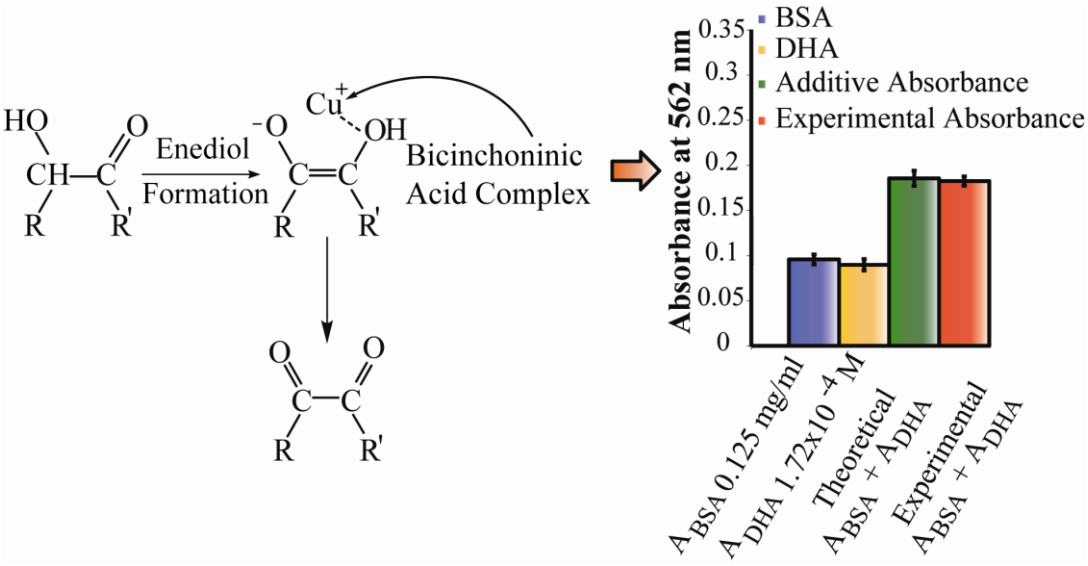

Reprinted from Analytical Biochemistry, 430(2), Jennifer R. Weiser, Nicole G. Ricapito, Alice Yueh, Ellen L. Weiser, David Putnam, A mechanistic analysis of the quantitation of α-hydroxy ketones by the bicinchoninic acid assay, 116-122., Copyright (2012), with permission from Elsevier.

3.1 Introduction

The bicinchoninic acid (BCA) assay, originally developed as a way to quantify the concentration of reducing sugars, is widely used as a powerful tool for protein quantification.[72-76] The BCA assay determines the total concentration of an analyte through the reduction of Cu^{2+} ions under alkaline conditions. This reduction event generates Cu^{1+} which reacts with bicinchoninic acid to form a complex that absorbs light strongly at 562 nm.[31, 32] The absorbance of this complex is then used to quantify an analyte's concentration either using Beer's law ($A=\varepsilon*b*c$) or according to a standard curve.

However, while the BCA assay is robust, a number of compounds interfere with it.[77-81] In the past few decades, a considerable number of compounds have been identified that can complicate the quantitation of specific analytes. The instructions of the most common BCA protein assay kit, produced by a number of manufacturers, acknowledge the potential of false readings from a number of compounds that can interfere with the assay. These include, but are not limited to, mercaptoethanol, phospholipids, hydrogen peroxide and sulfo-N-hydroxysuccinimide, all of which give erroneously high absorption readings.[77-81] Other compounds, such as ammonium sulfate and 2-D-pharmalyte, reduce the amount of color the BCA assay can produce, thereby leading to erroneously low absorption readings.[77] More recently the assay was used to determine sulfhydryl, N-hydroxysuccinimido carboxylate, aldehyde, and hydrazide functional groups on a variety of solid supports.[82]

Recently, we found that compounds from a previously unreported structure class, specifically the α-hydroxy ketone structure, influence the accuracy of the BCA assay to give erroneously high absorbance readings. The α-hydroxy ketone class of compounds is susceptible to autoxidation, and can enolize via an enediol intermediate during tautomerization.[83, 84] These α-

hydroxy ketone compounds also can undergo tauromerization in the same manner as reducing sugars.[84, 85] Under alkaline conditions, such as those found in the BCA assay (pH 11.25), reducing sugars isomerize to an equilibrium mixture of aldoses and ketoses via the same enediol intermediate.[86, 87] However, the α-hydroxy ketone class of compounds is far more effective at reducing the copper than reducing sugars, which causes a very strong absorbance reading in the BCA assay. We therefore hypothesized that the ability of α-hydroxy ketones, and by extension reducing sugars, to form an enediol intermediate is the mechanism through which these compounds are amenable to quantitation by the BCA assay. The ability of these chemicals to reduce Cu^{+2} and affect the BCA assay provides a very useful tool in quantifying these compounds. It is also important to note that if an α-hydroxy ketone is present in a sample, it may interfere with the accuracy of the results when conducting the BCA assay on solutions that contain other analytes, such as proteins. However, the ability of these chemicals to reduce Cu^{+2} and affect the BCA assay provides a very useful tool in quantifying α-hydroxy ketone compounds. By harnessing the BCA assay, there is now a tool able to track the degrading polymer backbone of dihydroxyacetone based polymers that are otherwise unable to be characterized using more common methods, such as GPC.

3.2 Experimental

3.2.1 Materials

1,3-Dihydroxyacetone dimer, dihydroxyacetone phosphate hemimagnesium salt hydrate, dextrose, fructose, DL-glyceraldehyde dimer, *p*-toluene sulfonic acid, bovine serum albumin (BSA), Bradford reagent, ninhydrin reagent and 2,2-dihydroxyindane-1,3-dione were purchased from Sigma-Aldrich (St. Louis, MO) and used as received. Acetoin, acetone, ethyl alcohol, ethyl

acetate, glycerol, triethyl orthoformate, sodium carbonate (Na_2CO_3), 0.1N silver nitrate, 28% w/w aqueous solution of ammonia, and 0.1N NaOH were purchased from VWR (West Chester, PA) and used as received. 1,5-Dihydroxypentan-3-one was purchased from Santa Cruz Biotechnology®, Inc. (Santa Cruz, CA) and used as received. Phosphate buffered saline (10.0 M, PBS) without calcium or magnesium was purchased from BioWhittaker® (Lancaster, MA) and diluted to 1.0 M with 18 Ω water. Corning® Costar® brand, clear, 96-well cell culture plates were purchased from Fisher (catalog number 3599). BCA Protein Assay kit (product number 23225) was purchased from Thermo Fisher Scientific, Inc.

3.2.2 Synthesis of (2,5-diethoxy-1,4-dioxane-2,5-dimethanol)

The protected 1,3-dihydroxyacetone (DHA) dimer was synthesized using a previously reported method.[25] A 500 mg round bottom flask was charged with dihydroxyacetone dimer (32 g, 177.8 mmol), triethyl orthoformate (60 mL, 360 mmol), and *p*-toluenesulfonic acid (128 mg) in 300 mL of ethyl alcohol. The mixture was stirred for 24 h, after which time 400 mg of Na_2CO_3 was added. The reaction mixture was stirred for an additional 30 min before filtration. The solvent and residual triethyl orthoformate were removed *in vacuo* and the product recrystallized from ethyl acetate to yield the title compound (31 g, 74%). ^{1}H NMR ($CDCl_3$) δ: 1.23-1.26 (6H), 3.53-3.95 (12H). Anal. Calcd: C, 50.85; H, 8.47. Found: C, 51.14; H, 8.70.

3.2.3 BCA assay

Various concentrations, ranging from 1.11×10^{-2} M to 1.72×10^{-4} M, were selected for each compound. All serial dilutions were done with 1X PBS buffer. The assay was run under standard conditions according to the manufacturer's directions, 50:1 bicinchoninic acid and tartrate in an

alkaline carbonate buffer (reagent A) to 4% copper sulfate pentahydrate solution (reagent B), and the relative intensity of the reading determined at 562 nm on a SpectraMAX Plus384 Microplate Reader (Molecular Devices Corporation) after an hour incubation at 37 °C.

3.2.4 Copper(II) ion ratios in the BCA assay working reagent

A standard curve for DHA with concentrations ranging from $4.44x10^{-2}$ M to $6.94x10^{-4}$ M was created in triplicate. All serial dilutions were done with 1X PBS buffer. The BCA assay solution was then prepared six times varying the copper concentration by changing the conditions of reagent B while holding the volume of reagent A fixed. The DHA samples were allowed to incubate for one hour at 37 °C with the various BCA working reagent conditions before the absorbance was read. Due to the saturation of the signal, each sample was diluted 10X post incubation, or in the case of the $4.4x10^{-2}$ M, 20X, and the relative percent absorbance as compared to the largest signal of $4.44x10^{-2}$ M DHA in a 50:3 working reagent ratio was determined.

3.2.5 Protein sample interference

A standard curve for BSA with six concentrations ranging from 0.5 mg/ml to $1.56x10^{-2}$ mg/ml and a standard curve for DHA with four concentrations ranging from 0.125 mg/ml to $1.56x10^{-2}$ mg/ml ($1.38x10^{-3}$ M to $1.72x10^{-4}$ M) were created in triplicate. All serial dilutions were made with 1X PBS buffer. To each interference trial, the BSA concentration was varied while a constant amount of DHA was added to each sample. This was repeated four times so that each concentration of DHA was added to the entire range of BSA concentrations. The mixed BSA and DHA samples were the run in the BCA assay in triplicate using the same conditions listed previously.

3.2.6 Bradford assay

A serial dilution for DHA with concentrations ranging from $1.11x10^{-2}$ M to $1.72x10^{-4}$ M was created in triplicate using 1X PBS buffer. The assay was run under the standard conditions as recommended by the supplier's instructions.

3.2.7 Ammoniacal silver nitrate (Tollen's reagent)

In a 20 mL glass vial was charged 150 mg of the α-hydroxy ketone based analyte in 1 mL 18 Ω water. To this was added 7.5 mL of 0.1N silver nitrate and 15 mL of 28% w/w solution of aqueous ammonia hydroxide. The vial was then rotated by hand continuously for approximately five minutes at room temperature until a silver mirror or finely divided black precipitate formed.

3.2.8 Ninhydrin protein assay

As per the assay guidelines from Sigma-Aldrich, a 50 μM solution of sample (DHA or glycine) was prepared in 0.05% glacial acetic acid. A 2 mL aliquot was added to a glass test tube to which 1 mL of ninhydrin reagent (2% solution of ninhydrin and hydrindantin in dimethyl sulfoxide and lithium acetate buffer, pH 5.2) was added. The test tubes were then allowed to sit in boiling water for 10 minutes before cooling to room temperature and the subsequent addition of 5 mL of 95% ethanol. Then 200 μl of each solution was then put in a 96 well plate and the absorbance determined at 570 nm.

3.2.9 Ninhydrin enediol test

In a 20 mL vial was charged equimolar amounts (1.0 mol) of 2,2-dihydroxyindane-1,3-dione (ninhydrin) and the α-hydroxy ketone compound DHA or DL-glyceraldehyde. To this was

added 10 mL of either 1X PBS, 18 Ω water, 0.1N NaOH or reagent A from the BCA assay kit. A 1mL aliquot was taken from each mixture and placed in a separate tube. To this was added 20 μL of reagent B and the solution thoroughly mixed at room temperature for 30 seconds. The tubes were then centrifuged for 1 minute at 3000 rpm to collect any precipitate. The precipitate was then recrystallized in acetone and dried in vacuo. ^{1}H NMR (DMSO-d_6) δ: 6.48 (s; 2H, OH), and 7.97 (s; 8H, aromatic H)

3.3 Results and Discussion

3.3.1 The role of structural arrangement of the analyte in the BCA assay

To highlight the impact α-hydroxy ketones have on the BCA assay, a variety of compounds either containing the α-hydroxy ketone arrangement, or lacking this arrangement, were subjected to the BCA assay. Using a consistent molar basis for the study and a number of compounds with similar structures, the percent reactivity, relative to DHA, were determined (Figure 3.1). Figure 3.1 shows that 1,3-dihydroxypropan-2-one, more commonly referred to as dihydroxyacetone (DHA), has the strongest response to the assay and was designated at 100%. DHA, which exists in equilibrium with its dimeric form in solution, has an extremely sensitive response to the BCA assay reagents. It produces a 30 times more sensitive response than glucose, a reducing sugar. DHA is also known to tautormerize readily to glyceraldehyde under alkaline conditions, which are the conditions present in the BCA assay (pH 11.25).[88-91] To support the hypothesis that the BCA assay is affected positively by the enol-diol tautomer formed by α-hydroxy ketones, and to put forward that this intermediate may be co-ordinating metal ions, structural analogs of DHA were investigated at equivalent concentrations.

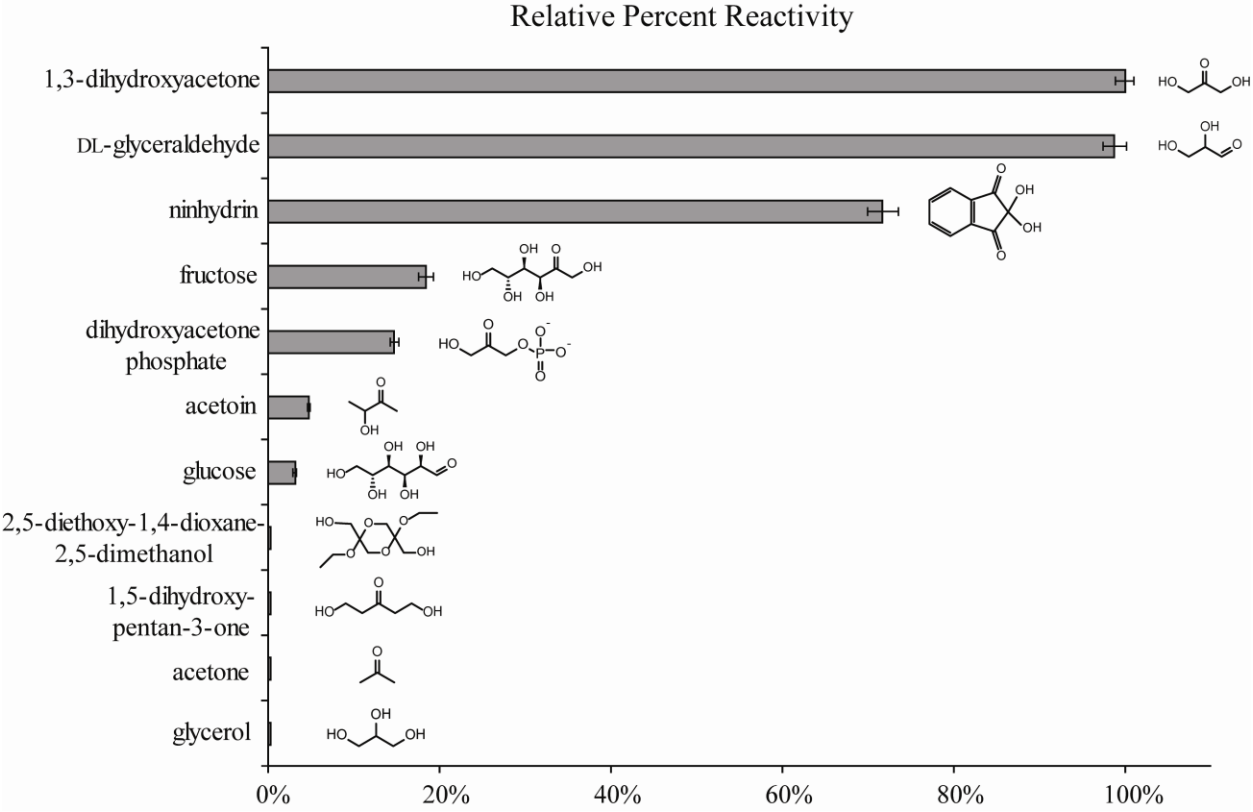

Figure 3.1. Percent reactivity of assayed compounds relative to 1,3-dihydroxyacetone dimer in the BCA assay on a molar basis of 2.75×10^{-3} M showing the strong response α-hydroxy ketones have within the assay.

The first derivative explored was a locked form of the DHA dimer, 2,5-diethoxy-1,4-dioxane-2,5-dimethanol, to determine whether the monomeric DHA or the dimeric form led to the signal in the BCA assay. This compound showed no response in the BCA assay, maintaining the posit that it is the monomeric DHA's ability to form the enediol tautomer that causes a response to the assay. To explore the significance of the α-hydroxy ketone structure, another variation of DHA, 1,5-dihydroxy-pentan-3-one, was tested. While it contains both hydroxyl groups and a ketone group, this structure has a β-hydroxy ketone arrangement. This compound showed no response to the assay and suggests that the proximity of the hydroxyl groups to the carbonyl is a structural necessity to reduce the Cu^{2+}.

To further show the significance of the α-hydroxy ketone structural arrangement, the simplest variation on DHA's structure, the common solvent acetone, was evaluated. Acetone lacks the hydroxyl groups, but does have the ketone group at the C2 position. Acetone showed no response to the assay under the same conditions as the previous compounds, again highlighting the importance of the proximity of a hydroxyl group. A final example that showed the relevance of the α-hydroxy ketone structure and the importance of its ability to enolize, is glycerol. Glycerol, a trihydric alcohol, does not possess a carbonyl and thus gave no response to the BCA assay. These data exemplify that it is not just the proximity of the two alcohol groups formed during enolization that may co-ordinate the copper, but that the movement of electrons during tautomerization causes a change in the metal ion's energy state.

Another variation of DHA that also exemplifies the structural arrangement of the hydroxyl groups to a keto group is acetoin. As expected, this simple compound with an α-hydroxy keto structure, does give a positive response in the BCA assay. This response, while weaker than that of DHA, is strong in comparison to that of non-ketone α-hydroxy reducing

sugars. A final derivative of DHA tested, dihydroxyacetone phosphate, showed about a 6-7 fold decrease in sensitivity to the assay compared to DHA, but still gave a remarkably strong signal. This weaker response may be attributed to the phosphate group's hindrance to the enediol tautomer formation.

One other unique α-hydroxy ketone that also was tested in the BCA assay and gave a characteristic response was fructose. Fructose, a reducing sugar, contains the α-hydroxy ketone backbone arrangement, unlike the majority of other common reducing sugars. Fructose is known to be one of the most sensitive of the reducing sugars in the BCA assay and this increased sensitivity was seen when compared with glucose in Figure 3.1.[73, 74, 92] The increased sensitivity to the assay may be correlated to the manner in which the enediol intermediate is formed. Like other α-hydroxy ketones, fructose has the ability to form a diketone intermediate with the C2 and C3 carbon as well as a ketoaldehyde intermediate between the C1 and C2 carbons, while other reducing sugars, such as glucose and galactose, form only the ketoaldehyde intermediate. [87, 93, 94] This diketone intermediate may attribute to why fructose gives a much stronger response than the other sugars in the BCA assay.

3.3.2 Copper(II) ion ratios in the working reagent of the BCA assay

As per the Thermo Fisher Scientific, Inc., Pierce® BCA Protein Assay Kit suggestions, copper concentrations in the working reagent are varied to study the affect of copper chelation versus copper reduction. As seen in Figure 3.2, there is a linear correlation in relative percent absorbance as the DHA and copper(II) ion were varied. This correlation indicates that the mechanism by which α-hydroxy ketones influence the assay is not by a copper chelating affect, but a reduction of the Cu^{2+} to Cu^{1+}.[80] In the standard working reagent ratio, 50:1 (reagent A:B), the DHA response is limited by the amount of copper present for the two highest DHA

concentrations reported ($4.44x10^{-2}$ M and $2.22x10^{-2}$ M). This trend is more pronounced as the amount of reagent B (the copper) in the working ratio is decreased and it is apparent that this is the limiting reagent for the majority of the DHA concentrations as evidenced by the signal plateau. Conversely, as the copper ratio in the working reagent increases, (an increase in reagent B), the DHA becomes the limiting reagent in the BCA assay, which leads to the signal plateau in the more concentrated DHA samples. This relationship is best represented by observing that higher concentrations of DHA still give a stronger relative percent absorbance than the DHA concentration that has a signal plateau. This direct proportionality supports the purported mechanism of direct cupric ion reduction by this class of analytes.

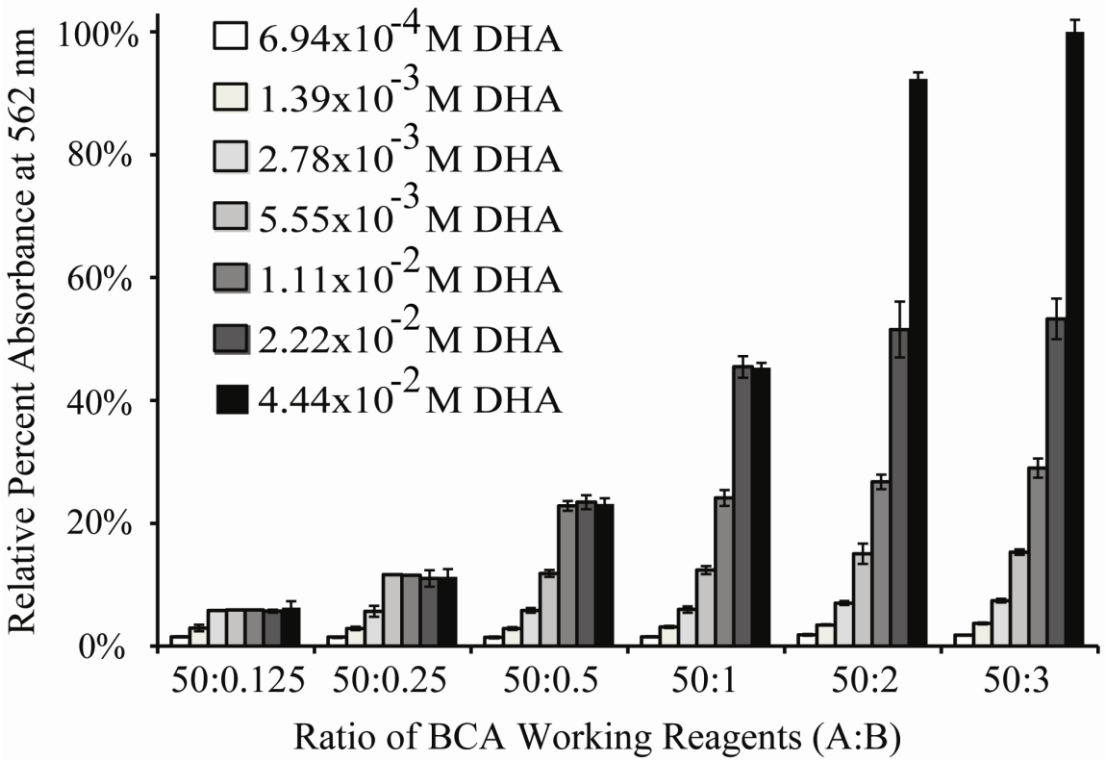

Figure 3.2. Relative percent absorbance readings for various concentrations of DHA ($4.44x10^{-2}$ M to $6.94x10^{-4}$ M) and amounts of copper (reagent B) in the BCA assay working reagent as compared to $4.44x10^{-2}$ M DHA in a 50:3 working reagent ratio. Standard working reagent conditions are 50:1 (reagent A to reagent B).

3.3.3 Analyte interference of protein quantitation in the BCA assay

To exemplify how an α-hydroxy ketone may interfere with protein quantitation, an array of DHA samples were added to standard curves created using the model protein, bovine serum albumin (BSA). The results of this experiment are shown in Figure 3.3. Over the entire range of concentrations, a direct relationship exists between the absorbance value obtained and the amount of α-hydroxy ketone added to the protein sample. Seen in Figure 3.4, the effect on the final absorbance values by adding DHA to BSA is consistent and additive. Calculating the

theoretical absorbance value by adding a BSA absorbance at a set concentration with a DHA absorbance at a set concentration yield values that are comparable to the experimental value obtained when combining these compounds prior to running the BCA assay. These results show the interference various concentrations of an α-hydroxy ketone can have on a protein sample. However, due to the additive nature of this effect, if the concentration of α-hydroxy ketone is known, then the concentration of the protein is quantifiable using the BCA assay.

3.3.4 The response of α-hydroxy ketones to the Bradford assay

To further support the unique quantification of α-hydroxy ketones in the BCA assay, other standard protein assays were investigated. The Bradford assay, based on the Coomassie Brilliant Blue G-250, run under acidic conditions, follows the conversion of a red form of the dye to a blue form at 595 nm.[95] This assay showed no colorimetric response to our model α-hydroxy ketone, DHA.

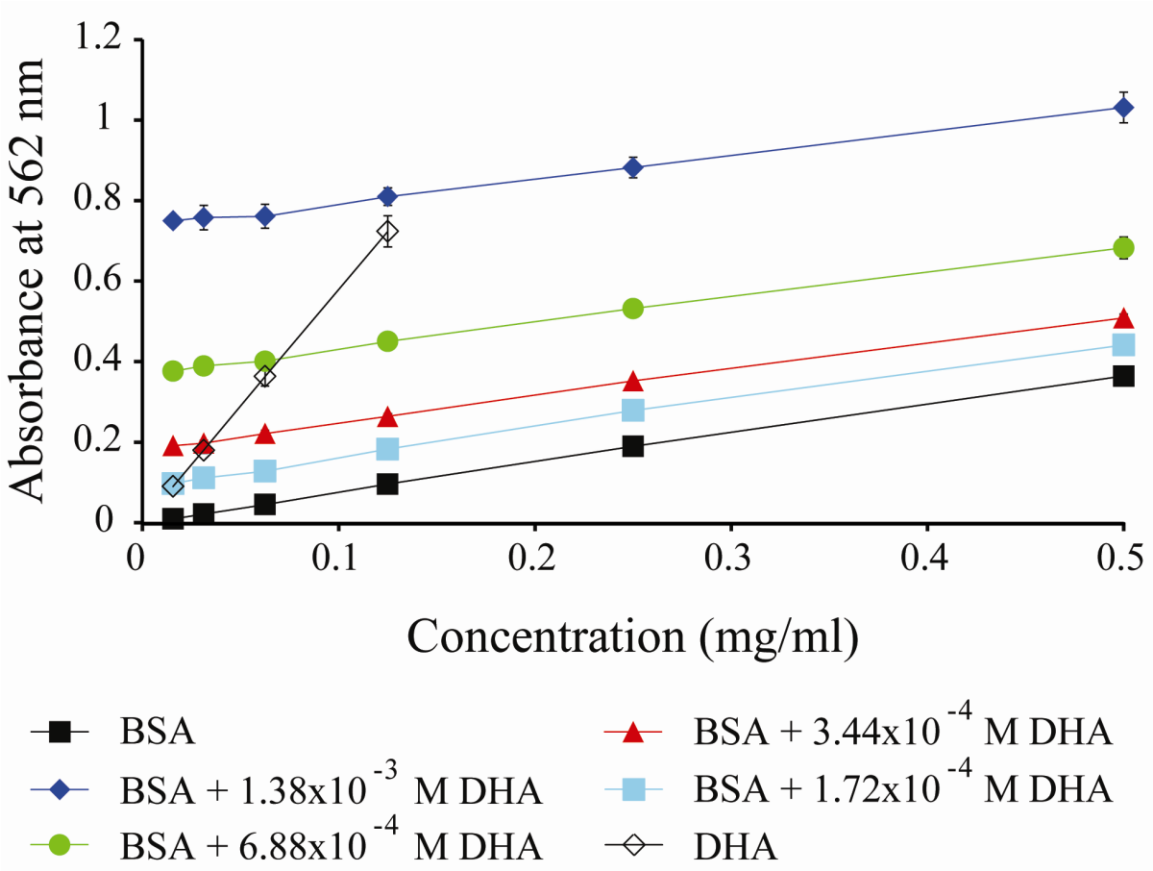

Figure 3.3. Absorbance readings for various concentrations BSA and DHA in the BCA protein assay. These values show the magnitude of interference an α-hydroxy ketone contaminate has on protein samples.

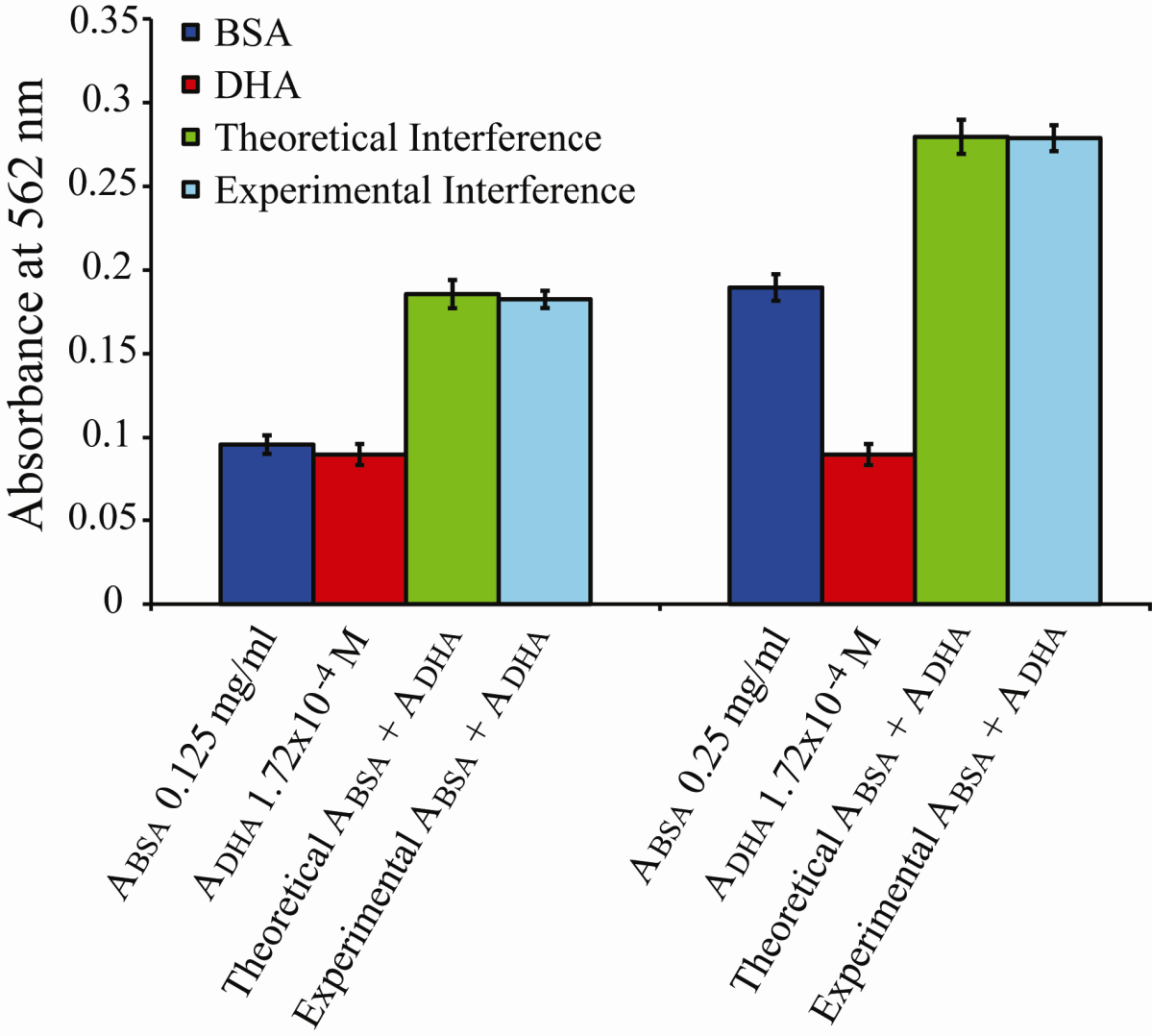

Figure 3.4. The colorimetric response at 562 nm in the BCA assay between BSA absorbance (A_{BSA} = 0.125 mg/ml or 0.25 mg/ml) added to DHA absorbance (A_{DHA} = 1.72x10^{-3} M), yielding a theoretical additive absorbance in comparison to the experimental absorbance obtained. The correlation between the theoretical and the experiment values show the consistent and additive affect to the absorbance reading an α-hydroxy ketone sample has when mixed with a protein sample.

3.3.5 The response of α-hydroxy ketones to Tollen's reagent

To confirm α-hydroxy ketone's ability to form enediol intermediates under BCA assay conditions, the ammoniacal silver nitrate reaction (Tollen's reagent) was performed. Tollen's reagent is typically used to differentiate between aldehydes and ketones, but in the case of α-hydroxy ketones, a positive response is also observed. The Tollen's reagent is run in similar conditions to the BCA assay, where the pH is basic (approximately 10) and the final response is a reduction of Ag^{1+} (aq) to Ag^{0} (s). Both DHA and glyceraldehyde formed the classic silver mirror coating on glass indicative of a positive result for the formation of an enediol intermediate (Figure 3.5). In the case of dihydroxyacetone phosphate (DHAP), a finely divided black precipitate was formed. The mechanism of action through which Tollen's reagent interacts with α-hydroxy ketones involves the formation of an enediol intermediate, which leads to silver reduction. These responses further support the implication of the enediol formation in the BCA assay.[96]

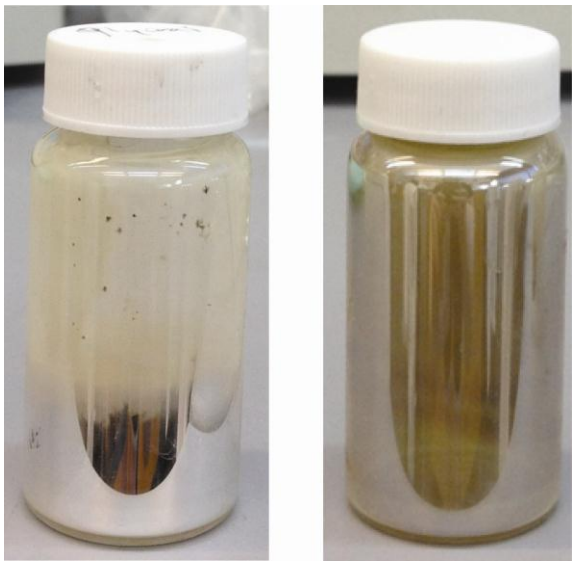

Glyceraldehyde Dihydroxyacetone

Figure 3.5. Result of the Tollen's reagent silver mirror test on glyceraldehyde and DHA.

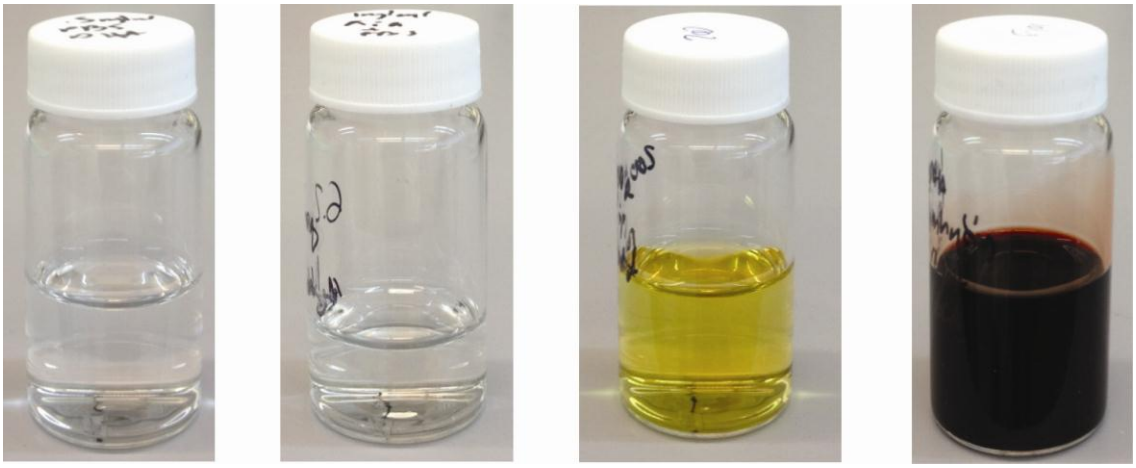

A B C D

Figure 3.6. Result of adding ninhydrin to DHA and reagent A of the BCA assay. (A) DHA in deionized water. (B) Ninhydrin in deionized water. (C) Ninhydrin in Reagent A (main component is 0.1 N NaOH). (D) Equimolar amounts of DHA and ninhydrin in Reagent A.

3.3.6 The response of α-hydroxy ketones to ninhydrin

To experimentally confirm the purported mechanism through which α-hydroxy ketones interact with the BCA assay, ninhydrin was utilized. The classic ninhydrin test for proteins did not show the formation of Rhuemann's purple for α-hydroxy ketones, a response typically observed when working with compounds containing ammonia and/or primary and secondary amines. A glycine control developed an expected strong color that was sensitive at 570 nm, however DHA solutions made with 0.05% glacial acetic acid or a DHA solution of 1.11×10^{-2} M in 1X PBS buffer turned light red upon heating(Figure 3.6). This result is significant because the red color is associated with ninhydrin being reduced to a monovalent anion, indanone-enediol structure. As the reduction of ninhydrin proceeds, a crystalline precipitate of hydrindantin forms.[96-99] This response is more strongly observed in dilute basic conditions, when solid

ninhydrin is combined with a compound that can form an enediol. Under these conditions, the ninhydrin is reduced while the other compound is oxidized via its enediol pathway. This precipitate was observed when equimolar amounts of DHA and ninhydrin were combined in only reagent A of the BCA assay or in 0.1N NaOH, the major component of reagent A, after a 24 hour time period. A ^{1}H NMR taken of the precipitate, Figure 3.7, correlates with known ^{1}H NMR spectra of hydrindantin.[100] No precipitate formed and there was no color change when the ninhydrin and DHA were placed in water or PBS over the course of 48 hours. Also of note is that, while aldehydes do react in the BCA assay as previously explored by Tyllianakis, et al., they do not react with ninhydrin in the same manner as α-hydroxy ketones.[82] The addition of propionaldehyde to ninhydrin in either reagent A or 0.1N NaOH saw no color shift to red or formation of a precipitate. From these observations we conclude that the mechanism through which aldehydes produce a colormetric response to the BCA assay is not the same mechanism through which α-hydroxy ketones elicit a colorimetric response.

The hydrindantin precipitate was observed to form much more rapidly when all of the BCA assay conditions were present. It was seen that ninhydrin alone in reagent A or in 0.1N NaOH was a yellow color, while DHA alone in either solvent was colorless. (Figure 3.6) However, when both ninhydrin and DHA were dissolved in either reagent A or 0.1N NaOH, the solution turned a deep red color. The red color was attributed to the oxidation of the α-hydroxy ketone's enediol intermediate in the basic conditions, while the ninhydrin was reduced. When the solutions are allowed to sit at room temperature for 24 hours, a precipitate of hydrindantin formed, a result that is in agreement with previous work using ascorbic acid and ninhydrin. [97-99]

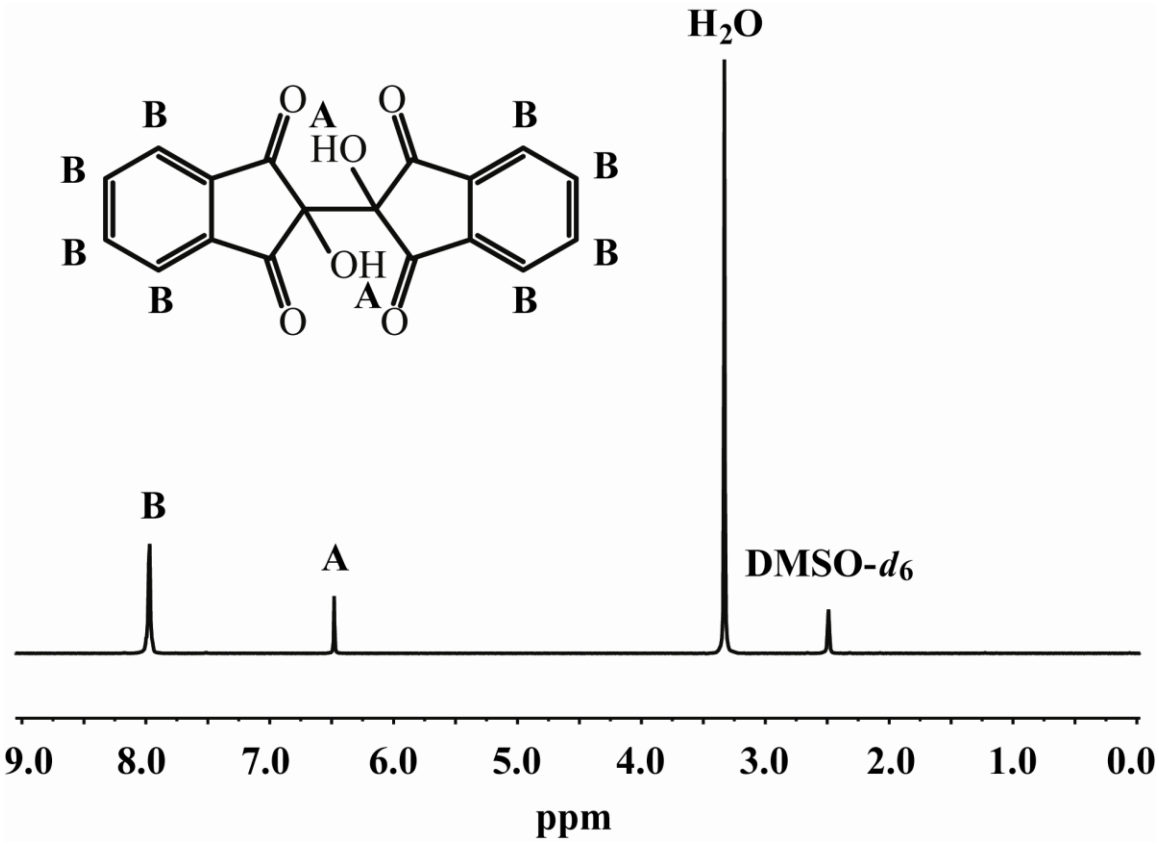

Figure 3.7. ^{1}H NMR spectrum of the hydrindantin precipitate in DMSO-d_6.

Upon addition of reagent B (the copper) to the solution of DHA and ninhydrin in reagent A, the deep red color shifted to a deep purple color along with the rapid formation of a precipitate. This purple color is likely in response to the Cu^{2+} reducing to Cu^{1+}, which then complexes with the bicinchoninic acid. The precipitate formed in the presence of both the ninhydrin and another α-hydroxy ketone is that of hydrindantin.[97, 98]. Conversely, adding reagent B to the deep red colored solution of DHA and ninhydrin in 0.1N NaOH, there was an immediate change of color to pale blue along with the precipitate. This response is a better way to visualize how the BCA assay is sensitive to enediol formation. The loss of the red color as the copper ion is added is likely a result of the indanone-enediol reoxidation as the copper is reduced. The subsequent addition of bicinchoninic acid to this solution via the addition of reagent A, yields the usual BCA assay color response as seen with an immediate shift in color to deep purple. These experiments were conducted in parallel with DL-glyceraldehyde as the model α-hydroxy ketone, and the results were the same as DHA. These responses confirm the proposed mechanism where the DHA and other α-hydroxy ketones need to form the enediol to proceed with the positive response in the BCA assay.

Further support for the enediol mechanism is that ninhydrin itself has an α-hydroxy ketone structure. When the solid form of ninhydrin is added to the BCA assay under the same conditions as the previously tested compounds, the assay gives a very strong purple colorimetric response similar to all the other α-hydroxy ketone compounds tested. No precipitate formed, a response only seen with the presence of another enediol in the solution. However, upon addition of the BCA assay working reagent, the color of the solution turned red before the deep purple color typical of the BCA assay began to develop. The initial appearance of the red color is indicative of ninhydrin forming an indanone-enediol and reinforces the proposed enediol

intermediate mechanism for the behavior of α-hydroxy ketones in the BCA assay.[97, 98]

3.3.7 Proposed mechanism of analyte interaction in the BCA assay

The proposed mechanism of how α-hydroxy ketones react in the BCA assay, shown in Scheme 3.1, is hypothesized given our results. We based this scheme on previously reported work by others using a copper oxidation system and have extended this correlation through our experiments to include the BCA assay system. Studies conducted by Marshall and Waters, Thornalley, and Singh focused on the creation of an enediol intermediate which directly correlated to a redox event involving metal ions, such as copper.[83-85, 101, 102] In some of the earliest studies, Marshall and Waters noticed that the enolization of α-hydroxy ketones occurred naturally to form enediol intermediates. These studies also found that when copper ions were present, they were reduced and formed complexes with the enediol radicals.

Other work by Thornalley explored the autoxidation of the α-hydroxy ketone, DL-glyceraldehyde under physiological conditions. To understand the mechanism of this oxidation event, an important iron porphyrin protein, cytochrome c, was monitored as it was reduced from the ferric state (+3) to the ferrous state (+2).[103] It was seen that a direct correlation existed between the DL-glyceraldehyde's uptake of iodine and the temperature dependence of the rate of ferricytochrome c reduction by DL-glyceraldehyde.[84] This uptake of iodine by α-hydroxy ketones is a typical response in the formation of the enediol tautomer, thus helping to link the reduction of the iron ion with the enediol intermediate.[104] In further studies, the formation of the α-ketoaldehyde enediol intermediate for glyceraldehyde and dihydroxyacetone, hydroxypyruvaldehyde, was monitored and shown to be directly related to the autoxidation event.[83] Also of note is the chemical synthesis of hydroxypyruvaldehyde used for components of Thornalley's study. The synthesis of this α-ketoaldehyde occurred via a modified version of a

scheme previously derived by oxidizing dihydroxyacetone in the presence of cupric acetate.[105]

Thornalley's work also made two other important correlations. The first was at high pH there is evidence for deprotonation of the enediol intermediate, which aligns with the conditions present in the BCA assay. The second was that enediol anion and enediol oxy radicals that form become metal ion coordinated, another finding in agreement with the hypothesized mechanism shown in Scheme 3.1.

Another study that supports the hypothesized mechanism of how α-hydroxy ketones enolize was conducted by Singh.[85] This group observed that the rate of autocatalysis of enolization increases at higher temperatures, which are the conditions found in the standard BCA assay. These studies provide mechanistic insight as to how reducing sugars and α-hydroxy ketones are quantified by the BCA assay.

Extensive work done by Richard, again supports the hypothesized mechanism purported for the conditions found in the BCA assay. Early work by Richard examined the enediol intermediate mechanism in which glyceraldehyde phosphate converts to dihydroxyacetone phosphate (DHAP).[106] Further studies working with DHAP and DHA also show the formation of this enediol intermediate when working in a variety of conditions such as higher pH or in the presence of metal cations.[107-109]

The final confirmation for this enediol intermediate is the response seen in the presence of ninhydrin. The observation of the red color due to the presence of an indanone-enediol and the subsequent precipitation of hydrindantin when other enediol forming α-hydroxy ketone compounds are present, enables a correlation to be made to the proposed mechanism. In keeping with the results seen by Marshall and Waters, Thornalley, Singh, and Richard, enediol formation is an important intermediate in the oxidation activity of α-hydroxy ketones in the BCA assay.

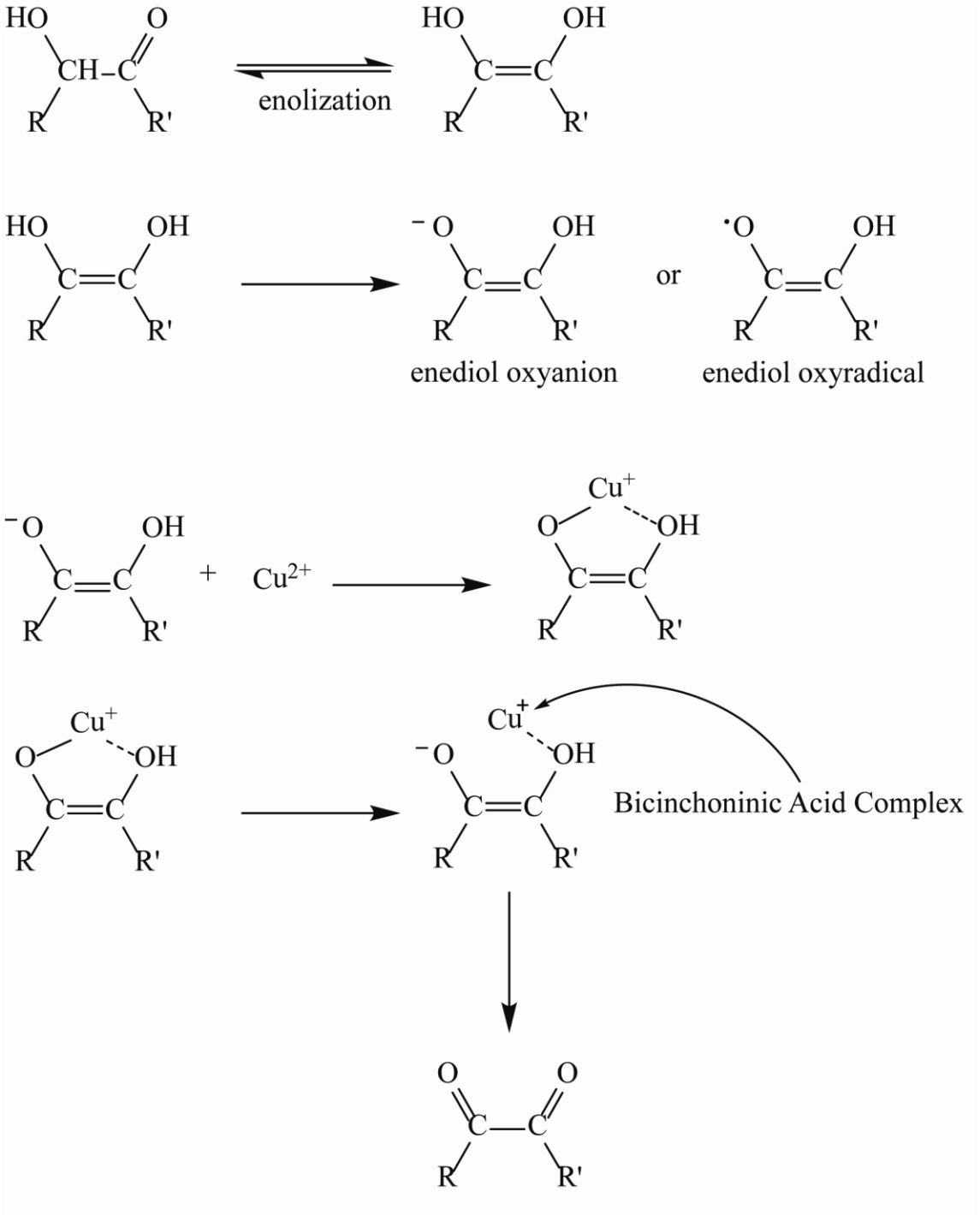

Scheme 3.1. Proposed mechanism for an enediol intermediate from α-hydroxy ketones responsible for the oxidation of copper in the BCA assay. Adapted from work by Marshall and Waters, Singh, and Thornalley. [83-85, 101, 102]

3.4 Conclusion

The BCA assay is a tool commonly used for the quantification of proteins. However, new explorations into the fundamentals of the assay show that it is a useful tool for quantifying α-hydroxy ketones. We propose that the ability of these compounds to reduce the copper present in the BCA assay is derived in the similar manner in which reducing sugars behave in the assay. Both these classes of compounds can undergo enolization, creating an enediol intermediate. This process may lead to a co-ordination event that reduces the copper ions, thereby allowing the bicinchoninic acid to chelate to the Cu^{1+} and produce a significant and measurable colorimetric response. It must also be taken into consideration that if working with solutions where α-hydroxy ketones may be present, elevated readings may result that could interfere with final concentration determinations.

CHAPTER 4 – CONTROLLED PROTEIN RELEASE FROM DIHYDROXYACETONE BASED POLY(CARBONATE-ESTER)S

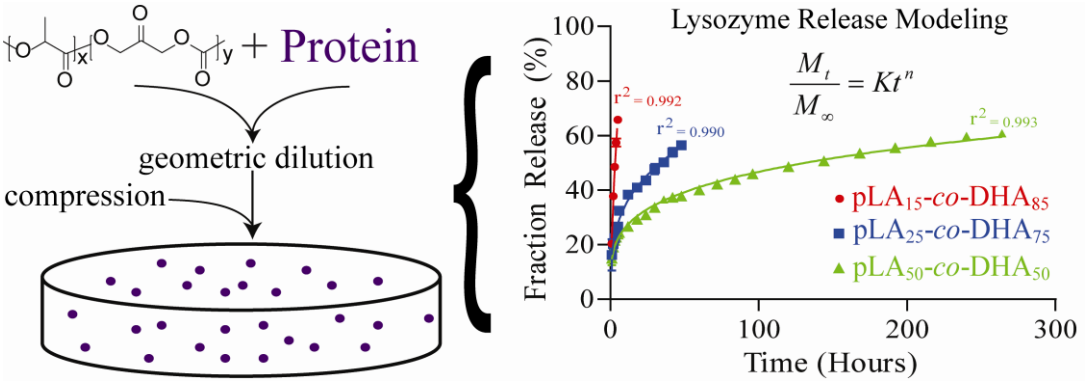

4.1 Introduction

The ability to control the release of therapeutics using polymer matrices is an important factor when designing new drug delivery systems.[10, 56, 110-112]The optimization of polymeric and copolymeric based biomaterials is important to successfully create a system that allow for a long-term, controlled release of therapeutics integrated into a polymer matrix.[113, 114] The delivery criterion of the therapeutic, specifically those that are protein based, will ultimately dictate the manner in which the polymeric material's characteristics are manipulated to influence its intended target. The criteria for release from biodegradable polymers include: high polymer purity and reproducibility, the mechanism by which the polymeric material degrades (i.e. hydrolytic vs. enzymatic), a well-defined release rate of degradation products that are non-toxic, and a predictable drug-release profile.[34, 57, 110, 113, 115] To ensure reliable, long term release of a protein, as well as to maintain its biological activity, biodegradable polymer matrices have been developed to facilitate a controlled diffusion of the active agent.[10, 113, 116, 117]

Early work on polymer matrices for controlled drug delivery focused on poly(α-ester) systems, specifically poly(α-hydroxy acid)s, such as those based on lactic acid and glycolic acid.[10, 110, 115] Originally, these polymer systems were designed to deliver low molecular weight compounds through the hydrolytic degradation of the polymer matrix.[10, 113] Slow diffusion of the compounds and non zero-order release kinetics due to the bulk degradation of the polymers make this type of polymer system poorly suited for the release of more fragile compounds, such as proteins.[10, 56, 110, 116] Additionally, the hydrolytic degradation of the polymer occurs via the random scission of the ester backbone which leads to bulk erosion and produces degradation products that ultimately affect the stability of the encapsulated drug or protein.[56, 57, 110, 116, 118, 119] For example, polyesters based on lactic acid can produce very low pH environments due to the

build up of the acidic end groups of the monomers.[30, 70, 71] The acidic monomers follow the same diffusion principles as the therapeutic being released, which translates to a slow diffusion out of the polymer matrix. The overall effect of this degradation pattern leads to a liquid core, surrounded by a hard "shell" and the potential degradation of the therapeutic inside the acidic environment. [30, 70, 71, 118]

Further exploration of polyester systems for long-term protein release focused on creating surface erodible biomaterials by manipulating the polymer main chain composition, such as synthesizing polyorthesters or by copolymerizing with other compounds.[57, 58, 60, 110, 116, 120-122] The surface degradation characteristics of a polycarbonate based on 1,3-trimethylene carbonate were previously reported, but the degradation of the polymer matrix was relatively slow.[123] Later work explored the creation of copolymers derived from DL-lactic acid and 1,3-trimethylene carbonate to produce a highly hydrophobic, surface eroding polymer with an increased rate of degradation.[58, 123, 124] The intent was to use the low water permeability, and subsequent high hydrophobicity, of the copolymer to allow for a solid form of a protein integrated into the polymer matrix to maintain its biological activity.

Based on the above principles and our previous study of poly(carbonate-ester) copolymers derived from the two naturally occurring biomolecules, lactic acid (LA) and a carbonate form of dihydroxyacetone (DHA), the protein release characteristics for these copolymers were explored.[125] The poly(carbonate-ester)'s unique in vitro degradation pattern, wherein the carbonate bond appears to be more labile than the ester bond, a phenomenon not typically seen, appeared to allow the material to degrade more via surface erosion than bulk degradation.[58-60] This manner of degradation should translate to a system that remains at a more stable internal matrix pH, a key aspect during the optimization of a system for the controlled

release of a protein based therapeutic.[10, 57, 71, 117, 126] Furthermore, the degradation products of dihydroxyacetone carbonate (DHAC)-based polymers were studied previously and found to ultimately degrade into CO_2 from the carbonate bond and DHA, materials that are biocompatible within the human body.[22-24] Similarly, the degradation products of LA-based polymers are well characterized and are known to be biocompatible. Additionally, polyesters based on LA are approved for clinical use.[56, 111, 117] LA based polymers eventually break down to monomeric lactic acid, which is metabolized through the tricarboxyclic acid cycle and eventually removed from the body as CO_2 via the respiratory system.[9, 127] This degradation behavior of the LA and DHAC poly(carbonate-ester)s is why the biomaterial was chosen for further controlled release studies.

These new studies using LA-DHAC poly(carbonate-ester)s were performed to further understand the degradation profile of the biomaterial. The degradation of the copolymer into DHA was explored via the bicinchoninic acid (BCA) assay. Using the BCA assay's ability to react with α-hydroxy ketones, a more complete degradation profile of DHA release from the copolymer was obtained.[128] The controlled release behavior of proteins from the copolymer matrix was determined using two model proteins, bovine serum albumin (BSA) and lysozyme, loaded at two different weight percentages. Chosen for their well-documented behavior in other controlled release systems, the rate of release of the BSA and lysozyme was quantified using the Bradford microassay.[16, 111] The activity of lysozyme was monitored by a biological activity assay to explore how the degradation characteristics of the copolymer might affect the structural stability of the released model protein. Mathematical modeling was used to analyze the mechanism of release of the proteins to obtain a better understanding of these poly(carbonate-ester)s.

4.2 Experimental

4.2.1 Materials

All copolymer compositions are defined according to the following abbreviations: LA_x = mol % lactic acid; $DHAC_y$ = mol % dihydroxyacetone carbonate. Three mole ratios of copolymers, pLA_{50}-*co*-$DHAC_{50}$, pLA_{25}-*co*-$DHAC_{75}$, pLA_{15}-*co*-$DHAC_{85}$, were synthesized as previously described (M_w ~70,000 g/mol).[125] Bovine serum albumin (BSA), lysozyme and *M. lysodeikticus* cells were purchased from Sigma-Aldrich (St. Louis, MO) and used as received. Phosphate buffered saline (10X, PBS) without calcium or magnesium was purchased from BioWhittaker® (Lancaster, MA) and diluted to 1X with 18 Ω water. Potassium phosphate monobasic, potassium phosphate dibasic, and Costar Brand Serocluster 96-well microtitration plates were purchased from VWR (West Chester, PA). BCA Protein Assay kit (product number 23225) was purchased from Thermo Scientific®. Quick Start™ Bradford Protein Assay 1X Dye Reagent (catalog number 500-0205) was purchased from Bio-Rad Laboratories, Inc.

4.2.2 Copolymer degradation analysis

Tablets were formed from the three copolymer ratios via direct mechanical compression of the copolymer powder using a Carver Press, model 3851-0 (Wabash, IN). The copolymers were first sized through a 250 μm sieve before direct compression of 20 mg of copolymer at 1000 psi for 10 seconds at room temperature. The tablets were placed in 1X PBS buffer solution (1.0 mL, pH 7.4) and incubated with rotation (N=3) at 37 ºC in 1.5 mL Eppendorf tubes. At predetermined time points, the entire buffer solution was isolated and replaced with fresh buffer. The majority of the removed buffer was immediately frozen, while a small aliquot was run under standard BCA conditions according to the manufacturer's directions: 50:1 bicinchoninic acid and

tartrate in an alkaline carbonate buffer (reagent A) to 4% copper sulfate pentahydrate solution (reagent B). The relative intensity of the reading was determined at 562 nm on a SpectraMAX Plus384 Microplate Reader (Molecular Devices Corporation).

4.2.3 Protein release quantification

Two different loading percentages of each protein, 5% and 10% by weight, were passed through a 250 μm sieve. The fine powder was then incorporated into the three different copolymer matrices, also sized through a 250 μm sieve, via geometric dilution with the copolymer powder. 20 mg of the subsequent mixture was then subjected to direct mechanical compression using a Carver Press, model 3851-0 (Wabash, IN) to 1000 psi for 10 seconds at room temperature to form tablets. The final cylindrical tablets had dimensions of approximately 5.32 ± 0.02 mm x 0.84 ± 0.02 mm (diameter x thickness) as measured by digital calipers. The tablets were placed in 1X PBS buffer solution (1.0 mL, pH 7.4) and incubated with rotation (N=3) at 37 ºC in 1.5 mL Eppendorf tubes. At predetermined time points, the entire buffer solution was exchanged and a 150 μl aliquot of appropriately diluted buffer sample placed in a clear polystyrene 96 well plate. To this was added 150 μl of Quick Start™ Bradford Protein Assay 1X Dye Reagent and the solution allowed to shake for two minutes before sitting at room temperature for 8 additional minutes. The relative intensity of the solution was determined at 595 nm on a SpectraMAX Plus384 Microplate Reader (Molecular Devices Corporation). The remaining buffer removed at each time point was immediately placed in a freezer set to -20ºC.

4.2.4 Activity assay

The biological activity of lysozyme was determined using *M. lysodeikticus* (0.01% w/v) suspended in potassium phosphate buffer (66mM, pH 6.24) freshly prepared from potassium phosphate monobasic and potassium phosphate dibasic crystals. A 15 µl aliquot of appropriately diluted released protein sample was placed in a 96 well plate and mixed with 200 µl of prepared *M. lysodeikticus* suspension. The plate was immediately placed in a SpectraMAX Plus384 Microplate Reader (Molecular Devices Corporation). The decrease in the absorbance was monitored by the UV spectrophotometer over a 5 minute period (450 nm, 25ºC). The activity of the lysozyme, defined in enzyme units (EUs) was determined using the slope of the linear portion in the plot of absorbance versus time.[129, 130] A unit of enzyme was defined as the quantity of enzyme that caused an absorbance decrease of .001 per minute at pH 6.24 (66 mM potassium phosphate buffer) and 25ºC. The biological activity of the sample was then compared to the native lysozyme sample to evaluate the effect of the formulation. If a 15 µl sample gave too weak of a signal, a 50 µl or 100 µl sample was used and compared to corresponding volumes of native lysozyme samples.

4.2.5 Protein release modeling

Modeling of protein release was conducted in Graphpad© using the mean values of the three samples from each time point. Models with the best fit had a correlation coefficient (r^2) closest to 1.0. The data for the Korsmeyer-Peppas model was only fit to approximately the first 60% of the fraction released as required by the model.[40]

4.3 Results and Discussion

4.3.1 DHA release from pLA_x-*co*-$DHAC_y$

Previous work explored the degradation behavior of pLA_x-*co*-$DHAC_y$ copolymer over an 8 week study (Chapter 2). This study tracked the loss of mass from the polymers at set time points. The results of this study showed that the carbonate bond appeared to be more labile to hydrolysis than the ester bond.[125] This behavior led to the copolymers with more DHAC, and subsequently more carbonate bonds in the backbone, to degrade more rapidly than those with more lactic acid. Also, the degradation of those tablets showed a behavior that aligned with many of the characteristics indicative of surface erosion as evidenced by scanning electron microscopy. However, due to the insolubility of the copolymers in common solvents, an accurate profile for the change in molecular weight and monomer release was unable to be obtained at that time.

To further explore the manner in which these pLA_x-*co*-$DHAC_y$ copolymers degrade, a new study was run under similar conditions to capture the change in monomer composition during degradation. Recently, we discovered that structures with an α-hydroxy ketone arrangement are quantifiable using the BCA assay (Chapter 3).[128] This assay is applicable due to α-hydroxy ketone's ability to form an enediol through a process that subsequently reduces the copper present in the BCA assay. The reduction of the copper in turn causes a colorimetric response by the bicinchoninic acid present. Due to DHA's ability to form this enediol, the release of DHA from the copolymer is able to be tracked using the BCA assay.

Three copolymers with monomer ratios were synthesized, pLA_{50}-*co*-$DHAC_{50}$, pLA_{25}-*co*-$DHAC_{75}$, pLA_{15}-*co*-$DHAC_{85}$, by varying the amount of initiator to obtain copolymers with a M_w ~70 kDa, as previously reported. The copolymer powder was formed into tablets via direct compression and placed into 1.5 mL Eppendorf tubes containing 1.0 mL of 1X PBS buffer. The

samples were then allowed to rotate at 37 °C to simulate in vivo conditions. At set time points, the entire volume of buffer was exchanged and the removed buffer assayed using the BCA assay for the presence of DHA.

The results, shown in Figure 4.1, follow the same trends as previously seen with the mass loss studies of these materials. The data, which is normalized to 100% DHA loss when the tablet completely eroded away, show the pLA_{15}-*co*-$DHAC_{85}$ to degrade the fastest. This ratio shows an almost zero order release of DHA from the backbone up to day 30, a pattern that may indicate a surface erosion type degradation behavior. What is more telling is that in a direct comparison of the percent release of monomer to the percent mass loss of the tablet from previous studies, the behavior is almost directly aligned, as seen in Figure 4.1. This result may signify a material with more surface eroding characteristics, but is not the only mechanism of erosion.

The monomer release for both pLA_{50}-*co*-$DHAC_{50}$ and pLA_{25}-*co*-$DHAC_{75}$ showed slower degradation profiles whose linear portion, up to day 45 for pLA_{25}-*co*-$DHAC_{75}$ and day 76 for pLA_{50}-*co*-$DHAC_{50}$, follow first order release kinetics. This result implied a more bulk erosion pattern is responsible for the degradation of the copolymers. While this type of degradation does not perfectly align with surface erosion, the release of the DHA in these two ratios is fairly consistent and controlled. Also, there is no burst release of the DHA from the material which is generally seen with bulk eroding polymers made of lactic acid. It should also be noted that the release of DHA, while reduced in magnitude, continued until the tablets had completed eroded away. As seen in Figure 4.1, a direct comparison of the percent release of monomer from pLA_{25}-*co*-$DHAC_{75}$ and pLA_{50}-*co*-$DHAC_{50}$ to the percent mass loss of the tablet shows similar behavior, but they are not perfectly aligned. The curves for these two ratios begin to show a more rapid loss of DHA after 10% of the DHA released. Once 10% of the DHA is released, the mass loss of

the tablet diverges from the amount of DHA that is released and would appear to indicate that bulk erosion is more responsible for the copolymer degradation.

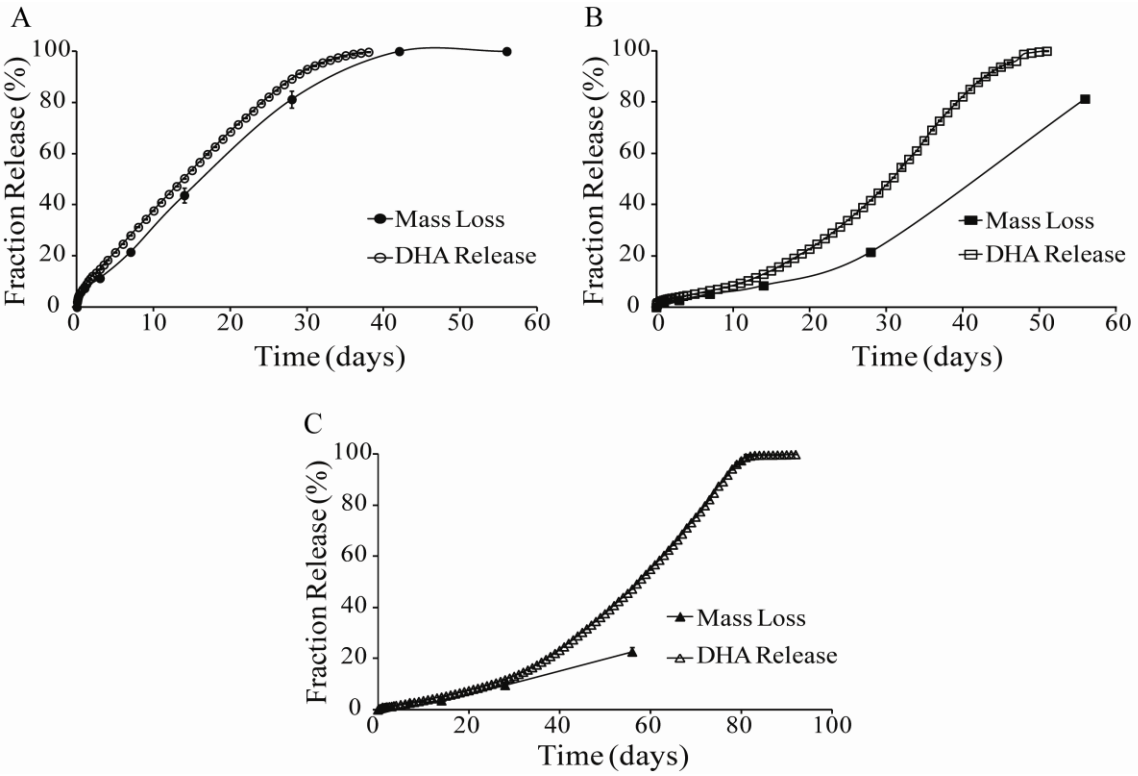

Figure 4.1. Fractional percent release of DHA from the copolymer matrix directly compared to the percentage mass loss, both as a function of degradation time (n=3).[125] (A) pLA_{15}-*co*-$DHAC_{85}$ (B) pLA_{25}-*co*-$DHAC_{75}$ (C) pLA_{50}-*co*-$DHAC_{50}$

4.3.2 Analysis of bovine serum albumin release

After monitoring how the copolymeric material behaves under in vitro degradation conditions, two model proteins were selected to monitor the release behavior from the copolymer matrix. Due to its well characterized behavior in release studies, BSA was incorporated into the copolymer matrix prior to tablet formation. To evaluate factors that affect the in vitro release, two different protein loading percentages, 5% and 10% by weight, were chosen for the study. Throughout the study, BSA was quantified using the Bradford microassay and the protein loaded copolymers kept in near sink conditions via the complete exchange of buffer no later than every 24 hours.[131, 132]

For all ratios, the release of the protein from the copolymer matrix follows a first order release pattern, with the pLA_{15}-*co*-$DHAC_{85}$ releasing the fastest and the pLA_{50}-*co*-$DHAC_{50}$ being the slowest, seen in Figure 4.2. This occurrence is expected due to previous degradation studies, which showed erosion occurring much more rapidly in the copolymers with more DHAC in the backbone.[125] However, the release profiles of BSA do not perfectly align with the mass loss of any of the copolymer ratios. This result, coupled with the new understanding of monomer release from the copolymers, indicates the materials show more bulk degradation characteristics. If this is the case, then some of the well defined rules in which proteins release from bulk degrading LA based polymers may be applicable to these poly(carbonate-ester)s.

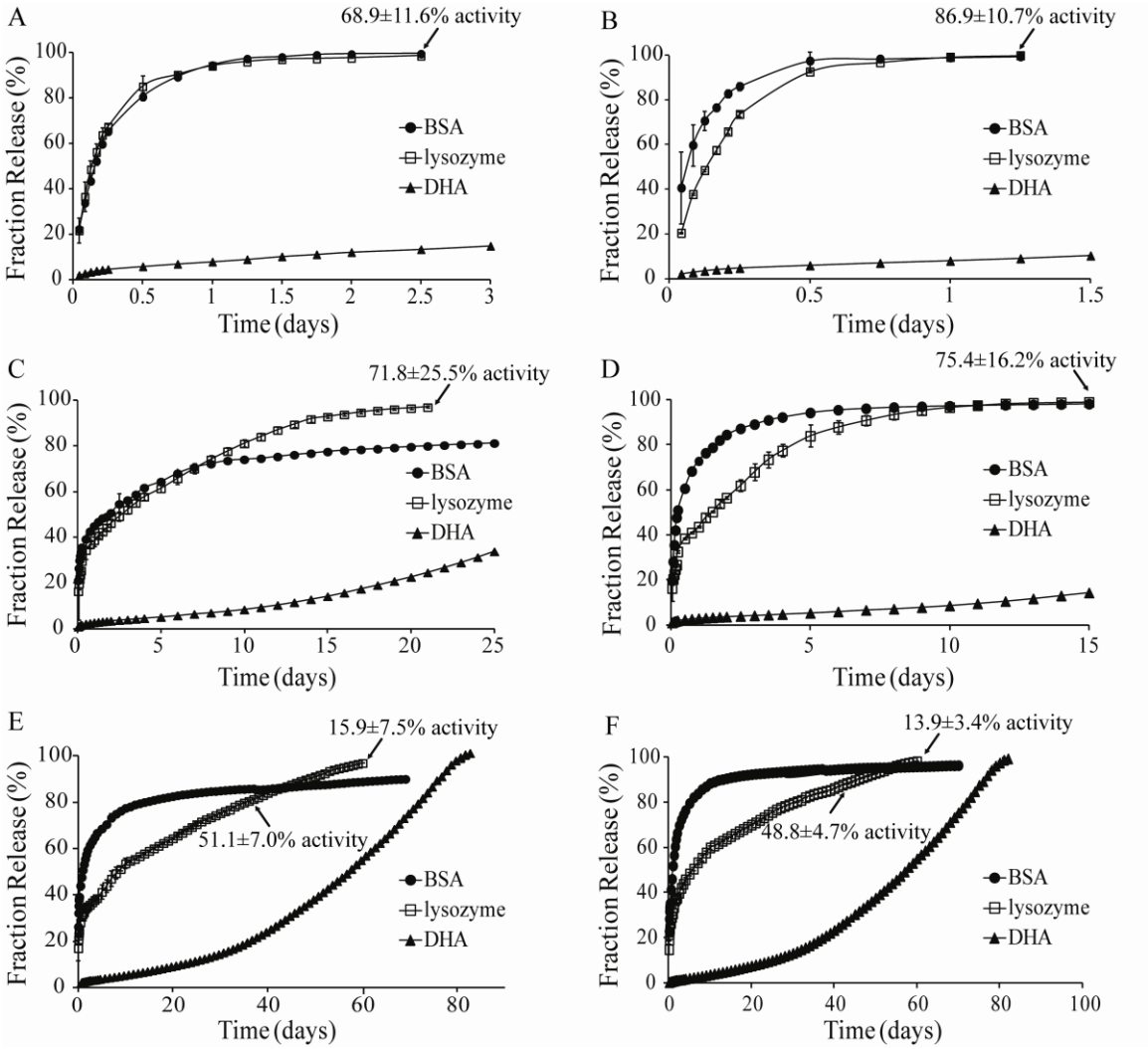

Figure 4.2. Fractional release percent of BSA and lysozyme compared to fractional release of monomer from the copolymer matrix as a function of time (n=3). BSA (●), lysozyme (□), fractional monomer release (▲). (A) pLA_{15}-*co*-$DHAC_{85}$, 5 wt% loading (B) pLA_{15}-*co*-$DHAC_{85}$, 10 wt% loading (C) pLA_{25}-*co*-$DHAC_{75}$, 5 wt% loading (D) pLA_{25}-*co*-$DHAC_{75}$, 10 wt% loading (E) pLA_{50}-*co*-$DHAC_{50}$, 5 wt% loading (F) pLA_{50}-*co*-$DHAC_{50}$, 10 wt% loading.

During the release of a protein from PLGA based systems, there are three phases observed. An initial release of protein due to surface bound or poorly encapsulated drug through aqueous pores, a second phase attributed to diffusional release through pores or through the dense polymer, and a third phase generally regarded as release due to erosion of the polymer matrix.[117, 133-135] The earlier onset of erosion impacts the formation of pores in the matrix, which is generally regarded as the release mechanism for similar LA based matrices.[56, 135] However, the diffusional release may also be due to the protein's diffusion through the polymer, osmotic pumping, or erosion of the encapsulating polymer. Yet, it is the transport through pores in the matrix that is the most common method of release due to the fact that transport of higher M_w molecules, such as peptides, are too large and too hydrophilic to transport through the polymer phase. Also, a protein may release from the polymer matrix before any mass loss is observed.

Directly comparing these poly(carbonate-ester)s with the release of BSA from PLGA tablets and microspheres under similar conditions, there appears to be a similar in vitro release behavior. A study done by Bodmer, et al., exemplified this type of system with BSA released from directly compressed PLGA tablets with a range of molecular weights, up to 76,000, as seen in Figure 4.3.[133] The PLGA tablets (55:45 lactic acid:glycolic acid) had a 20 wt% BSA loading and showed bulk erosion type of degradation. The release from these tablets showed an initial burst of ~28%, which is slightly higher, but comparable to the DHAC based matrices, which had ~20% release of protein in the first hour. This initial burst release was true of all of the ratios and loading percentages, except for the 10 wt% loading of pLA_{15}-*co*-$DHAC_{85}$, which released ~40% of the BSA within the first hour. The initial burst effect, generally attributed to the rapid diffusion of protein located at or near the surface of the polymer matrix, usually is increased by higher loading percentages.[56, 117, 136] The higher loading percent of pLA_{15}-*co*-$DHAC_{85}$ and the

fact that this copolymer ratio begins to degrade much more rapidly than the other ratios of DHAC based copolymers, may explain the higher initial burst. Comparing the initial burst of the DHAC based copolymer to Bodmer's PLGA polymers appear to be in agreement due to Bodmer's higher loading percent of protein. However, comparing the DHAC based tablet to PLGA microspheres show a large difference in the initial burst effect. Certain PLGA microspheres showed ~10% initial burst for less than 2% protein loading by weight, while studies done with 10 wt% BSA loading saw a 30-58% initial burst. Furthermore, both of these studies saw the classic problem of slow, incomplete protein release.[117, 136, 137] The higher initial burst seen in the microsphere preparation is generally attributed to the manner in which they are made and are highly dependent on the solvents used in preparation, method of fabrication, and release medium.[56, 136-140]

	Polymer	System	Copolymer ratio	Molecular Weight	Loading wt%	Burst Release	Total Release	Onset of Erosion	Activity
BSA	PLGA[133]	matrix	55:45	75K	20%	~28%	~100 in 4.5 days	day 18	-
	PLGA[137]	microsphere	50:50	100K	10%	30-58%	55-80% in 45 days	day 40	-
	PLGA[136]	microsphere	70:30	74K	2%	~3%	7.5% in 250 days	-	-
	pLA_x-*co*-$DHAC_y$	matrix	50:50	70K	10%	~20%	~90-95% in 70 days	day 1	-
Lysozyme	PLGA[136]	microsphere	80:20	45K	5%	~3%	13% in 250 days	day 40	active
	PLGA[145]	microsphere	50:50	8.6K	10%	~6%	<10% in 25 days	-	not active
	pLA_x-*co*-$DHAC_y$	matrix	50:50	70K	10%	~15%	~100% in 60 days	day 1	13.9% ~50% 43 day

Figure 4.3. Comparison of release properties of BSA and lysozyme from pLA_x-co-$DHAC_y$ systems as compared to PLGA systems.

Bodmer, et al., also observed that the PLGA release system showed near complete release of the protein from the matrix before the system lost any mass, as seen in Figure 4.3. This behavior is typical of the bulk degradation of higher molecular weight lactic acid based tablet matrices, while low molecular weight polymers may begin to lose mass immediately.[133, 141] Both the DHAC and PLGA systems of comparable molecular weight had similar protein release profiles and close to 100% protein release, however the manner in which these PLGA matrices degrade is quite different than the DHAC based polymers. What is interesting about the similar protein release profiles for PLGA and these DHAC based copolymers of comparable M_w is that, unlike studies involving PLGA based polymers, the mass of the DHAC based tablet decreases from the onset of the study. This phenomenon was observed previously and is shown in Figure 4.1.[125] However, through GPC analysis of PLGA polymers, there is a noticeable molecular weight change in the polymers starting at day 0, showing the polymer backbone degradation begins upon the onset of the study.[10, 50, 133] This occurrence was tracked for the DHAC based copolymers using BCA analysis of the monomer produced from the degrading copolymer backbone and the same conclusion drawn. These findings suggest that the pores that form in the DHAC based polymers from the onset not only help to transport the protein out, but may help transport degraded LA and DHA from the polymer matrix. Another piece of evidence that supports this theory is the fact that the copolymers do not form a liquid core. This phenomenon is seen during the degradation of PLGA based polymer tablets due to the buildup of lactic acid and subsequent pH decrease.[10, 56, 57, 71, 140] Due to the pore formation, we hypothesize that the pH of the DHAC based copolymers stays more neutral under sink conditions, which leads to a more amenable environment for the therapeutics being delivered. All of this evidence suggests that the manner in which proteins release from the DHAC based polymers does not exactly follow the

three phase system of release like that of PLGA matrices.

In contrast, PLGA microspheres show less efficient cumulative protein release, as seen in Figure 4.3. As shown in Figure 4.2, the DHAC based materials have an 80% or greater release efficiency, while studies by Igartua, et al, used PLGA microspheres (50:50, Mw ~30k-70k, 10 wt% loading) and only saw a cumulative release of BSA of less than 80%, with the lowest being 40%, over a 45 day study.[137] Other work reported protein aggregation within the microspheres that led to a significant reduction in the percent of BSA released.[136, 139, 142] This protein aggregation was quite pronounced in the studies done by Viswanathan, et al., who saw only a 7.5% release of BSA from PLGA microspheres (70:30, Mw ~74.5k, 2 wt% loading) over an extended study.[136] At the end of the 250 day study, an insoluble mass of protein equivalent to 78.9% of the total BSA loaded into the microspheres was extracted from the remaining PLGA microspheres. This reduction in the total release of encapsulated proteins is widely observed by many researchers and is attributed to the degradation or aggregation of the protein within the degrading polymer matrix or during microsphere preparation.[117, 136, 139, 140] There are a number of theories as to why the degradation or aggregation of the protein occurs within the microspheres, which include formation of intermolecular linkages, the formation of non-specific physical or chemical adsorption between polymer and protein, or the hydrolysis of the protein. These reasons may explain why the release from the DHAC based copolymers did not show 100% recovery of BSA.

4.3.4 Analysis of lysozyme release

The release of lysozyme from the copolymer matrix was done in the same manner and under the same conditions as the release of BSA. Shown in Figure 4.2, the release of lysozyme

generally followed the same release profile as that of the BSA. However, the release was more controlled and the point at which the release of lysozyme began to slow down tended to be closer to the total percent released as compared to the BSA. This phenomenon, commonly seen in drug release, is attributed to the increasing difficulty of the protein or drug from the center of the tablet to diffuse out of the matrix, as a result the release rate will begin to slow down.[143, 144] The lysozyme release study also had a higher percent of total release than the BSA, with all of the ratios and loading percentages having a greater than 95% total release, as seen in Figure 4.2. Furthermore, the lysozyme release saw a consistent, slightly lower initial burst amount between 14-21% of the total drug for all of the samples. The difference in initial burst is possibly due to the difference in chemical and physical properties of each protein that affected the initial release.[143]

A key aspect of the lysozyme release study was to monitor the biological activity of the protein and assess how the degrading copolymer matrix affected the protein. Over the course of the study, the lysozyme's activity remained fairly high for most of the study. In the studies using the pLA_{15}-*co*-$DHAC_{85}$ ratio, the activity of the lysozyme was quite high, with the 5 wt% loading having about a 69% activity and the 10 wt% loading having about 87%. This trend of the 10 wt% loading showing higher activity was seen for all the ratios and is attributed to the fact that the 10 wt% loading tablets normally released the protein faster than the 5 wt% loading. The release from the pLA_{25}-*co*-$DHAC_{75}$ copolymer ratio saw about a 72% and 75% biological activity for the 5 wt% and 10 wt% loading, respectively. However, the pLA_{50}-*co*-$DHAC_{50}$ ratio had much lower activity values, approximately 15% and 14% for the 5 wt% and 10 wt% loading, respectively. This lower activity, as compared to the other two ratios, is attributed to the longer lysozyme release profile. The pLA_{15}-*co*-$DHAC_{85}$ and the pLA_{25}-*co*-$DHAC_{75}$ ratios release in less

than a third of the time that the pLA_{50}-*co*-$DHAC_{50}$ ratio releases lysozyme. Also of note is that pLA_{50}-*co*-$DHAC_{50}$ kept ~50% of its activity for the first 37 days in the 5 wt% loading and 42 days in the 10 wt% loading. These findings suggest that the environment created by the degradation of the LA and DHAC within the matrix is not excessively harsh on sensitive proteins located in the interior.

Comparing the release of lysozyme from this system to that of PLGA microspheres, again there was seen a lower cumulative release efficiency in the system, as seen in Figure 4.3. In studies done by Viswanathan, et al., PLGA microspheres (80:20, Mw ~45000, 1.6 wt% loading) saw a similar release profile to that of BSA.[136] Over the time course of this study there was only a 5.7% release of lysozyme and at the end of 250 days, a 90.7% insoluble mass of lysozyme was recovered from the microspheres. A second study with the same PLGA microspheres containing ~5 wt% loading of lysozyme showed a slightly higher cumulative release of about 13%. Both of the release experiments showed the released lysozyme was still biologically active. Other studies by Park, et al., saw similar cumulative release values. PLGA microspheres (50:50, Mw ~8600, ~10 wt% loading) showed less than 10% lysozyme release over 25 days, the majority of which came from the initial burst effect followed by a very slow release. However, this study found that lysozyme had very little biological activity compared to the native over the 25 day period.[145]

4.3.5 Mechanism of release

Theoretically, the release mechanism of the model proteins from these matrices relies on the penetration of the dissolution fluid into the matrix through pores, the dissolution of the soluble component of the matrix, and the transport of the drug out of the matrix into the bulk

dissolution medium.[35, 37-39, 135, 146, 147] To understand the mechanism that controls the release of protein from the copolymer matrices in vitro, five commonly used models were used to fit the data; the zero-order equation, the first-order equation, the Higuchi equation, the Hixson-Crowell, and the Korsmeyer-Peppas models. The zero-order equation describes the release of a drug as independent of concentration.[33, 148]

$$C = k_O t \tag{1}$$

Where C is the concentration of drug released, k_O is the zero-order rate constant, and t represents time.

The first-order equation, which implies the release rate is concentration dependent, is used to describe drug dissolution in dosage forms containing water soluble drugs in porous matrices.[33, 148]

$$\log C = \log C_O - \frac{kt}{2.303} \tag{2}$$

Where C is the concentration of drug released, C_O is in initial concentration of drug, k is the first-order rate constant, and t represents time.

The Higuchi equation is a Fickian based diffusion model that describes the release of a drug from an insoluble matrix as a square root of time dependent process. The model is used to describe drug release of water soluble drugs from non-swellable or dissolvable matrices and a high correlation indicates drug release via diffusion.[35]

$$Q = k_H t^{1/2} \tag{3}$$

Where Q is the percent of drug released, k_H is the rate constant of the Higuchi system, and t represents time.

The Hixson-Crowell model, which models the release from a matrix that has changing surface area or diameter of particles or tablets, is applicable to systems in which dissolution occurs in planes that are parallel to the drug surface if the matrix dimensions diminish proportionally.[36] A high correlation using this model indicates protein release by dissolution and with changes in surface area and diameter of the tablets.

$$Q_O^{1/3} - Q_t^{1/3} = k_{HC}t \tag{4}$$

Where Q_O is the initial amount of the drug, Q_t is the amount of drug released at time t, k_{HC} is the rate constant of the Hixon-Crowell system, and t represents time.

The Korsmeyer-Peppas model is a semi-empirical equation that uses a power law expression to describes the drug release from a swelling controlled system.[37-39, 149]

$$\frac{M_t}{M_\infty} = kt^n \tag{5}$$

Where M_t/M_∞ is the fraction of drug released at time t, k is the rate constant of the Korsmeyer-Peppas system, t represents time, and value of n is used to characterize the release mechanism for cylindrical shaped matrices. The n value indicates the manner of protein release, either by Fickian diffusion, a combination of diffusion and matrix erosion, or solely by erosion of the polymeric matrix. A summation of the n values and the mechanisms associated with these values is found in Table 4.1.

Upon fitting the data to these five models, the best fit of the release data was with the Korsmeyer-Peppas model, seen in Figure 4.4. This model is used when the release mechanism is not well known or when more than one type of release (diffusion, erosion, or swelling) controls

the system. The r^2 values for both BSA release and lysozyme release have the highest correlation with this model compared to the others and the values are located in Table 4.2 and 4.3. The value of n calculated using the model gives an idea of the mechanism of release and is found in Table 4.4. For the pLA_{15}-*co*-$DHAC_{85}$ copolymers loaded with either 5 wt% or 10 wt% of BSA or lysozyme, the n value for a cylindrical shape is within the $0.89 > n > 0.45$ range, indicating an anomalous or non-Fickian transport mechanism.[40] When $n = 0.45$ or $n = 0.89$, a Fickian or Case II transport mechanism is observed for this system, respectively. Non-Fickian or anomalous diffusion occurs when the diffusion and relaxation rates are comparable and is associated with the rate at which the structure of the polymer rearranges to accommodate water molecules.[40, 150] This transport is partially controlled by viscoelastic relaxation of the polymeric matrix as water penetrates the system. In Case I, or Fickian diffusion, the mobility of the penetrant is much slower than the segmental relaxation rate. In Case II diffusion, the mobility of the penetrant is much higher than the segmental relaxation rate. Non-Fickian diffusion contains intermediate characteristics of both Case I and Case II diffusion and depends on the polymer-penetrant system, the penetrant activity and the temperature.[40, 151] Deviation from Fick's law is observed when the penetrant diffusion is at a temperature below the glass transition (T_g) temperature.[151] This is the case for all of these poly(carbonate-ester)s, which have T_g values around 60 °C.[125]

The other ratios and loading percents fell outside of the anomalous transport region, with values less than 0.45. These n values indicate a pseudo-Fickian release mechanism. This pseudo-Fickian behavior suggests that the release mechanism is quite complex, and may depend on numerous other factors such as drug diffusion, porosity, the crystallinity, polymeric swelling, and polymer erosion.[147, 152, 153] Pore distribution and size greatly affects the release rate of the drug as it follows a tortuous path through the matrix. The pore arrangement intrinsic to the system may

explain one trend seen with the pLA_{50}-*co*-$DHAC_{50}$ and pLA_{25}-*co*-$DHAC_{75}$ matrices. In general, the n value increased with increasing loading percent, which may be a function of the increased number of pores created in the system as the protein diffused out. The formation of pores is due to void spaces created by the solubilized protein or by the erosion of copolymer matrix which is a rate-controlling process.[135] Another observed trend for the pLA_{50}-*co*-$DHAC_{50}$ and pLA_{25}-*co*-$DHAC_{75}$ is the values of n decrease as the LA content within the copolymers increased. This may correlate to the possibility for increasing crystalline microdomains within the copolymer matrix that affect the mechanism of transport.

For all of the ratios, statistical effects that pertain to the differences in polymer and drug distribution throughout the system may lead to deviations from the ideal Fickian behavior.[147, 154] The degradation of the copolymer's backbone, visualized using the BCA assay to track the release of degraded DHA from the copolymer backbone, may decrease the rigidity of the polymer chains and alter the porosity of the degrading polymer tablet.[133, 135, 147] There is also increasing hydrophilicity of the polymer due to an increase in the number of terminal carboxylate and hydroxyl end groups from a build up of monomer degradation. This monomer build up is much more rapid in the pLA_{15}-*co*-$DHAC_{85}$ as compared to the pLA_{50}-*co*-$DHAC_{50}$ and pLA_{25}-*co*-$DHAC_{75}$ ratios. The increase in hydrophilicity leads to an increase in solubility of the undissolved polymer and thus the porosity of the matrix. However, in the copolymer ratios with more LA, there is an increase in the carboxylate end group as compared to the hydroxyl end group. The increase in carboxylate end groups may interact with the positively charged proteins or other cationic structures, thus impeding their release.[117, 126, 133, 135, 140, 155] If this is the case, the release of protein from pLA_{15}-*co*-$DHAC_{85}$ may not only be due to faster copolymer degradation kinetics, but because it has the least number of ionizable groups compared to the other

copolymer ratios containing more LA.

The increase in the number of ionizable groups also aligns when comparing the release of BSA to the release of lysozyme. As seen in Figure 4.2, lysozyme releases slightly slower than BSA. This observation is most evident when directly comparing the graphs of the 10 wt% loading. Due to the increase in carboxylate end groups from the degrading LA, coupled with the possibility that the pH of the system may decrease, the positively charged lysozyme (pI 11.35) may be attracted to the carboxylate groups while the negatively charged BSA (pI 4.7) is repelled.[156, 157] The attraction of lysozyme to the degrading lactic acid based matrix was previously noted in studies by Park, et al., when salt was needed to break up the ionic interaction of the protein and matrix in an attempt to raise the total percent of lysozyme released.[145] Thus, the BSA would release faster from this copolymer matrix.

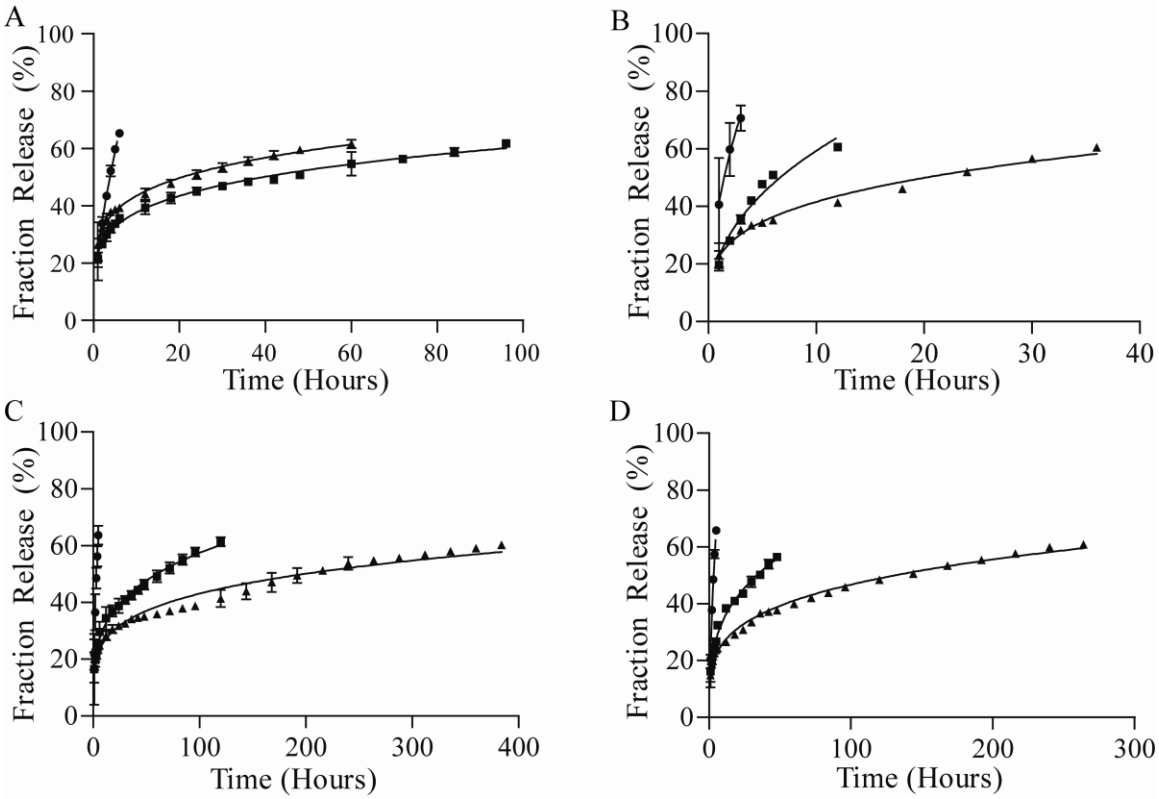

Figure 4.4. The calculated trend lines of the Korsmeyer-Peppas model overlaid on the fraction release percent of protein from the three copolymer ratios: pLA_{15}-*co*-$DHAC_{85}$ (●), pLA_{25}-*co*-DHAC75 (■), and pLA_{50}-*co*-$DHAC_{50}$ (▲). (A) 5 wt% loading of BSA (B) 10 wt% loading of BSA (C) 5 wt% loading of lysozyme (D) 10 wt% loading of lysozyme.

Release exponent (n)	Drug transport mechanism	Rate as a function of time	Mechanism
n<0.45	Psuedo-Fickian	t^{n-1}	Complex and depends on drug diffusion, porosity, the crystallinity, polymeric swelling, and polymer erosion
0.5	Fickian diffusion	$t^{-0.5}$	Penetrant mobility is slower than polymer segmental relaxation rate
n > 0.45 n < 0.89	Non-Fickian (Anomalous) transport	t^{n-1}	Contains characteristics of Fickian diffusion and Case II transport - glassy polymers
0.89	Case II transport	Zero-order relase	Penetrant mobility is faster than polymer segmental relaxation rate - swelling
n > 0.89	Super case II transport	t^{n-1}	Like Case II, however there is rapid increase in rate at a certain time

Table 4.1. Korsmeyer-Peppas drug transport mechanism from cylindrical polymer matrices. For clarity this table has been repeated from Table 1.1.

	5 wt% BSA loading					
	pLA_{15}-*co*-DHA_{85}		pLA_{25}-*co*-DHA_{75}		pLA_{50}-*co*-DHA_{50}	
Model	k	r^2	k	r^2	k	r^2
Zero Order	2.334 (h^{-1})	0.8215	0.1450 (h^{-1})	0.7824	0.0479 (h^{-1})	0.6809
First Order	0.2083 (h^{-1})	0.9758	$7.001x10^{-4}$ (h^{-1})	0.7404	$3.790x10^{-4}$ (h^{-1})	0.6597
Higuchi	16.41 ($h^{-1/2}$)	0.9312	1.769 ($h^{-1/2}$)	0.8677	1.281 ($h^{-1/2}$)	0.8132
Hixson-Crowell	$1.288x10^{-2}$($h^{-1/3}$)	0.8833	$2.034x10^{-4}$($h^{-1/3}$)	0.7198	$1.125x10^{-4}$($h^{-1/3}$)	0.6427
Korsmeyer-Peppas	22.44 (h^{-n})	0.9990	23.41 (h^{-n})	0.9919	27.93 (h^{-n})	0.9944

	10 wt% BSA loading					
	pLA_{15}-*co*-DHA_{85}		pLA_{25}-*co*-DHA_{75}		pLA_{50}-*co*-DHA_{50}	
Model	k	r^2	k	r^2	k	r^2
Zero Order	4.473 (h^{-1})	0.7559	0.8819 (h^{-1})	0.7890	0.4127 (h^{-1})	0.8368
First Order	0.1029 (h^{-1})	0.8685	$1.568x10^{-2}$ (h^{-1})	0.8717	$6.660x10^{-3}$ (h^{-1})	0.9141
Higuchi	22.24 ($h^{-1/2}$)	0.8946	8.893 ($h^{-1/2}$)	0.9238	5.582 ($h^{-1/2}$)	0.9686
Hixson-Crowell	$2.314x10^{-2}$($h^{-1/3}$)	0.8238	$4.235x10^{-3}$($h^{-1/3}$)	0.8451	$1.878x10^{-3}$($h^{-1/3}$)	0.8905
Korsmeyer-Peppas	41.36 (h^{-n})	0.9937	22.63 (h^{-n})	0.9595	22.64 (h^{-n})	0.9843

Table 4.2. Calculated kinetic parameters from fitting the release of BSA from the pLA_x-*co*-$DHAC_y$ copolymer matrix to the five different release models (k is the release rate constant and r^2 is the correlation coefficient).

	5 wt% Lysozyme loading					
	pLA_{15}-*co*-$DHAC_{85}$		pLA_{25}-*co*-$DHAC_{75}$		pLA_{50}-*co*-$DHAC_{50}$	
Model	k	r^2	k	r^2	k	r^2
Zero Order	2.196 (h^{-1})	0.7636	0.1120 (h^{-1})	0.9169	0.1540 (h^{-1})	0.8974
First Order	0.594710^{-2} (h^{-1})	0.8669	$3.019x10^{-3}$ (h^{-1})	0.9672	$8.532x10^{-4}$ (h^{-1})	0.9820
Higuchi	15.66 ($h^{-1/2}$)	0.8909	3.813 ($h^{-1/2}$)	0.9879	2.061 ($h^{-1/2}$)	0.9984
Hixson-Crowell	$1.175x10^{-2}$($h^{-1/3}$)	0.8262	$7.941x10^{-4}$($h^{-1/3}$)	0.9483	$2.355x10^{-4}$($h^{-1/3}$)	0.9710
Korsmeyer-Peppas	23.21 (h^{-n})	0.9938	16.69 (h^{-n})	0.9939	15.77 (h^{-n})	0.9744

	10 wt% Lysozyme loading					
	pLA_{15}-*co*-$DHAC_{85}$		pLA_{25}-*co*-$DHAC_{75}$		pLA_{50}-*co*-$DHAC_{50}$	
Model	k	r^2	k	r^2	k	r^2
Zero Order	6.110 (h^{-1})	0.8732	0.6751 (h^{-1})	0.9302	0.2299 (h^{-1})	0.8827
First Order	0.2219 (h^{-1})	0.9987	$6.473x10^{-3}$ (h^{-1})	0.9383	$8.776x10^{-4}$ (h^{-1})	0.9493
Higuchi	16.99 ($h^{-1/2}$)	0.8689	4.861 ($h^{-1/2}$)	0.9509	2.071 ($h^{-1/2}$)	0.9870
Hixson-Crowell	$1.525x10^{-2}$($h^{-1/3}$)	0.8158	$1.377x10^{-3}$($h^{-1/3}$)	0.8950	$2.363x10^{-4}$($h^{-1/3}$)	0.9304
Korsmeyer-Peppas	22.67 (h^{-n})	0.9920	16.67 (h^{-n})	0.9899	14.76 (h^{-n})	0.9926

Table 4.3. Calculated kinetic parameters from fitting the release of lysozyme from the pLA_x-*co*-$DHAC_y$ copolymer matrix to the five different release models (k is the release rate constant and r^2 is the correlation coefficient).

	pLA_{15}-*co*-$DHAC_{85}$		pLA_{25}-*co*-$DHAC_{75}$		pLA_{50}-*co*-$DHAC_{50}$	
Loading %	n	Release Mechanism	n	Release Mechanism	n	Release Mechanism
5 wt% BSA	0.6022	Anomalous Transport	0.2066	Pseudo-Fickian	0.1924	Pseudo-Fickian
10 wt% BSA	0.4965	Anomalous Transport	0.4179	Pseudo-Fickian	0.2638	Pseudo-Fickian
5 wt% Lysozyme	0.6371	Anomalous Transport	0.2681	Pseudo-Fickian	0.2182	Pseudo-Fickian
10 wt% Lysozyme	0.6703	Anomalous Transport	0.3121	Pseudo-Fickian	0.2502	Pseudo-Fickian

Table 4.4. Calculated Korsmeyer-Peppas values of the exponent, n, and release mechanism for the release of BSA and lysozyme from the pLAx-co-DHACy copolymer matrix.

4.4 Conclusion

Various poly(carbonate-ester)s based on lactic acid and a carbonate form of dihydroxyacetone were formed into tablets via direct compression. The degradation of these copolymer matrices was explored using the BCA assay to track DHA release from the copolymer backbone. A trend toward faster DHA release was seen in the copolymers with more DHAC in the backbone and that the release of the monomer followed a similar trend as that of mass loss for each tablet. However, the deviation of percent monomer released compared to percent mass loss indicates bulk degradation may play a more important part in the degradation of the copolymer matrix.

The poly(carbonate-ester)s unique intrinsic characteristics, such as the increased degradation rate with copolymers more rich in carbonate bonds and the apparent lack of a viscous core formation due to lactic acid build up in the interior of the tablet, influence they way in which they release therapeutics. This degradation pattern makes for a more amenable environment for the release of sensitive proteins, as evidenced by the release of two model proteins, BSA and lysozyme. The poly(carbonate-ester)s achieved greater than 80% release for both model proteins at both 5 wt% and 10 wt% loading. The release of lysozyme had high levels of activity for the duration of release from pLA_{15}-*co*-$DHAC_{85}$ and pLA_{25}-*co*-$DHAC_{75}$, and greater than 50% activity for the first month of release from pLA_{50}-*co*-$DHAC_{50}$. It was seen that the release of both proteins fit the Korsmeyer-Peppas model with a high correlation, which may indicate that the release mechanism is a combination of diffusion and erosion based release. These poly(carbonate-ester)'s non-ideal Fickian behavior is greatly affected by the protein's diffusion, the matrix's porosity, the crystallinity of the polymers, polymeric swelling, and polymer erosion.

CHAPTER 5 – CLIMB GK-12 FELLOWS: BRINGING BME TO THE K-12 CLASSROOM

5.1 Introduction

The ability to successfully convey new ideas and concepts, particularly those regarding science and math, is an essential component to developing new teaching pedagogies.[158-161] The Cornell Learning Initiative in Medicine and Bioengineering (CLIMB) is part of the National Science Foundation's (NSF) GK-12 program which allows science, technology, engineering, and math (STEM) graduate students to understand this new facet of scientific education. The CLIMB program offers graduate students the chance to be visiting scientific scholars to area kindergarten through 12th grade (K-12) schools, be scientists-in-residence and bring the graduate fellows' research to the classroom. The scientific knowledge and experience that each fellow is able to share with area K-12 students may begin to bridge the gap between classic text book learning and the practical tools of laboratory science. A STEM Fellow's presence in the classroom has the potential to enhance the content of the basic K-12 science curriculum.

The GK-12 program allows STEM Fellows the opportunity to prepare lectures, provide demonstrations, become a mentor, expand on traditional lessons and implement a multi-day inquiry based experiment to highlight practical, relatable applications of the required curriculum. The tools and resources available to a BME graduate student unites math, chemistry, biology, medicine and engineering in such a way that opens K-12 students to new perspectives on science. The NSF GK-12 program also benefits the graduate fellow by improving on basic communication and teaching skills by challenging their abilities to relay scientific knowledge to an audience with a much less in-depth scientific background.

5.1.1 Classroom background

The aforementioned work in the CLIMB program partnered the STEM Fellow with Laura

Austen, a teacher for the New York State biology course entitled, The Living Environment. During the 2009-2010 academic year, the student traveled to Southside High School in Elmira, NY to help teach this New York State Regent's level course. Student enrollment was approximately 90 students spread over 4 classes, with students ranging from 13-17 years old.

5.2 Example lessons

5.2.1 Viscoelastic polymers

To introduce the field of polymer science, the students were asked to create Silly Putty. This viscoelastic polymer demonstrated the properties of both a viscous material and an elastic material. An overview was given of the basic structure of what comprises ordinary glue and how, in the presence of borate ions, the polymer structure crosslinks to create the abovementioned viscoelastic structure. This activity was done simply by mixing glue (mainly polyvinyl acetate) with borax (borate ions). The protocol used required preparing a supersaturated solution of Borax in tap water. To this was slowly added a 1:1 glue:tap water mixture, with constant stirring, to achieve the proper consistency.

5.2.2 Physical properties of polymers

Another polymer-based experiment involved the creation of bouncy balls. This experiment did not produce the best example of a bouncy ball (ie. the balls didn't bounce as well as store bought ones), but it was feasible with the limited resources of the classroom. The experimental protocol is as follows:

> Pour 2 tablespoons warm tap water and 1/2 teaspoon borax powder into a cup. Stir the mixture to dissolve the borax and add food coloring, if desired. Pour 1 tablespoon of glue

into a different cup. Without stirring, add 1/2 teaspoon of the borax solution previously prepared and 1 tablespoon of cornstarch. Allow the ingredients to sit for 10-15 seconds and then stir them together to fully mix. Once stirring becomes ineffective, take it out of the cup and mold the ball with your hands.

5.2.3 Hydrogels

Another short polymer demonstration included exploring everyday polymers. A number of diapers were brought in and the students were asked to open them up and separate out the 4-5 grams of a polyacrylic acid polymer found within the cotton layers. To give the students a basic understanding of hydrogels and hydrophilic polymers, tap water was added to about 2 grams of the polymer. The students then observed the material swell to about 50 times its original size. After the material reached its fullest size, a salt solution was added to the beaker and the students observed the polymer shrink back down. Aligned with this day's demonstration, there were a few other polymeric materials Ms. Austen had on hand that offered other examples of polymeric hydrogels. One material, Instant Snow Polymer, when hydrated mimicked the appearance of snow, while Water Gel Crystals took on the appearance of cubes of ice when hydrated.

5.2.4 Alginate

To try and make a real world connection between polymers and everyday life, a talk was given about joint replacement and this topic tied into the food concept of molecular gastronomy. An explanation was provided about how people in biomedical research create scaffolds upon which to create new biologically inspired devices by borrowing two medial meniscus molds from the Bonassar lab at Cornell University. To demonstrate how these molds work, a 2% w/w

solution of both alginate and calcium sulfate was prepared. These solutions were injected in a 2:1 alginate to calcium sulfate mixture into a mold and then the mold immediately submerged into a solution of calcium chloride for 20 minutes. To explore how these polymeric scaffolds are affected by the experimental conditions, the students varied the alginate/calcium sulfate mixtures to see how this would change the "tissue's" properties. Following this, a link was provided between this type of medical laboratory science to cooking by demonstrating how, when the alginate is rapidly dropped into calcium sulfate, it forms a gel. However, if done right, the inside remains a liquid while only a thin outer layer becomes a gel. This example was then tied into how a number of restaurants around the world use this and other laboratory techniques to redefine fine dining experiences with science.

5.2.5 Non-Newtonian fluids

Another laboratory demonstration involved showing the students the properties of non-Newtonian fluids. To teach the student's about non-Newtonian fluids, a substance colloquially known as "oobleck" was created using 1 part tap water to 1.5-2 parts corn starch. This experiment was a huge success with the students and had far greater participation than most other experiment. A number of students even commented on trying this experiment at home.

5.2.6 Cells and microscopy

In the very beginning of the year a short talk on cells was aligned with their unit regarding this subject. A number of pictures of cells taken with different imaging techniques were shown to try and exemplify how they are a dynamic, living, 3-D structure. Along with this presentation, an explained was provided regarding the basic concepts of microscopy, specifically

scanning electron microscopy, and its usefulness in research. A number of actual pictures taken from one of Cornell's SEM machines were shown to the students as well as Au/Pd sputter coated samples. The students were then asked to compare non magnified samples to ones magnified 15,000 times.

5.2.7 Properties of bone

During the student's unit on the human body, a short demonstration was provided on the properties of bones. The students were given turkey bones that were either demineralized with 1M HCl overnight or had the organic components (collagen and elastin) removed using bleach overnight. This visually grabbing and tactile experiment caught the student's attention immediately. It was effective in explaining how bones are not the completely rigid materials that most people assume.

5.2.8 Heart valves

During this demo, a number of different porcine and bovine heart valves were brought to the classroom. A talk was given about the different kinds of heart valves and the surgery that would be required to implant such a device. This lesson had a large majority of the students interested due to the personal connections some made with these materials and the knowledge that family members have these devices implanted.

5.2.9 Biomedical devices

Another hands on talk was about different biomedical devices. A variety of medical devices such as endoscopes, different models of pacemakers used throughout the years, and

internal defibrillators were brought in to show the students the evolution of medical devices. The student's learned about how the devices have changed with time and what things might impact the newer technologies (i.e. better microprocessors).

5.2.10 Biochemistry

During the unit on biochemistry, a discussion about pH and different methods to assess this intrinsic property of certain materials was held. In an attempt to have the students think about the tools they have in their everyday environment, a head of red cabbage was brought to the classroom. The cabbage was cut up and boiled for 20 minutes. Upon cooling, the extracted liquid was used as a pH indicator. The student's were taught that this liquid was a pH indicator because it contains the anthocyanin, flavin. In the presence of very acidic solutions it will turn anthocyanins a red color. Neutral solutions are a purplish color, like the extracted color from the cabbage, and basic solutions will be greenish-yellow. This experiment was also the first time the students started questioning everyday objects they use, such as their sodas, cleaning spray, etc.

Another activity that was created with different biochemistry techniques in mind was a Thanksgiving themed laboratory involving the concepts of lipids, proteins, carbohydrates, and pH. To help reinforce mandatory New York State laboratory requirements, the students took all of the components found in a traditional Thanksgiving meal and decided which food (turkey, gravy, stuffing, pumpkin pie, etc.) and what test (starch test with iodine, Benedict's solution for sugar, etc.) they would like to perform. Due to this activity being relatable, a larger number of students became more involved as compared to other standard laboratory assignments that were trying to exemplify the same concepts

5.2.11 Ideal gas law

In another attempt to teach the students science in a non-traditional manner, dry ice was provided to the students. The goal was to show them sublimation and how gases expand. To do this, dry ice was added to a lab glove, sealed, and the students observed its expansion. Also, dry ice was added to water to watch it bubble as the gas escaped. However, the biggest thrill for them was when a tiny bit of dry ice was added to a 1.5mL Eppendorf tube filled with tap water and capped. On top of the fun popping noise, it showed them that the expanding gas caused enough pressure to build up to uncap the tube, thus subtlety teaching them the ideal gas law, PV=nRT.

A final experiment brought in involved the use of liquid nitrogen to try and once again examine the ideal gas law. The students used liquid nitrogen to condense the air/moisture in a blown up balloon and then watched it re-expand when removed from the liquid nitrogen. Other items, such as flowers and bananas, were flash frozen to show how the liquid trapped inside these materials can freeze and cause seemingly solid objects to shatter when dropped. Finally, the students used the liquid nitrogen to make ice cream in an attempt to not only have fun, but also open them up to new ideas and other ways of thinking about common items in the world around them. This experiment showed them that the faster the rate of undercooling of a material, the smaller the new forming crystals will become, thus creating a creamier ice cream that they had never tasted before.

5.3 Inquiry-based curriculum development

Part of the CLIMB program involved the development of an inquiry-based experiment. The work in this thesis focuses on the unit of genetics and teaching two inquiry-based laboratory experiments on gel electrophoresis. The goal of the first experiment was to have students

understand how gels are made for DNA separation and how altering the composition can affect the experimental parameters and mechanical properties of the gel. A module template for the agarose electrophoresis mini experiment can be found in the Appendix A.1. The goal of the second experiment was to run a SDS-PAGE electrophoresis to compare known and unknown protein samples. The experiment itself was designed by Cornell Institute of Biology Teachers (CIBT) and gave the students an opportunity to employ SDS-PAGE to compare different animal proteins, figure out an unknown "mystery meat" sample, and answer their own questions (ie. how similar are fresh water fish vs. salt water, etc.).

During both the agarose gel mini lab and the SDS-PAGE four day lab, the feedback from students was overall very positive. During this unit it was found that more students who normally do not ask questions or participate were more active and engaged within their lab group throughout the experiment. This was especially true while loading the gels with their protein samples. In the beginning, more than half the students said they did not want to participate. However, upon seeing their classmates use micropipetters to load the gels, all of the reluctant students began vying for the chance to load protein samples into the acrylamide gel.

However, it should also be noted that this experiment was not a 100% inquiry-based success. Due to the lack of inquiry-based labs in their daily curriculum, many students struggled with the experiment design being so open ended. They had difficulty devising a question they would want to explore about the different types of meat and then designing an experiment to answer said question. Regardless of its average success rate for student comprehension of inquiry-based science, an overall positive response was observed for the majority of the students.

5.4 Data analysis

To quantify the impact that my presence had during the year, two metrics were used to assess their science and math knowledge and attitude. Both of these metrics were administered before the STEM Fellow began at Southside High School and at the end of the school year to student's with which the Fellow interacted and students with which Fellow had no contact. A fourteen question, basic science inventory was created drawing from the concepts of other educational designed metrics.[162, 163] The first 10 questions were designed to assess the scientific knowledge of the students and the last 4 questions were designed to assess their attitude toward math and science (A.2) These first 10 questions were designed to include basic concepts that are incorporated into the NY State Reagent's level biology course and new areas of knowledge the STEM Fellow wished to cover during their time at Southside High School. The second metric was the draw a scientist test (DAST), which is a method in which to assess the student's attitude toward science and scientists.[164] The manner in which these scientists are drawn (i.e. what they look like, any symbols of science in the picture, etc.) give an indication toward the student's attitude towards the members of the scientific community.

Analyses were conducted to investigate whether students' knowledge of science and attitude toward science changed during the school year as a function of having a STEM Fellow present in the classroom. In order to examine these questions, 2 x 2 mixed design analyses of variance (ANOVAs) were run, with time as a within-subjects variable (pre- and post-school year) and class as a between-subjects variable (Laura Austen's class with a STEM Fellow present and a control class). Main effects of time and class were explored, as well as a time x teacher interaction. It was hypothesized that a STEM Fellow's presence in the classroom would positively impact the student's breadth and depth of scientific knowledge, as well as their

attitude toward science. Only students who completed both the pre-test and post-test were included in the analyses that follow.

Students completed a 10-question knowledge of science survey at the beginning and end of the school year. These questions were administered at both assessments and are found in appendix 2. There was a statistically significant main effect of time, such that students' mean score on the science knowledge survey was higher at the end of the school year (M = 1.74, *standard error (SE)* = 0.32) than at the beginning of the school year (M = 0.44, SE = 0.14), $F(1, 41) = 19.56$, $p < .0001$. There was also a statistically significant main effect of class, with the mean knowledge score for students in the class with the STEM Fellow (M = 1.69, SE = 0.21) being greater than the mean knowledge score for students in the control class without the STEM Fellow (M = 0.49, SE = 0.33), $F(1, 41) = 9.52$, $p = .004$. These main effects were qualified by a statistically significant time x class interaction, $F(1, 41) = 16.56$, $p < .0001$. Paired samples t tests were conducted to examine the change in students' knowledge of science from the beginning to the end of the school year in each class separately. As predicted, students in the class with the STEM Fellow showed a statistically significant increase in knowledge of science from the beginning of the school year (M = 0.44, SE = 0.14) to the end of the school year (M = 2.94, SE = 0.39), $t(30) = -7.00$, $p < .0001$. In contrast, there was no significant change in knowledge of science over the school year for students in the control class without a STEM Fellow, $t(11) = -0.58$, $p = .58$ (M_{beg} = 0.44, SE_{beg} = 0.24, M_{end} = 0.54, SE_{end} = 0.15). This interaction is depicted in Figure 5.1.

Similar changes over the course of the school year were observed in students' attitude toward science. There was a statistically significant time x class interaction, $F(1, 44) = 4.85$, $p = .03$. As above, the interaction was evaluated by conducting paired sample t tests for change in

attitude over time for each class separately. In the class with the STEM Fellow, there was a significant increase in students' attitude toward science from the beginning of the school year (M = 2.55, SE = 0.25) to the end of the school year (M = 3.16, SE = 0.14), $t(30) = -3.26$, $p = .003$. This pattern of results is consistent with students viewing science more positively over time. Throughout the course of the school year, the students' appeared more engaged in the in-class activities and State required laboratories. In contrast, there was no significant change in students' attitude toward science in the control class without the STEM Fellow from the beginning of the school year (M = 2.95, SE = 0.23) to the end of the school year (M = 2.70, SE = 0.35), $t(14) = 0.61$, $p = .55$. While there was a decrease in the control class's attitude toward science, this was not statistically significant and may be due to random fluctuations. These results are shown in Figure 5.2.

The second metric used to assess the student's attitude toward science was the DAST. The original criteria of the DAST included items such as the presence of a lab coat or eyeglass, symbols of research or knowledge, or any relevant captions.[164] However, only two criteria were used to assess the Southside High School DAST results. It was hypothesized that the presence of a younger, female STEM Fellow might impact the student's attitude toward the scientific community. Therefore, the DAST results were evaluated using a chi-squared test for age and gender of the scientist depicted in their drawing. The results show a statistically significant change in their perception of what characteristics are associated with scientists, with a drop from approximately 90% considering scientists as male to almost an even ratio of male to female by the end of the school year, as shown in Figure 5.3 ($\chi^2 = 15.99$, df = 1, $p<0.0001$). The age of the scientific figure in the drawing also saw a statistically significant shift from figures that looked older in the initial drawings, to younger figures in the final drawings ($\chi^2 = 6.134$, df = 2,

p=.0465). Examples of these drawings can be seen in Figure 5.4.

The students were also asked to write who they think scientists are before meeting their STEM Fellow and again at the end of the school year. The results of asking the question, "who are scientists?", also saw a shift in perception. Out of 72 students who answered this question before the presence of a STEM Fellow, approximately 11% used wording that they are normal people or implied this descriptor. However, this number rose to 44% when this question was answered by 50 students at the end of the school year. A more qualitative assessment of the student's answers saw another shift from answering the question with words and phrases that only used symbols of scientists, such as lab coat or goggles, to answering the question with phrases like, "you and I", "Ms. Austen or Ms. Weiser", or "anyone".

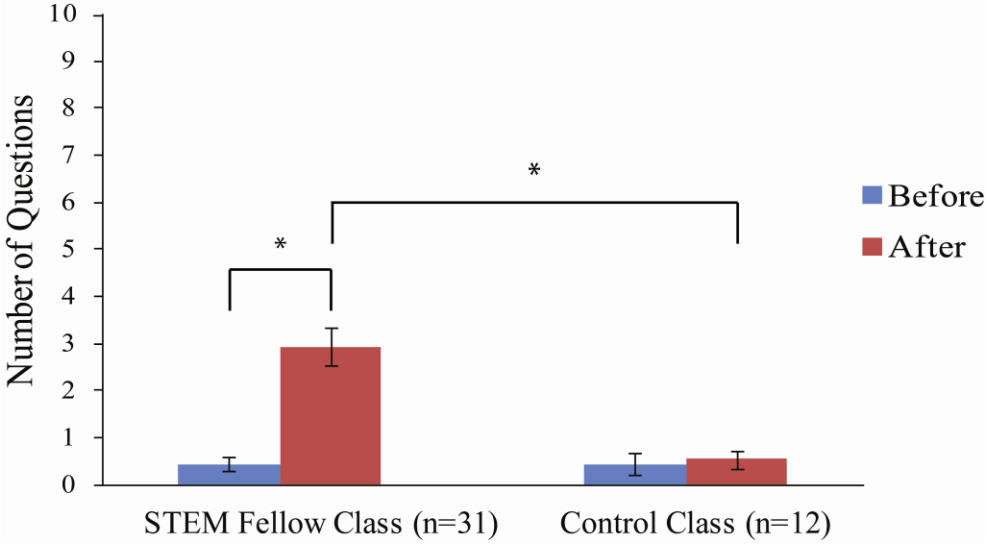

Figure 5.1. Science knowledge pre-school year and post-school year for the classes that interacted with a STEM Fellow and a control class

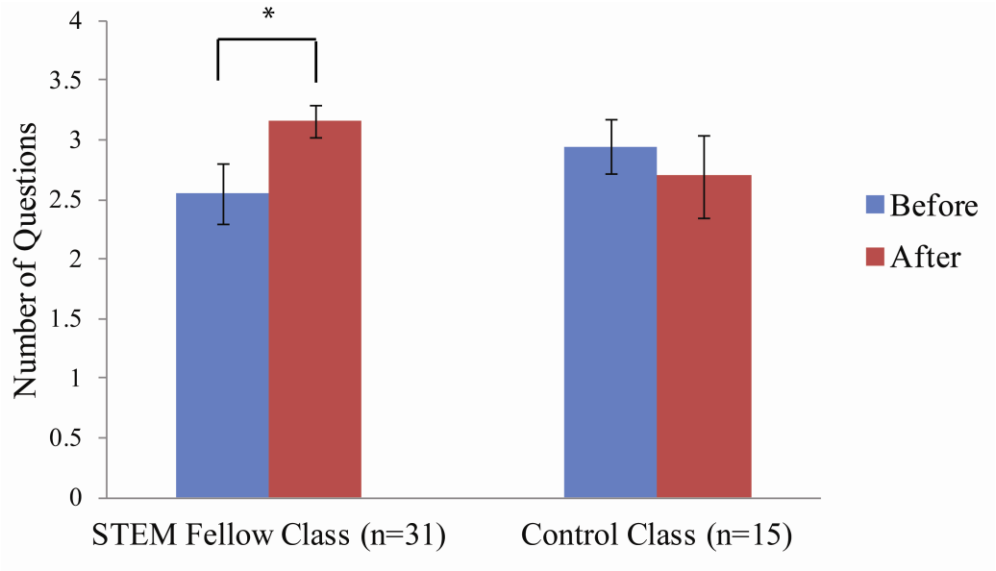

Figure 5.2. Attitude toward science pre-school year and post-school year for the classes that interacted with a STEM Fellow and a control class.

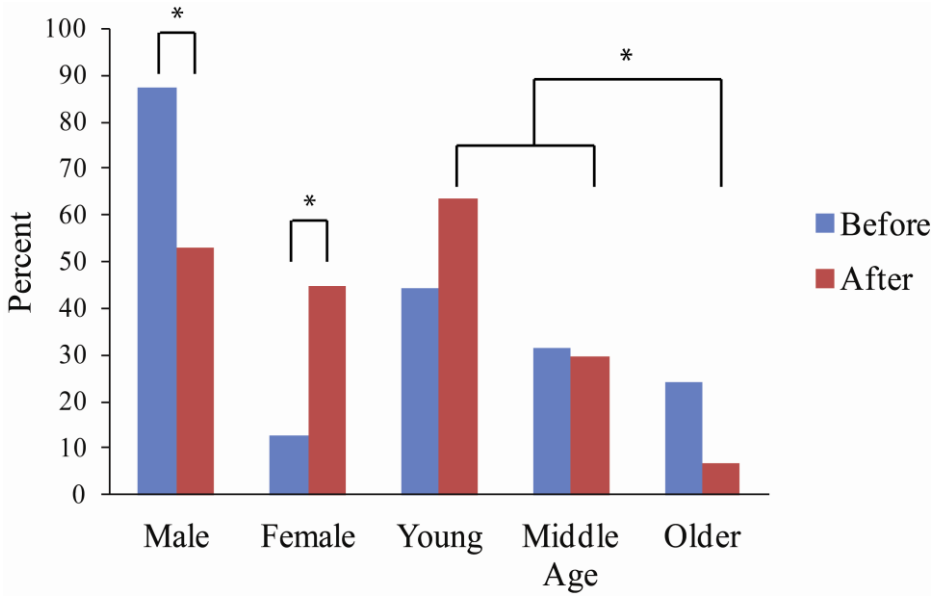

Figure 5.3. Assessment of gender and age of the responses pre- and post-school year to the "Draw a Scientist Test".

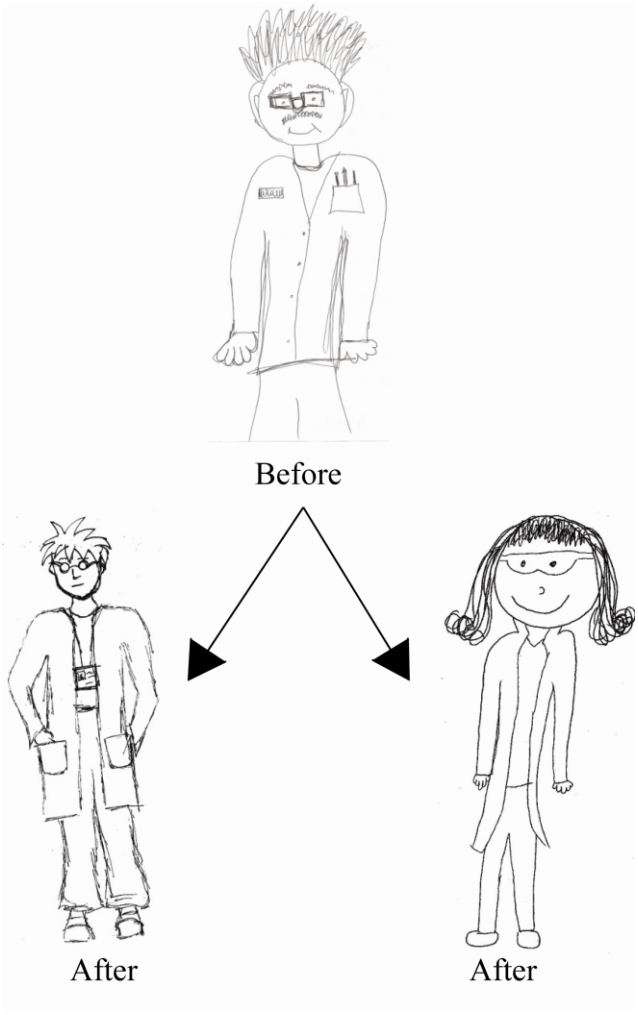

Figure 5.4. Examples of responses pre- and post-school year to the "Draw a Scientist Test".

5.5 Conclusion

The GK-12 experience was overall a positive one. The ability to interact with young students benefits both the STEM Fellow, by improving communication skills, and the students, who had a positive experience by the presence of a STEM Fellow in the classroom. The implementation of inquiry-based learning and more "hands on" lessons attempted to enhance the state designed curriculum for the biology-based, The Living Environment, high school course. The responses of students to the question, "has your view on science changed throughout the year?", were overall very positive. Students gave responses such as, "My views for science have changed because I have been taught a whole new perspective", "My views of science changed a lot. After taking this class I want to get involved in science as a career", and "Science can be fun… not boring". Of course not every student appeared to benefit from a STEM Fellow in their classroom, but to the majority of students, the presence of a STEM Fellow appeared to help supplement their high school science experience.

CHAPTER 6 – FUTURE DIRECTIONS

6.1 Introduction

The focus of future work using dihydroxyacetone as a copolymer component is to continue to elucidate the structure-function relationship of new DHA based copolymers. This work will include the synthesis of new copolymers based on DHA with both glycerol and various diacid alkanes (DAs) in the backbone as well as continued work on MPEG-pDHAC copolymers. The overall goal is to be able to understand how DHA incorporated into a copolymer backbone will affect its intrinsic characteristics and subsequently be able to harness certain aspects for new biomaterial-based medical devices.

6.2 Diacid alkanes

The goal of the first work is to understand the effect of adding a free hydroxyl, as well as the introduction of alternate esters into the polymer backbone, will have on the polymer's intrinsic characteristics. The synthesis of DHA and DA copolymers has been initiated and their usefulness as biomaterials studied.[165, 166] We hypothesize that by varying the type and ratios of the monomers within the copolymer backbone that we can study the structure/function relationship of each component within the material and ultimately create new biomaterials based on DHA.

In an effort to further harness DHA's inherent characteristics, such as its ability to form Schiff bases that can be reduced to secondary amines, or its ability to act as a physical crosslinker to make a gel if the polymer is too water soluble, the synthesis of alternate copolymers should continue to be explored.[20-22] The decision to incorporate both glycerol and diacid alkanes (DAs) into the polymer backbone is due to their inherent characteristics that both provide. Glycerol, an tri-alcohol monomer, is a very desirable building block to use for creating

polyesters or poly(carbonate-ester)s because it has a history of being biocompatible, is FDA approved and inexpensive. Polymers containing glycerol also have in a secondary hydroxyl group in the backbone that can hydrogen bond and is amenable to further functionalization. [51, 54, 167-169] On the other hand, diacid alkanes, such as sebacic acid, a diacid monomer, are a natural metabolic intermediate in ω-oxidation from medium to long chain fatty acids.[19] Like glycerol, a variety of diacid alkane containing polymers have also been approved by the FDA for medical applications and shown to be safe in vivo.[18, 170, 171] The potential DA's have a long history of biocompatibility, easily undergo hydrolytic degradation, and have wide range of applications, such as controlled drug delivery devices or use in medical devices such as biodegradable elastomers.[19, 51, 170, 171] Despite well-established work involved in the synthesis of poly(glycerol-sebacate) materials, these materials are crosslinked thermosets. The ability to synthesize linear polymers with a reactive, physical crosslinking site, promoted the proposed exploration of polyesters derived from adipoyl chloride, sebacoyl chloride, or suberoyl chloride polymerized with dihydroxyacetone and glycerol. The addition of the glyerol's free hydroxyl is an intriguing candidate to add to the polymer backbone making this three component copolymer an attractive, potentially bioadhesive, material to study.[165, 166, 172]

6.2.1 Preliminary synthesis

To synthesize copolymers based on DHA, glycerol, and DAs, a Schötten-Baumann, one step acylation was carried out. The synthetic scheme, based on one previously used to create poly(DHA_x-*co*-DA_y) copolymers, is shown in Scheme 6.1.[165, 166] Briefly, DHA (0.350 g, 3.89 mmol) and glycerol (0.358 mg, 3.89 mmol) were charged to a 10 mL airfree single neck reaction flask fitted with a 2 mm stopcock and magnetic stir bar stored at temperatures above 100 ºC. The

flask was kept under N_2 flow at temperatures below 0 ºC during the addition of an organic solvent (chloroform, or a chloroform/dimethyl sulfoxide mixture are both candidates to address solubility and freezing point issues) (15 mL). The solution was allowed to stir before the slow addition of the diacid chloride (DC), ex. sebacoyl dichloride (0.83 mL, 3.89 mmol) at a syringe rate of 1 mL per minute. After which, pyridine (0.75 mL, 9.31 mmol) was added via syringe at the same rate. Following the addition of all of the reagents, the N_2 flow was stopped, the reaction vented and the reaction allowed to proceed for thirty minutes.

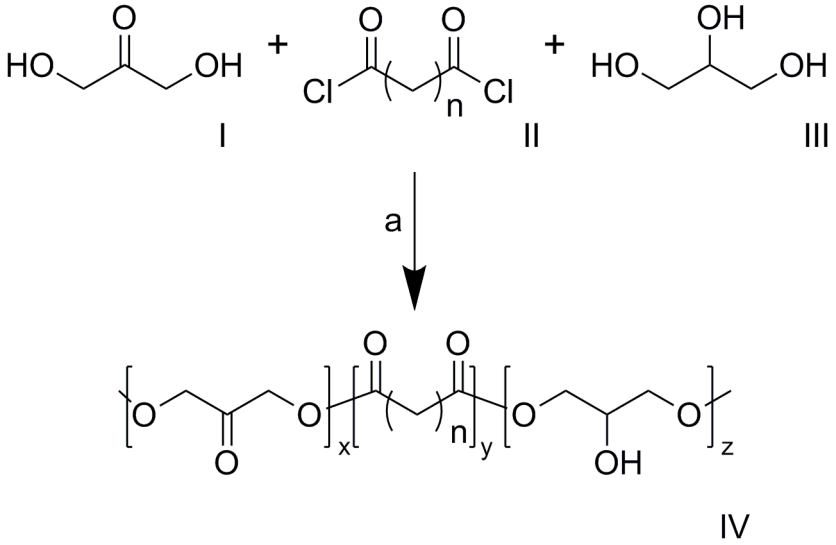

Scheme 6.1. Proposed synthetic route to p(DHA_x-*co*-DA_y-*co*-GLY_z) (IV). a) chloroform/DMSO, pyridine, N_2(g), -78ºC, 30 minutes.

The material synthesized precipitated out of solution as the reaction proceeded and the resulting polymers were moderately adhesive to the touch. This behavior is indicative of the formation of a networked polymer that is crosslinked. These crosslinks were formed due to the reaction of the secondary alcohol in the glycerol monomer, as well as the primary alcohols. However, the intent was to create linear polymers using this one step synthesis. One change to the synthetic protocol that may help to achieve this goal is to reduce the temperature further by the use of an acetone/dry ice bath. The addition of dimethly sulfoxide to the chloroform enables the temperature to be reduced close to the -78 ºC an acetone/dry ice bath achieves due to chloroform's freezing point residing at -63.5 ºC. The end goal is to synthesize a library of different mole feed ratios at two different molecular weights and with three different diacid chlorides (adipoyl chloride, sebacoyl chloride, and suberoyl chloride) to help understand how each monomer contributes to the function of the copolymer as a whole (Table 6.1).

Mole Feed Percents		
% DHA	% DC*	% GLY
0	50	50
50	50	0
40	50	10
25	50	25
10	50	40

*DC denotes adipoyl chloride, sebacoyl chloride, and suberoyl chloride

Table 6.1. Potential prepared mole feed percents of p(DHAx-co-DAy-co-GLYz) copolymers.

6.3 MPEG-pDHAC based copolymers

The goal of the second work was to attempt to increase the time it takes for the MPEG-pDHAC, diblock copolymer to degrade. Earlier work on this copolymer was effective in the treatment of seroma, however, the material's original application was designed for use in post surgical tissue adhesions. The copolymer did not properly address this issue due to its rapid degradation in vivo.[20-22]

Two different approaches to accomplish this are by end-capping the DHAC portion of the copolymer backbone and by incorporating LA into the copolymer to create a tripolymer. The copolymer of MPEG-pDHAC gave positive results for the potential creation of a biomaterial that is useful as a physical barrier to effectively reduce post-operative tissue adhesion. Post surgical tissue adhesion is a complex inflammatory disorder that occurs when tissues in the body grows into each other. These adhesions normally occur within the peritoneum after abdominal surgery; however, they may also form from infection, burns, irradiation, trauma, allergic reactions, repeated peritoneal dialysis, and the presence of debris.[27, 173, 174] Post surgical abdominal tissue adhesions are a significant a factor in the onset of chronic abdominal and pelvic pain, perforated bowel, infertility, and small bowel obstruction.[27, 173, 174] Abdominal adhesions also may require secondary surgeries that increase the total cost to the hospital and the patient over $2 billion dollars annually in the United States alone.[175, 176]

To create an effective post-operative adhesion physical barrier, the material should be biocompatible and absorbable, remain in place without sutures or staples, cover and separate raw or injured surfaces, prevent fibrin strand formation, and be easy to handle during application.[27, 173, 174] Previous work has seen that MPEG-pDHAC holds promise as a physical barrier, however, this material degrades in less than 24 hours, while the material should last 48 to 72h in vivo.[21, 22,

[27, 173, 174] The hypothesis is that the terminating alcohol group from DHAC may be catalyzing the rapid degradation of the copolymer backbone, effectively "unzipping" the copolymer leading to its rapid degradation. Work with the previous, DHAC and LA based poly(carbonate-ester)s would seem to indicate that the degradation should be slightly slower for DHAC based materials. Therefore, the process of end-capping the MPEG-pDHAC or incorporation of LA into the backbone may increase the time in which the copolymers take to degrade.

6.3.1 Preliminary synthesis

The synthetic strategy to create the two potential new copolymers, the end-capped version of MPEG-pDHAC or the $MPEG_x$-(pLA_y-co-$DHAC_z$), can follow the same synthetic scheme as previous described by Zawaneh, et al and can be seen in Scheme 6.2 and 6.3.[21, 22] In short, dihydroxyacetone dimer (II) can be converted to a ring by first locking the C2 carbonyl using a dimethoxy acetal protecting group. Structure III can then ben cyclized to a six member ring (IV). Structure VI can then be created via the polymerization of structure IV with a 5000 M_w polymer of monomethoxy-polyethylene glycol (V) in the presence of $Sn(Oct)_2$ and heat. In the case of the $MPEG_x$-(pLA_y-co-$DHAC_z$) copolymer, LA will be added during this step. The copolymer can then be deprotected using TFA and water or I_2/acetone to potentially afford structure VII (poly(MPEG-b-2-oxopropylene carbonate); MPEG-pDHAC).

Based on other work, the end-capping of the DHAC and ultimate creation of structure VIII in Scheme 6.2, may be possible by using acetic anhydride in the presence of pyridine or a 4-dimethylaminopyridine (DMAP) catalyst.[177-180] The amount of time and temperature would need to be explored to find out the optimum conditions for this end-capping reaction to proceed forward. The work would also focus on optimizing the DHAC block length to understand and

control the copolymer's degradation characteristics.

6.4 Structural characterization

The employment of similar characterization techniques to those of the previously made poly(carbonate-ester)s will help to understand the inherent properties of these potentially new materials. GPC can be used to analyze the molecular weight and molecular weight distribution of each sample synthesized. ^{1}H NMR and ^{13}C NMR can help to confirm the structure and determine the distribution of monomers within the polymer backbone. Thermally characterization techniques, such as thermogravimetric analysis detect the degradation temperatures of the samples while differential scanning calorimetry determines the glass transition temperature and the presence of a melting temperature.

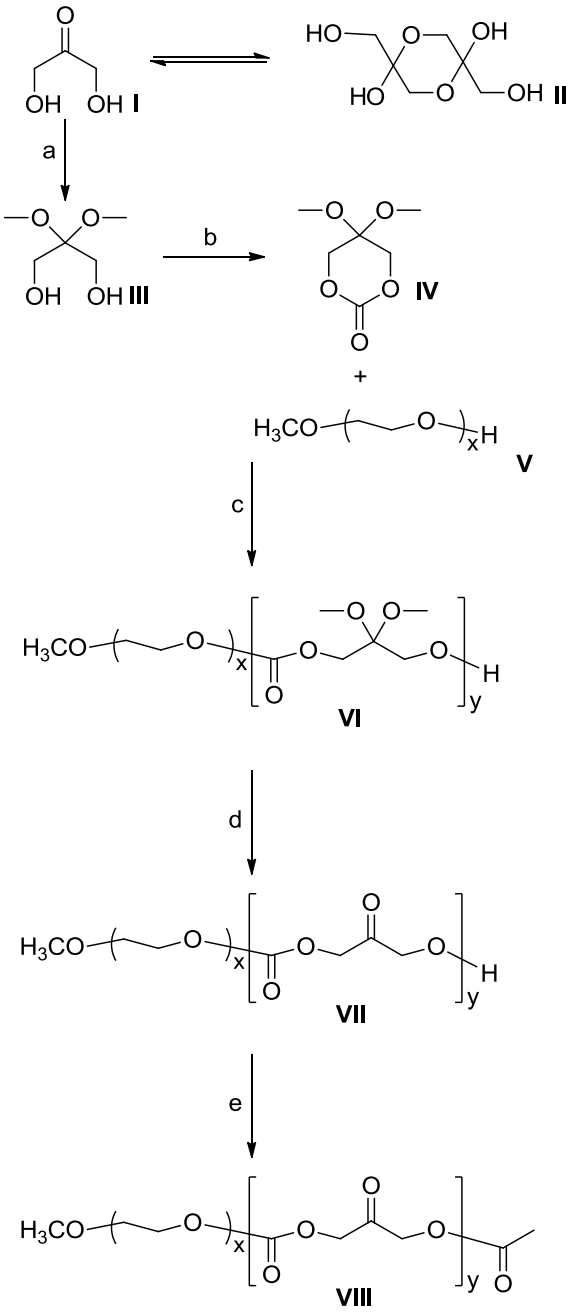

Scheme 6.2. Proposed synthetic route to end-capped MPEG-pDHAC (VIII). a) trimethyl orthoformate, *p*-toluene sulfonic acid, methanol, 24 h; sodium carbonate, 24 h. b) ethylchloroformate, triethylamine, tetrahydrofuran, 3 h. c) stannous octoate, 100ºC, 1-2 h. d) trifluoroacetic acid, water, 12 h, room temperature or I_2, acetone, 1h, reflux. e) acetic anhydride, pyridine or DMAP.

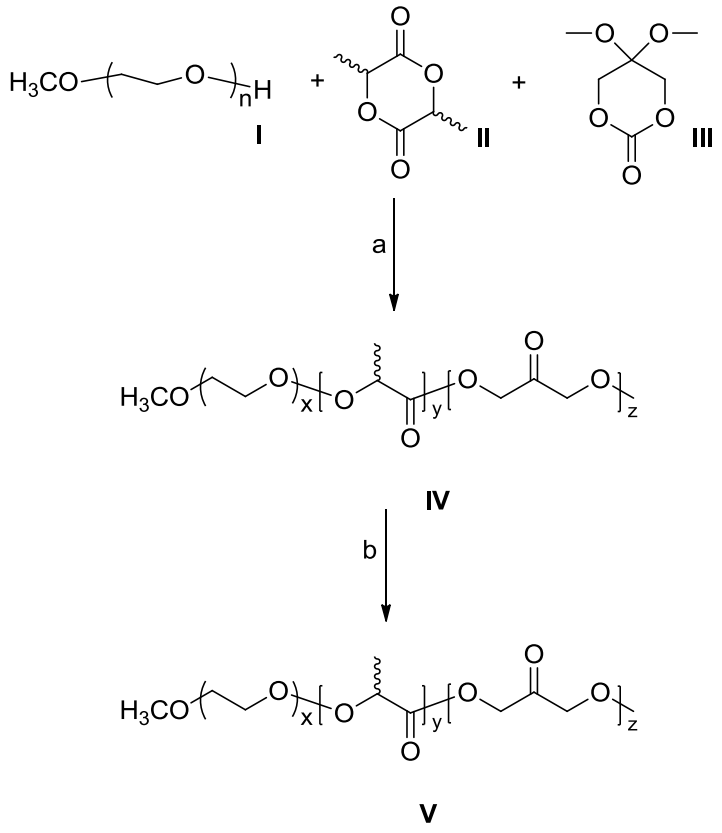

Scheme 6.3. Proposed synthetic route to $MPEG_x$-(pLA_y-*co*-$DHAC_z$) (V). a) stannous octoate, 130ºC, 1-2 h. b) trifluoroacetic acid, water, 12 h, room temperature or I_2, acetone, 1h, reflux.

6.5 Mechanical characterization

Following these structural characterization methods, studies regarding the physical nature of the polymers should commence. To estimate how long the copolymers may remain within an in vivo environment, studies similar to those conducted with the p(LA_x-*co*-$DHAC_y$) copolymers will be performed. The copolymers could be incubated in PBS (pH 7.4, 37ºC) and PBS (pH 7.4, 37ºC, 1% esterase) for pre-determined time points (n=3). The use of this second PBS solution with the added esterase will be important to mimic how enzymes may affect the material's degradation and can begin to mimic in vivo conditions.[22] Upon sample recovery, the materials can be lyophilized and the change in mass and dimension recorded. If these polymers are soluble in THF or other common organic solvents, GPC studies to track the molecular mass loss could also occur. If not, the BCA assay may once again be used to determine the rate at which degraded DHA is leaving the copolymer backbones

Another mechanical characterization method could be designed to explore the tissue adhesion kinetics of the polymer to quantify its bioadhesive behavior, which could be the ultimate goal of this class of biomaterial. These experiments could yield data on the Young's Modulus and the yield point (i.e. mechanical characteristics) of the copolymers. Previous in vitro models to test the effect of varying amounts of DHAC within the copolymer have already been established.[181] Additionally, the tissue adhesion kinetic studies, derived from earlier protocols, are able to mimic organ tissues surfaces, the origin of post-operative tissue adhesions. To accurately create the model tissue surface, collagen Type I derived from bovine calf skin could be cast and allowed to adhere to glass microscope slides. The adhesion characteristics can then be quantified by tensile strength analysis (Instron). The Young's modulus and yield strength of the adhesion layer could be determined on different samples at various time points to produce a

strength vs. time profile for each polymeric material.

APPENDIX

A.1 GK-12 genetics module

Introduction to Agarose Gel Electrophoresis: A Precursor to CIBT's DNA Profiling or Protein Gel Electrophoresis laboratories

Author: Jennifer Weiser and Laura Austen
Date Created: 2010
Subject: Molecular Biology and Genetics
Level: High School
Standards: *New York State- The Living Environment*
(http://www.emsc.nysed.gov/ciai/mst/pub/livingen.pdf)
Standard 1: Inquiry and Design
Standard 4.2.1: Genetics
Schedule: One 90 minute class period

Objectives:

To introduce students to the concepts of gel electrophoresis without requiring all the equipment needed to run a full gel electrophoresis experiment. The goal is to have students understand how gels are made for DNA separation and how altering the composition can affect the experimental parameters.

Students will:

- Mix and pour agarose gels of varying consistencies
- Predict how changing the percent agarose will effect the outcome
- Practice micropipetting

Vocabulary:

Gel Electrophoresis **Buffer**
Gel Chamber **Agarose**
Micropipette

Materials:

For Each Pair:

2-3 grams agarose
100 ml 1x Tris/Borate/EDTA (TBE) Buffer
Gel casting tray and comb
High walled container to (plastic box, tray, etc)
0-20 µl micropipette (for every 3-4 pairs)
Water
Hot/stir plate (for every 3-4 groups)
Erlenmeyer flask
Stir bar
Balance (for class)
Food coloring
Gloves
Goggles

Safety:

All students should use gloves and goggles. Caution should be used while heating and dissolving agarose in TBE buffer.

Science Content for the Teacher:

Gel Electrophoresis is a technique widely used in professional laboratory settings. There are a number of types of electrophoresis, but one of the most basic is that of agarose gel electrophoresis. This technique is used in laboratories all over the world to separate DNA based on size. To do this, a sample of DNA is amplified millions of times using Polymerase Chain Reaction (PCR) and then cut up into smaller segments using restriction enzymes. This DNA sample is then loaded into an agarose gel using a micropipette and exposed to an electric current. This current causes the DNA to move along the gel away from the negative electrode (anode) to the positive (cathode). This movement is impeded by the agarose gel's composition, separating the DNA solely based on size (molecular weight). A molecular weight marker is often also used for later comparison. Once run, a visualization technique can be used to see the bands of different sized DNA along the gel.

Agarose: Agarose is a linear polymer that is derived from red algae. Upon mixing with buffer and allowed to set, a gel matrix forms. This matrix, which can be thought of as a rubber band maze, impedes the flow of DNA. Larger DNA fragments become more entangled and take longer to move through this matrix while the smaller fragments can navigate through the pores of the matrix more easily. By adjusting the concentration of agarose used in the gel you can manipulate the porosity (size and number of holes). The more concentrated the gel, the smaller the pores and thus DNA would take longer to move. Larger fragments would not move as far through the gel, however, this would cause a better separation of smaller sized (lower molecular weight) DNA fragments. Conversely, the less concentrated the gel, the faster the fragments will move through the gel. This change in gel concentration would result in poorer resolution between the smaller DNA fragments since there are more pores through which the may move.

DNA: Deoxyribonucleic acid, DNA, is essentially the blue prints for all living organisms. DNA is a polymer based on four repeating nucleotides that is arranged in a double helix. Due to the inherent negative charge of these nucleotides, DNA is a negatively charged molecule. It is this feature that allows gel electrophoresis to separate the pieces of DNA based only on size.

PCR: Polymerase Chain reaction is a simple technique to make an exponential number of copies of the DNA in question. This is done to make it easier to visualize the DNA after the experiment has run. The basics of this technique are three stages that keep repeating until stopped. First the double strand is denatured or broken apart at a high temperature. Next extra free floating copies of the four nucleotides anneal or attach to each strand making a new, complimentary strand. Then these new, complimentary strands elongate or add more nucleotides to match the exact length of the strand it is copying. This process, as mentioned before, can go on indefinitely until the user stops the reaction or the reagents, such as the free floating nucleotides, run out.

Restriction Enzymes: These are enzymes that target specific nucleotide sequences within the DNA. By being so specific, each strand of DNA is cut at the exact same place as all of the other copies made by PCR amplification.

Molecular Weight Marker: This is a standard sample that has a known molecular weight for each fragment it contains. By comparing the sample you have run to the standard, you can get an approximate size for each of your DNA fragments.

Micropipette: This is a very exact tool used by scientists to deliver a set amount of material. The pipette is variable and can deliver very precise amounts just by adjusting the value located on the side. When using the micropipette to deliver a DNA sample or in this lab's case, colored dye, it is important not to pierce the agarose gel by going to far into the well each comb

has produced. It is also important not to inject the sample too violently or trapped air bubbles will push out the sample

Preparation:

1. Each group should have an Erlenmeyer flask with 100 ml 1x TBE buffer, gel casting tray and comb, gloves, and secondary container with walls higher than those of the gel casting tray.
2. If TBE buffer can not purchased it can be made beforehand. To make a 5x concentrated TBE stock solution, which can be diluted to 1x later on, you must first create a 0.5 M EDTA stock solution. Weigh out 93.05 g EDTA disodium salt and dissolve this in 400 mL deionized water. Adjust the pH to 8 using sodium hydroxide and then add more deionized water to equal 500 mL. In a separate container add 54 g tris base and 27.5 g boric acid to 900 mL deionized water. Add 20 mL of the EDTA stock solution previously prepared and add more deionized water to equal 1L. Dilute to 1x before using.
3. Pre-heat the stir/hot plates prior to the beginning of class

Classroom Procedure:

Engage (Time: 15 minutes)

Show the students all of the electrophoresis equipment and micropipettes. Let them know what an agarose gel is and how it works. Ask the students to predict what would happen if you would change the formula to make a standard 1% gel. Also, show the students the proper pipetting technique before the start of the experiment. This can be done while you are waiting for the gels to solidify.

Explore (Time: 60 minutes)

Split the students up into groups of 2 and have them go to a work station. Have each group decide on a different percent agarose gel to make. Allow each group to weigh out the proper amount of agarose on the balance and have them add it to their 100 ml of TBE buffer. Put the flask on the hot plate with a stir bar running slowly (Note: If you do not have a stir plate you can use a metal spatula to help stir it gently). Once the agarose has dissolved allow it to cool before pouring it into the gel tray. Add the comb and allow the mixture to solidify (at least 30 minutes depending on the percent agarose in the gel).

You can take this time to explain a little about the properties of agarose gels and how they are used in laboratories.

Once the gels have set, have the students (with gloves on) feel the gels and compare their relative strengths. Ask them to see how their findings match up with their initial predictions.

Optional: Have the students keep track of how long each percent gel takes to solidify.

Place the gels in the secondary container and add enough water to cover the gel. Carefully remove the combs from the gels and have the students try to pipette 8 µl of food

coloring into the well.

Explain (Time: 15 minutes)

You can use the time during gel solidification to begin to explain the concepts of gel electrophoresis. After finishing the hands on part, have the students discuss how their initial predictions compared to what they actually observed. Then ask the students to try and explain how altering the percentage weight of the gel might affect a gel electrophoresis experiment.

Assessment:

The following rubric can be used to assess students during each part of the activity. The term "expectations" here refers to the content, process and attitudinal goals for this activity. Evidence for understanding may be in the form of oral as well as written communication, both with the teacher as well as observed communication with other students. Specifics are listed in the table below.

1= exceeds expectations

2= meets expectations consistently

3= meets expectations occasionally

4= not meeting expectations

	Engage	Explore	Explain
	Shows leadership in the discussion and offers creative ideas reflecting a good understanding of electrophoresis.	Completes work accurately while providing an explanation for what is observed. Works very well with partner.	Provides an in-depth explanation of findings, making connections with real world applications
	Participates in prediction and shows an understanding of gel electrophoresis.	Completes work accurately and works cooperatively with partner.	Provides clear explanation of findings.
	Contributes to the predictions, but shows little understanding of gel electrophoresis.	Works cooperatively with partner, but makes some mistakes with the procedure.	Provides a limited explanation of findings.
	Does not participate. Shows no understanding of laboratory concepts.	Has trouble working with partner. Does little to complete the procedure.	Is not clear in explanation of findings.

Extension Activities:

This lab is a precursor to Cornell's Institute for Biology Teachers lab's entitled DNA Profiling – Paternity Testing (http://cibt.bio.cornell.edu/labs/dl/DNAP.PDF) or Using Protein Gel Electrophoresis to Study Evolution (http://cibt.bio.cornell.edu/labs/dl/PGEL.pdf)

Safety:

All students must have on the proper safety equipment when working with the agarose

gels (goggles and gloves). Care should be taken when using the hot plate or removing the heated agarose/TBE buffer mixture.

Acknowledgments:

Dr. Shivaun Archer, Department of Biomedical Engineering, Cornell University

Dr. Christopher Schaffer, Department of Biomedical Engineering, Cornell University

Nev Singhota, Director of EPO, Cornell University

A.2 GK-12 Survery 2009-2010

Biochemistry

What is an organic compound? Can you name one example?

What is a polymer? Can you name one example?

What is an enzyme? What do we mean when we say enzymes are specific?

How is a protein made?

Physiology

What is biomedical engineering? Name one application of current biomedical research.

What is a biomaterial? Can you name one example?

Name two components of bone and why do they make it unique?

Cell

What is chromatography? Can you name one type of chromatography?

Genetics

What is gel electrophoresis? Can you name one application?

What does polymerase chain reaction (PCR) do?

Extra

Do you use science in your everyday life?

Do you use math in your everyday life?

Do you think you will use science or math in your everyday life after high school?

Would you be interested in a career in science or math?

REFERENCES

1. Dee, K., Puleo, D, Bizios, R, *An Introduction to Tissue-Biomaterial Interactions*. John Wiley & Sons, Inc.: 2002.

2. Shastri, V. P., Non-degradable biocompatible polymers in medicine: past, present and future. *Curr Pharm Biotechnol* **2003,** *4* (5), 331-337.

3. Peppas, N. A.; Langer, R., New Challenges in Biomaterials. *Science* **1994,** *263* (5154), 1715-1720.

4. Anderson, J. M., The future of biomedical materials. *Journal of Materials Science-Materials in Medicine* **2006,** *17* (11), 1025-1028.

5. Moore, D. B.; Harris, A.; Siesky, B., The world through a lens: the vision of Sir Harold Ridley. *British Journal of Ophthalmology* **2010,** *94* (10), 1277-1280.

6. Reisch, M. S., Medical polymers renaissance. *Chemical & Engineering News* **2007,** *85* (45), 14-17.

7. Langer, R.; Vacanti, J. P., Tissue Engineering. *Science* **1993,** *260* (5110), 920-926.

8. Putnam, D., DRUG DELIVERY The heart of the matter. *Nature Materials* **2008,** *7* (11), 836-837.

9. Albertsson, A. C.; Varma, I. K., Recent developments in ring opening polymerization of lactones for biomedical applications. *Biomacromolecules* **2003,** *4* (6), 1466-1486.

10. Holland, S. J.; Tighe, B. J.; Gould, P. L., Polymers for biodegradable medical devices. 1. The potential of polyesters as controlled macromolecular release systems. *Journal of Controlled Release* **1986,** *4* (3), 155-180.

11. Frazza, E. J.; Schmitt, E. E., A new absorbable suture. *J Biomed Mater Res* **1971,** *5* (2), 43-58.

12. Brem, H.; Lawson, H. C., The development of new brain tumor therapy utilizing the local and sustained delivery of chemotherapeutic agents from biodegradable polymers. *Cancer* **1999,** *86* (2), 197-199.

13. Dang, W. B.; Daviau, T.; Brem, H., Morphological characterization of polyanhydride biodegradable implant GLIADEL® during in vitro and in vivo erosion using scanning electron microscopy. *Pharmaceutical Research* **1996,** *13* (5), 683-691.

14. Kumar, N.; Langer, R. S.; Domb, A. J., Polyanhydrides: an overview. *Advanced Drug Delivery Reviews* **2002,** *54* (7), 889-910.

15. Vacanti, C. A.; Langer, R.; Schloo, B.; Vacanti, J. P., Synthetic-Polymers Seeded with Chondrocytes Provide a Template for New Cartilage Formation. *Plastic and Reconstructive Surgery* **1991,** *88* (5), 753-759.

16. Cohen, S.; Yoshioka, T.; Lucarelli, M.; Hwang, L. H.; Langer, R., Controlled Delivery Systems for Proteins Based on Poly(Lactic Glycolic Acid) Microspheres. *Pharmaceutical Research* **1991,** *8* (6), 713-720.

17. Freed, L. E.; Vunjaknovakovic, G.; Biron, R. J.; Eagles, D. B.; Lesnoy, D. C.; Barlow, S. K.; Langer, R., Biodegradable Polymer Scaffolds for Tissue Engineering. *Bio-Technology* **1994,** *12* (7), 689-693.

18. Sundback, C. A.; Shyu, J. Y.; Wang, Y. D.; Faquin, W. C.; Langer, R. S.; Vacanti, J. P.; Hadlock, T. A., Biocompatibility analysis of poly(glycerol sebacate) as a nerve guide material. *Biomaterials* **2005,** *26* (27), 5454-5464.

19. Wang, Y. D.; Ameer, G. A.; Sheppard, B. J.; Langer, R., A tough biodegradable elastomer. *Nature Biotechnology* **2002,** *20* (6), 602-606.

20. Henderson, P. W.; Kadouch, D. J. M.; Singh, S. P.; Zawaneh, P. N.; Weiser, J.; Yazdi, S.; Weinstein, A.; Krotscheck, U.; Wechsler, B.; Putnam, D.; Spector, J. A., A rapidly resorbable hemostatic biomaterial based on dihydroxyacetone. *Journal of Biomedical Materials Research Part A* **2010,** *93A* (2), 776-782.

21. Zawaneh, P. N.; Doody, A. M.; Zelikin, A. N.; Putnam, D., Diblock copolymers based on dihydroxyacetone and ethylene glycol: Synthesis, characterization, and nanoparticle formulation. *Biomacromolecules* **2006,** *7* (11), 3245-3251.

22. Zawaneh, P. N.; Singh, S. P.; Padera, R. F.; Henderson, P. W.; Spector, J. A.; Putnam, D., Design of an injectable synthetic and biodegradable surgical biomaterial. *Proceedings of the National Academy of Sciences of the United States of America* **2010,** *107* (24), 11014-11019.

23. Soler, C.; Soley, M., Rapid and Delayed-Effects of Epidermal Growth-Factor on Gluconeogenesis. *Biochemical Journal* **1993,** *294*, 865-872.

24. Levy, S. B., Dihydroxyacetone-Containing Sunless or Self-Tanning Lotions. *Journal of the American Academy of Dermatology* **1992,** *27* (6), 989-993.

25. Zelikin, A. N.; Putnam, D., Poly(carbonate-acetal)s from the dimer form of dihydroxyacetone. *Macromolecules* **2005,** *38* (13), 5532-5537.

26. Zelikin, A. N.; Zawaneh, P. N.; Putnam, D., A functionalizable biomaterial based on dihydroxyacetone, an intermediate of glucose metabolism. *Biomacromolecules* **2006,** *7* (11), 3239-3244.

27. Zawaneh, P. N.; Putnam, D., Materials in Surgery: A Review of Biomaterials in Postsurgical Tissue Adhesion and Seroma Prevention. *Tissue Engineering Part B-Reviews* **2008,** *14* (4), 377-391.

28. von Burkersroda, F.; Schedl, L.; Gopferich, A., Why degradable polymers undergo surface erosion or bulk erosion. *Biomaterials* **2002,** *23* (21), 4221-4231.

29. Gopferich, A., Polymer bulk erosion. *Macromolecules* **1997,** *30* (9), 2598-2604.

30. Li, S. M.; Vert, M., Morphological-Changes Resulting from the Hydrolytic Degradation of Stereocopolymers Derived from L-Lactides and DL-Lactides. *Macromolecules* **1994,** *27* (11), 3107-3110.

31. Walker, J. M., The bicinchoninic acid (BCA) assay for protein quantitation. *Methods Mol Biol* **1994,** *32*, 5-8.

32. Garcia, E.; Johnston, D.; Whitaker, J. R.; Shoemaker, S. P., Assessment of Endo-1,4-Beta-D-Glucanase Activity by a Rapid Colorimetric Assay Using Disodium 2,2'-Bicinchoninate. *Journal of Food Biochemistry* **1993,** *17* (3), 135-145.

33. Dash, S.; Murthy, P. N.; Nath, L.; Chowdhury, P., Kinetic Modeling on Drug Release from Controlled Drug Delivery Systems. *Acta Poloniae Pharmaceutica* **2010,** *67* (3), 217-223.

34. Katti, D. S.; Lakshmi, S.; Langer, R.; Laurencin, C. T., Toxicity, biodegradation and elimination of polyanhydrides. *Advanced Drug Delivery Reviews* **2002,** *54* (7), 933-961.

35. Higuchi, T., Mechanism of Sustained-Action Medication - Theoretical Analysis of Rate of Release of Solid Drugs Dispersed in Solid Matrices. *Journal of Pharmaceutical Sciences* **1963,** *52* (12), 1145-&.

36. Hixson, A. W.; Crowell, J. H., Dependence of reaction velocity upon surface and agitation I - Theoretical consideration. *Industrial and Engineering Chemistry* **1931,** *23*, 923-931.

37. Korsmeyer, R. W.; Gurny, R.; Doelker, E.; Buri, P.; Peppas, N. A., Mechanisms of Solute Release from Porous Hydrophilic Polymers. *International Journal of Pharmaceutics* **1983,** *15* (1), 25-35.

38. Korsmeyer, R. W.; Vonmeerwall, E.; Peppas, N. A., Solute and Penetrant Diffusion in Swellable Polymers .2. Verification of Theoretical-Models. *Journal of Polymer Science Part B-Polymer Physics* **1986,** *24* (2), 409-434.

39. Peppas, N. A., Analysis of Fickian and non-Fickian drug release from polymers. *Pharm Acta Helv* **1985,** *60* (4), 110-111.

40. Peppas, N. A.; Brannon-Peppas, L., Water Diffusion and Sorption in Amorphous Macromolecular Systems and Foods. *Journal of Food Engineering* **1994,** *22* (1-4), 189-210.

41. Hubbell, J. A., Synthetic biodegradable polymers for tissue engineering and drug delivery. *Current Opinion in Solid State & Materials Science* **1998,** *3* (3), 246-251.

42. Li, W. J.; Laurencin, C. T.; Caterson, E. J.; Tuan, R. S.; Ko, F. K., Electrospun nanofibrous structure: a novel scaffold for tissue engineering. *J Biomed Mater Res* **2002,** *60* (4), 613-621.

43. Engelberg, I.; Kohn, J., Physicomechanical Properties of Degradable Polymers Used in Medical Applications - a Comparative-Study. *Biomaterials* **1991,** *12* (3), 292-304.

44. Soler, C.; Soley, M., Rapid and delayed effects of epidermal growth factor on gluconeogenesis. *Biochem J* **1993,** *294 (Pt 3)*, 865-872.

45. Du, Y. J.; Lemstra, P. J.; Nijenhuis, A. J.; Vanaert, H. A. M.; Bastiaansen, C., ABA Type Copolymers of Lactide with Poly(Ethylene Glycol) - Kinetic, Mechanistic, and Model Studies. *Macromolecules* **1995,** *28* (7), 2124-2132.

46. Ovitt, T. M.; Coates, G. W., Stereochemistry of lactide polymerization with chiral catalysts: New opportunities for stereocontrol using polymer exchange mechanisms. *Journal of the American Chemical Society* **2002,** *124* (7), 1316-1326.

47. Park, T. G., Degradation of Poly(Lactic-Co-Glycolic Acid) Microspheres - Effect of Copolymer Composition. *Biomaterials* **1995,** *16* (15), 1123-1130.

48. Zhu, G. Z.; Mallery, S. R.; Schwendeman, S. P., Stabilization of proteins encapsulated in injectable poly (lactide-co-glycolide). *Nature Biotechnology* **2000,** *18* (1), 52-57.

49. Anderson, J. M.; Shive, M. S., Biodegradation and biocompatibility of PLA and PLGA microspheres. *Advanced Drug Delivery Reviews* **1997,** *28* (1), 5-24.

50. Reed, A. M.; Gilding, D. K., Biodegradable Polymers for Use in Surgery - Poly(Glycolic)-Poly(Lactic Acid) Homo and Co-Polymers .2. Invitro Degradation. *Polymer* **1981,** *22* (4), 494-498.

51. Ray, W. C.; Grinstaff, M. W., Polycarbonate and poly(carbonate-ester)s synthesized from biocompatible building blocks of glycerol and lactic acid. *Macromolecules* **2003,** *36* (10), 3557-3562.

52. Liu, R.; Wade, J. E.; Wolinsky, J. B.; Winer, J. H.; Catalano, P. J.; Wagner, A. J.; Grinstaff, M. W.; Colson, Y. L.; Raut, C. P., Paclitaxel-Eluting Polymer Film Reduces Locoregional Recurrence in Mouse Model of Sarcoma: A Novel Investigational Therapy. *Annals of Surgical Oncology* **2010,** *17*, S31-S32.

53. Liu, R.; Wolinsky, J. B.; Walpole, J.; Southard, E.; Chirieac, L. R.; Grinstaff, M. W.; Colson, Y. L., Prevention of Local Tumor Recurrence Following Surgery Using Low-Dose Chemotherapeutic Polymer Films. *Annals of Surgical Oncology* **2010,** *17* (4), 1203-1213.

54. Wolinsky, J. B.; Ray, W. C.; Colson, Y. L.; Grinstaff, M. W., Poly(carbonate ester)s based on units of 6-hydroxyhexanoic acid and glycerol. *Macromolecules* **2007,** *40* (20), 7065-7068.

55. Sun, J. W.; Dong, Y. M.; Cao, L. Y.; Wang, X. Y.; Wang, S. Z.; Hu, Y. F., Highly efficient chemoselective deprotection of O,O-acetals and O,O-ketals catalyzed by molecular iodine in acetone. *Journal of Organic Chemistry* **2004,** *69* (25), 8932-8934.

56. Alexis, F., Factors affecting the degradation and drug-release mechanism of poly(lactic acid) and poly[(lactic acid)-co-(glycolic acid)]. *Polymer International* **2005,** *54* (1), 36-46.

57. Heller, J., Controlled Drug Release from Poly(Ortho Esters). *Annals of the New York Academy of Sciences* **1985,** *446*, 51-66.

58. Pego, A. P.; Poot, A. A.; Grijpma, D. W.; Feijen, J., In vitro degradation of trimethylene carbonate based (Co)polymers. *Macromolecular Bioscience* **2002,** *2* (9), 411-419.

59. Yang, J.; Liu, F.; Yang, L.; Li, S. M., Hydrolytic and enzymatic degradation of poly(trimethylene carbonate-co-D,L-lactide) random copolymers with shape memory behavior. *European Polymer Journal* **2010,** *46* (4), 783-791.

60. Jie, C.; Zhu, K. J., Preparation, characterization and biodegradable characteristics of poly(D,L-lactide-co-1,3-trimethylene carbonate). *Polymer International* **1997,** *42* (4), 373-379.

61. Schmidt, P.; Keul, H.; Hocker, H., Copolymerization of 2,2-dimethyltrimethylene carbonate and L,L-lactide. *Macromolecules* **1996,** *29* (11), 3674-3680.

62. Espartero, J. L.; Rashkov, I.; Li, S. M.; Manolova, N.; Vert, M., NMR analysis of low molecular weight poly(lactic acid)s. *Macromolecules* **1996,** *29* (10), 3535-3539.

63. Zell, M. T.; Padden, B. E.; Paterick, A. J.; Thakur, K. A. M.; Kean, R. T.; Hillmyer, M. A.; Munson, E. J., Unambiguous determination of the C-13 and H-1 NMR stereosequence assignments of polylactide using high-resolution solution NMR spectroscopy. *Macromolecules* **2002,** *35* (20), 7700-7707.

64. Thakur, K. A. M.; Kean, R. T.; Hall, E. S.; Kolstad, J. J.; Lindgren, T. A.; Doscotch, M. A.; Siepmann, J. I.; Munson, E. J., High-resolution C-13 and H-1 solution NMR study of poly(lactide). *Macromolecules* **1997,** *30* (8), 2422-2428.

65. Chabot, F.; Vert, M.; Chapelle, S.; Granger, P., Configurational Structures of Lactic-Acid Stereocopolymers as Determined by C-13-Labeled (H-1)-Nmr. *Polymer* **1983,** *24* (1), 53-59.

66. *ChemBioDraw Ultra 11*, CambridgeSoft: 2007.

67. Celikkaya, E.; Denkbas, E. B.; Piskin, E., Poly(DL-lactide)/Poly(ethylene glycol) copolymer particles .1. Preparation and characterization. *Journal of Applied Polymer Science* **1996,** *61* (9), 1439-1446.

68. Fox, T. G.; Flory, P. J., The Glass Temperature and Related Properties of Polystyrene - Influence of Molecular Weight. *Journal of Polymer Science* **1954,** *14* (75), 315-319.

69. Ueberreiter, K.; Kanig, G., Self-Plasticization of Polymers. *Journal of Colloid Science* **1952,** *7* (6), 569-583.

70. Li, S. M.; Garreau, H.; Vert, M., Structure Property Relationships in the Case of the Degradation of Massive Aliphatic Poly-(Alpha-Hydroxy Acids) in Aqueous-Media .1. Poly(DL-Lactic Acid). *Journal of Materials Science-Materials in Medicine* **1990,** *1* (3), 123-130.

71. Li, S. M.; Garreau, H.; Vert, M., Structure Property Relationships in the Case of the Degradation of Massive Poly(Alpha-Hydroxy Acids) in Aqueous-Media .2. Degradation of Lactide-Glycolide Copolymers - Pla37.5ga25 and Pla75ga25. *Journal of Materials Science-Materials in Medicine* **1990,** *1* (3), 131-139.

72. Mopper, K.; Gindler, E. M., New Noncorrosive Dye Reagent for Automatic Sugar Chromatography. *Analytical Biochemistry* **1973,** *56* (2), 440-442.

73. McFeeters, R. F., A manual method for reducing sugar determinations with 2,2'-bicinchoninate reagent. *Anal Biochem* **1980,** *103* (2), 302-306.

74. Waffenschmidt, S.; Jaenicke, L., Assay of reducing sugars in the nanomole range with 2,2'-bicinchoninate. *Anal Biochem* **1987,** *165* (2), 337-40.

75. Smith, P. K.; Krohn, R. I.; Hermanson, G. T.; Mallia, A. K.; Gartner, F. H.; Provenzano, M. D.; Fujimoto, E. K.; Goeke, N. M.; Olson, B. J.; Klenk, D. C., Measurement of Protein Using Bicinchoninic Acid. *Analytical Biochemistry* **1985,** *150* (1), 76-85.

76. Wiechelman, K. J.; Braun, R. D.; Fitzpatrick, J. D., Investigation of the Bicinchoninic Acid Protein Assay - Identification of the Groups Responsible for Color Formation. *Analytical Biochemistry* **1988,** *175* (1), 231-237.

77. Brown, R. E.; Jarvis, K. L.; Hyland, K. J., Protein measurement using bicinchoninic acid: elimination of interfering substances. *Anal Biochem* **1989,** *180* (1), 136-139.

78. Kessler, R. J.; Fanestil, D. D., Interference by Lipids in the Determination of Protein Using Bicinchoninic Acid. *Analytical Biochemistry* **1986,** *159* (1), 138-142.

79. Baker, W. L., Potential Interference of Hydrogen-Peroxide in the 2,2'-Bicinchoninic Acid Protein Assay. *Analytical Biochemistry* **1991,** *192* (1), 212-214.

80. Vashist, S. K.; Zhang, B. B.; Zheng, D.; Al-Rubeaan, K.; Luong, J. H. T.; Sheu, F. S., Sulfo-N-hydroxysuccinimide interferes with bicinchoninic acid protein assay. *Analytical Biochemistry* **2011,** *417* (1), 156-158.

81. Hill, H. D.; Straka, J. G., Protein Determination Using Bicinchoninic Acid in the Presence of Sulfhydryl-Reagents. *Analytical Biochemistry* **1988,** *170* (1), 203-208.

82. Tyllianakis, P. E.; Kakabakos, S. E.; Evangelatos, G. P.; Ithakissios, D. S., Direct Colorimetric Determination of Solid-Supported Functional-Groups and Ligands Using Bicinchoninic Acid. *Analytical Biochemistry* **1994,** *219* (2), 335-340.

83. Thornalley, P.; Wolff, S.; Crabbe, J.; Stern, A., The Autoxidation of Glyceraldehyde and Other Simple Monosaccharides under Physiological Conditions Catalyzed by Buffer Ions. *Biochimica Et Biophysica Acta* **1984,** *797* (2), 276-287.

84. Wolff, S. P.; Crabbe, M. J. C.; Thornalley, P. J., The Autoxidation of Glyceraldehyde and Other Simple Monosaccharides. *Experientia* **1984,** *40* (3), 244-246.

85. Singh, S. V.; Saxena, O. C.; Singh, M. P., Mechanism of Copper(II) Oxidation of Reducing Sugars .1. Kinetics and Mechanism of Oxidation of D-Xylose, L-Arabinose, D-Glucose, D-Fructose, D-Mannose, D-Galactose, L-Sorbose, Lactose, Maltose, Cellobiose, and Melibiose by Copper(II) in Alkaline Medium. *Journal of the American Chemical Society* **1970,** *92* (3), 537-541.

86. Carey, F. A., *Organic Chemistry*. Fifth ed.; McGraw-Hill New York, 2003.

87. Rangappa, K. S.; Manjunathaswamy, H.; Raghavendra, M. P.; Gowda, D. C., Oxidation of threose-series pentoses and hexoses by sodium N-chloro-p-toluenesulfonamide. *Carbohydrate Research* **1998,** *307* (3-4), 253-262.

88. Morrison, R. T., *Organic Chemistry*. 4th ed.; Allyn and Bacon, Inc.: Newton, 1983.

89. Garrett, R. H.; Grisham, C. M., *Biochemistry*. 4th ed.; Cengage Learning: Boston, 2009.

90. Yaylayan, V. A.; Harty-Majors, S.; Ismail, A. A., Investigation of DL-glyceraldehyde-dihydroxyacetone interconversion by FTIR spectroscopy. *Carbohydrate Research* **1999,** *318* (1-4), 20-25.

91. Rhein, L. D.; Schlossman, M.; O'Lenick, A.; Somasundaran, P., *Surfactants in Personal Care Products and Decorative Cosmetics*. Third ed.; CRC Press: 2006.

92. Milton, J. D.; Mullen, P. J., The Effect of Reducing and Nonreducing Sugars on the Bicinchoninic Acid Reaction for Protein Determination. *Clinica Chimica Acta* **1992,** *208* (1-2), 141-143.

93. Cerchiaro, G.; Saboya, P. L.; Ferreira, A. M. D.; Tomazela, D. M.; Eberlin, M. N., Keto-enolic equilibria of an isatin-Schiff base copper(II) complex and its reactivity toward carbohydrate oxidation. *Transition Metal Chemistry* **2004,** *29* (5), 495-504.

94. Yaylayan, V. A.; Ismail, A. A., Investigation of the Enolization and Carbonyl Group Migration in Reducing Sugars by Ftir Spectroscopy. *Carbohydrate Research* **1995,** *276* (2), 253-265.

95. Bradford, M. M., Rapid and Sensitive Method for Quantitation of Microgram Quantities of Protein Utilizing Principle of Protein-Dye Binding. *Analytical Biochemistry* **1976,** *72* (1-2), 248-254.

96. Buehler, C. A., Hindered + Chelated 1,2-Enediols. *Chemical Reviews* **1964,** *64* (1), 7-18.

97. Macfadyen, D. A.; Fowler, N., On the Mechanism of the Reaction of Ninhydrin with Alpha-Amino Acids .2. A Spectrophotometric Study of Hydrindantin Reactions. *Journal of Biological Chemistry* **1950,** *186* (1), 13-22.

98. Joullie, M. M.; Thompson, T. R.; Nemeroff, N. H., Ninhydrin and Ninhydrin Analogs - Syntheses and Applications. *Tetrahedron* **1991,** *47* (42), 8791-8830.

99. West, E. S.; Rinehart, R. E., Reaction of ninhydrin with ascorbic acid and other endiol compounds - Decarboxylation of dehydroascorbic acid. *Journal of Biological Chemistry* **1942,** *146* (1), 105-108.

100. Wigfield, D. C.; Buchanan, G. W.; Croteau, S. M., On Ruhemanns Purple. *Canadian Journal of Chemistry-Revue Canadienne De Chimie* **1980,** *58* (3), 201-205.

101. Marshall, B. A.; Waters, W. A., Oxidations of Organic Compounds by Cupric Salts .1. Kinetics of the Oxidations of Glucose and Acetoin. *Journal of the Chemical Society* **1960,** (Jun), 2392-2398.

102. Marshall, B. A.; Waters, W. A., Oxidations of Organic Compounds by Cupric Salts .2. Oxidation of Benzoin. *Journal of the Chemical Society* **1961,** (Apr), 1579-1582.

103. Dickerson, R.; Takano, T.; Eisenber.D.; Kallai, O. B.; Samson, L.; Cooper, A.; Margoliash, E., Ferricytochrome C .1. General Features of Horse and Bonito Proteins at 2.8 a Resolution. *Journal of Biological Chemistry* **1971,** *246* (5), 1511-1535.

104. Wolfrom, M. L.; Lewis, W. L., The reactivity of the methylated sugars II The action of dilute alkali on tetramethyl glucose. *Journal of the American Chemical Society* **1928,** *50*, 837-854.

105. Reeves, H. C.; Ajl, S. J., Enzymatic Synthesis and Metabolism of Hydroxypyruvic Aldehyde. *Journal of Biological Chemistry* **1965,** *240* (2), 569-573.

106. Richard, J. P., Acid-Base Catalysis of the Elimination and Isomerization-Reactions of Triose Phosphates. *Journal of the American Chemical Society* **1984,** *106* (17), 4926-4936.

107. Nagorski, R. W.; Richard, J. P., Mechanistic imperatives for aldose-ketose isomerization in water: Specific, general base- and metal ion-catalyzed isomerization of glyceraldehyde with proton and hydride transfer. *Journal of the American Chemical Society* **2001,** *123* (5), 794-802.

108. O'Donoghue, A. M. C.; Amyes, T. L.; Richard, J. P., Hydron transfer catalyzed by triosephosphate isomerase. products of isomerization of dihydroxyacetone phosphate in D_2O. *Biochemistry* **2005,** *44* (7), 2622-2631.

109. Amyes, T. L.; Richard, J. P., Enzymatic catalysis of proton transfer at carbon: Activation of triosephosphate isomerase by phosphite dianion. *Biochemistry* **2007,** *46* (19), 5841-5854.

110. Nair, L. S.; Laurencin, C. T., Biodegradable polymers as biomaterials. *Progress in Polymer Science* **2007,** *32* (8-9), 762-798.

111. Cleland, J. L.; Langer, R., Formulation and Delivery of Proteins and Peptides - Design and Development Strategies. *Formulation and Delivery of Proteins and Peptides* **1994,** *567*, 1-19.

112. Heller, J., Polymers for Controlled Parenteral Delivery of Peptides and Proteins. *Advanced Drug Delivery Reviews* **1993,** *10* (2-3), 163-204.

113. Domb, A. J., Polymeric Carriers for Regional Drug-Therapy. *Molecular Medicine Today* **1995,** *1* (3), 134-139.

114. Orloff, L. A.; Domb, A. J.; Teomim, D.; Fishbein, I.; Golomb, G., Biodegradable implant strategies for inhibition of restenosis. *Advanced Drug Delivery Reviews* **1997,** *24* (1), 3-9.

115. Okada, M., Chemical syntheses of biodegradable polymers. *Progress in Polymer Science* **2002,** *27* (1), 87-133.

116. Pitt, C. G., The Controlled Parenteral Delivery of Polypeptides and Proteins. *International Journal of Pharmaceutics* **1990,** *59* (3), 173-196.

117. Giteau, A.; Venier-Julienne, M. C.; Aubert-Pouessel, A.; Benoit, J. P., How to achieve sustained and complete protein release from PLGA-based microparticles? *International Journal of Pharmaceutics* **2008,** *350* (1-2), 14-26.

118. Witt, C.; Kissel, T., Morphological characterization of microspheres, films and implants prepared from poly(lactide-co-glycolide) and ABA triblock copolymers: is the erosion controlled by degradation, swelling or diffusion? *European Journal of Pharmaceutics and Biopharmaceutics* **2001,** *51* (3), 171-181.

119. Uhrich, K. E.; Cannizzaro, S. M.; Langer, R. S.; Shakesheff, K. M., Polymeric systems for controlled drug release. *Chemical Reviews* **1999,** *99* (11), 3181-3198.

120. Buchholz, B., Analysis and Characterization of Resorbable DL-Lactide Trimethylene Carbonate Copolyesters. *Journal of Materials Science-Materials in Medicine* **1993,** *4* (4), 381-388.

121. Albertsson, A. C.; Eklund, M., Synthesis of Copolymers of 1,3-Dioxan-2-One and Oxepan-2-One Using Coordination Catalysts. *Journal of Polymer Science Part a-Polymer Chemistry* **1994,** *32* (2), 265-279.

122. Jie, C.; Zhu, K. J.; Yang, S. L., Preparation, characterization and biodegradable characteristics of poly(1,3-trimethylene carbonate-co-glycolide). *Polymer International* **1996,** *41* (4), 369-375.

123. Zhu, K. J.; Hendren, R. W.; Jensen, K.; Pitt, C. G., Synthesis, Properties, and Biodegradation of Poly(1,3-Trimethylene Carbonate). *Macromolecules* **1991,** *24* (8), 1736-1740.

124. Cai, J.; Zhu, K. J.; Yang, S. L., Surface biodegradable copolymers - poly(D,L-lactide-co-1-methyl-1,3-trimethylene carbonate) and poly(D,L-lactide-co-2,2-dimethyl-1,3-trimethylene carbonate): preparation, characterization and biodegradation characteristics in vivo. *Polymer* **1998,** *39* (18), 4409-4415.

125. Weiser, J. R.; Zawaneh, P. N.; Putnam, D., Poly(carbonate-ester)s of Dihydroxyacetone and Lactic Acid as Potential Biomaterials. *Biomacromolecules* **2011,** *12* (4), 977-986.

126. Bilati, U.; Allemann, E.; Doelker, E., Strategic approaches for overcoming peptide and protein instability within biodegradable nano- and microparticles. *European Journal of Pharmaceutics and Biopharmaceutics* **2005,** *59* (3), 375-388.

127. Inkinen, S.; Hakkarainen, M.; Albertsson, A. C.; Sodergard, A., From Lactic Acid to Poly(lactic acid) (PLA): Characterization and Analysis of PLA and Its Precursors. *Biomacromolecules* **2011,** *12* (3), 523-532.

128. Weiser, J. R.; Ricapito, N. G.; Yueh, A.; Weiser, E. L.; Putnam, D., A mechanistic analysis of the quantitation of α-hydroxy ketones by the bicinchoninic acid assay. *Analytical Biochemistry* **2012,** *430* (2), 116-122.

129. Shugar, D., The Measurement of Lysozyme Activity and the Ultra-Violet Inactivation of Lysozyme. *Biochimica Et Biophysica Acta* **1952,** *8* (3), 302-309.

130. Lee, Y. C.; Yang, D., Determination of lysozyme activities in a microplate format. *Analytical Biochemistry* **2002,** *310* (2), 223-224.

131. Carlsson, N.; Borde, A.; Wolfel, S.; Akerman, B.; Larsson, A., Quantification of protein concentration by the Bradford method in the presence of pharmaceutical polymers. *Analytical Biochemistry* **2011,** *411* (1), 116-121.

132. Sapan, C. V.; Lundblad, R. L.; Price, N. C., Colorimetric protein assay techniques. *Biotechnology and Applied Biochemistry* **1999,** *29*, 99-108.

133. Bodmer, D.; Kissel, T.; Traechslin, E., Factors Influencing the Release of Peptides and Proteins from Biodegradable Parenteral Depot Systems. *Journal of Controlled Release* **1992,** *21* (1-3), 129-137.

134. Tabata, Y.; Takebayashi, Y.; Ueda, T.; Ikada, Y., A Formulation Method Using D,L-Lactic Acid Oligomer for Protein Release with Reduced Initial Burst. *Journal of Controlled Release* **1993,** *23* (1), 55-64.

135. Fredenberg, S.; Wahlgren, M.; Reslow, M.; Axelsson, A., The mechanisms of drug release in poly(lactic-co-glycolic acid)-based drug delivery systems-A review. *International Journal of Pharmaceutics* **2011,** *415* (1-2), 34-52.

136. Viswanathan, N. B.; Patil, S. S.; Pandit, J. K.; Lele, A. K.; Kulkarni, M. G.; Mashelkar, R. A., Morphological changes in degrading PLGA and P(DL)LA microspheres: implications for the design of controlled release systems. *Journal of Microencapsulation* **2001,** *18* (6), 783-800.

137. Igartua, M.; Hernandez, R. M.; Esquisabel, A.; Gascon, A. R.; Calvo, M. B.; Pedraz, J. L., Influence of formulation variables on the in-vitro release of albumin from biodegradable microparticulate systems. *Journal of Microencapsulation* **1997,** *14* (3), 349-356.

138. Viswanathan, N. B.; Thomas, P. A.; Pandit, J. K.; Kulkarni, M. G.; Mashelkar, R. A., Preparation of non-porous microspheres with high entrapment efficiency of proteins by a (water-in-oil)-in-oil emulsion technique. *Journal of Controlled Release* **1999,** *58* (1), 9-20.

139. Crotts, G.; Park, T. G., Protein delivery from poly(lactic-co-glycolic acid) biodegradable microspheres: release kinetics and stability issues. *Journal of Microencapsulation* **1998,** *15* (6), 699-713.

140. Park, T. G.; Lu, W. Q.; Crotts, G., Importance of in-Vitro Experimental Conditions on Protein Release Kinetics, Stability and Polymer Degradation in Protein Encapsulated Poly(D,L-Lactic Acid-Co-Glycolic Acid) Microspheres. *Journal of Controlled Release* **1995,** *33* (2), 211-222.

141. Hutchinson, F. G.; Furr, B. J. A., Biodegradable Polymer Systems for the Sustained-Release of Polypeptides. *Journal of Controlled Release* **1990,** *13* (2-3), 279-294.

142. Crotts, G.; Sah, H.; Park, T. G., Adsorption determines in-vitro protein release rate from biodegradable microspheres: Quantitative analysis of surface area during degradation. *Journal of Controlled Release* **1997,** *47* (1), 101-111.

143. Huang, X.; Brazel, C. S., On the importance and mechanisms of burst release in matrix-controlled drug delivery systems. *Journal of Controlled Release* **2001,** *73* (2-3), 121-136.

144. Lee, P. I., Effect of Non-Uniform Initial-Drug Concentration Distribution on the Kinetics of Drug Release from Glassy Hydrogel Matrices. *Polymer* **1984,** *25* (7), 973-978.

145. Park, T. G.; Lee, H. Y.; Nam, Y. S., A new preparation method for protein loaded poly(D,L-lactic-co-glycolic acid) microspheres and protein release mechanism study. *Journal of Controlled Release* **1998,** *55* (2-3), 181-191.

146. Zimm, K. R.; Schwartz, J. B.; O'Connor, R. E., Drug release from a multiparticulate pellet system. *Pharm Dev Technol* **1996,** *1* (1), 37-42.

147. Wind, M. M.; Lenderink, H. J. W., A capacitance study of pseudo-Fickian diffusion in glassy polymer coatings. *Progress in Organic Coatings* **1996,** *28* (4), 239-250.

148. Lassalle, V.; Ferreira, M. L., PLGA based drug delivery systems (DDS) for the sustained release of insulin: insight into the protein/polyester interactions and the insulin release behavior. *Journal of Chemical Technology and Biotechnology* **2010,** *85* (12), 1588-1596.

149. Ritger, P. L.; Peppas, N. A., A simple equation for description of solute release I. Fickian and non-fickian release from non-swellable devices in the form of slabs, spheres, cylinders or discs. *Journal of Controlled Release* **1987,** *5* (1), 23-36.

150. Frisch, H. L., Sorption and Transport in Glassy-Polymers - Review. *Polymer Engineering and Science* **1980,** *20* (1), 2-13.

151. Wu, J. C.; Peppas, N. A., Numerical-Simulation of Anomalous Penetrant Diffusion in Polymers. *Journal of Applied Polymer Science* **1993,** *49* (10), 1845-1856.

152. Natu, M. V.; Gil, M. H.; de Sousa, H. C., Supercritical solvent impregnation of poly(epsilon-caprolactone)/poly(oxyethylene-b-oxypropylene-b-oxyethylene) and poly(epsilon-caprolactone)/poly(ethylene-vinyl acetate) blends controlled release applications. *Journal of Supercritical Fluids* **2008,** *47* (1), 93-102.

153. Liu, C. P. A.; Neogi, P., Sorption of Methylene-Chloride in Semicrystalline Polyethylene Terephthalate. *Journal of Macromolecular Science-Physics* **1992,** *B31* (3), 265-279.

154. Bhatia, S. K., Stochastic-Theory of Transport in Inhomogeneous-Media. *Chemical Engineering Science* **1986,** *41* (5), 1311-1324.

155. Blanco, M. D.; Alonso, M. J., Development and characterization of protein-loaded poly(lactide-co-glycolide) nanospheres. *European Journal of Pharmaceutics and Biopharmaceutics* **1997,** *43* (3), 287-294.

156. Wetter, L. R.; Deutsch, H. F., Immunological Studies on Egg White Proteins .4. Immunochemical and Physical Studies of Lysozyme. *Journal of Biological Chemistry* **1951,** *192* (1), 237-242.

157. Radola, B. J., Isoelectric Focusing in Layers of Granulated Gels .1. Thin-Layer Isoelectric Focusing of Proteins. *Biochimica Et Biophysica Acta* **1973,** *295* (2), 412-428.

158. Edelson, D. C.; Gordin, D. N.; Pea, R. D., Addressing the challenges of inquiry-based learning through technology and curriculum design. *Journal of the Learning Sciences* **1999,** *8* (3-4), 391-450.

159. Abd-El-Khalick, F.; Lederman, N. G., Improving science teachers' conceptions of nature of science: a critical review of the literature. *International Journal of Science Education* **2000,** *22* (7), 665-701.

160. Smith, K. A.; Sheppard, S. D.; Johnson, D. W.; Johnson, R. T., Pedagogies of engagement: Classroom-based practices. *Journal of Engineering Education* **2005,** *94* (1), 87-101.

161. Hmelo-Silver, C. E.; Duncan, R. G.; Chinn, C. A., Scaffolding and achievement in problem-based and inquiry learning: A response to Kirschner, Sweller, and Clark (2006). *Educational Psychologist* **2007,** *42* (2), 99-107.

162. Kind, P.; Jones, K.; Barmby, P., Developing attitudes towards science measures. *International Journal of Science Education* **2007,** *29* (7), 871-893.

163. Bowling, B. V.; Acra, E. E.; Wang, L.; Myers, M. F.; Dean, G. E.; Markle, G. C.; Moskalik, C. L.; Huether, C. A., Development and evaluation of a genetics literacy assessment instrument for undergraduates. *Genetics* **2008,** *178* (1), 15-22.

164. Chambers, D. W., Stereotypic images of the scientist: The draw-a-scientist test. *Science Education* **1983,** *67* (2), 255-265.

165. Korley, J., One-step Synthesis of Polyesters Containing Dihydroxyacetone. *in preparation* **2010**.

166. Korley, J., Biocompatibility of polyesters containing dihydroxyacetone. *in preparation* **2010**.

167. You, Z. W.; Cao, H. P.; Gao, J.; Shin, P. H.; Day, B. W.; Wang, Y. D., A functionalizable polyester with free hydroxyl groups and tunable physiochemical and biological properties. *Biomaterials* **2010,** *31* (12), 3129-3138.

168. Carnahan, M. A.; Grinstaff, M. W., Synthesis and characterization of poly(glycerol-succinic acid) dendrimers. *Macromolecules* **2001,** *34* (22), 7648-7655.

169. Carnahan, M. A.; Grinstaff, M. W., Synthesis and characterization of polyether-ester dendrimers from glycerol and lactic acid. *Journal of the American Chemical Society* **2001,** *123* (12), 2905-2906.

170. Pomerantseva, I.; Krebs, N.; Hart, A.; Neville, C. M.; Huang, A. Y.; Sundback, C. A., Degradation behavior of poly(glycerol sebacate). *Journal of Biomedical Materials Research Part A* **2009,** *91A* (4), 1038-1047.

171. Pryor, H. I.; O'Doherty, E.; Hart, A.; Owens, G.; Hoganson, D.; Vacanti, J. P.; Masiakos, P. T.; Sundback, C. A., Poly(glycerol sebacate) films prevent postoperative adhesions and allow laparoscopic placement. *Surgery* **2009,** *146* (3), 490-497.

172. Korley, J., Dihydroxyacetone-based polyesters: design, synthesis, characterization and evaluation as a biomaterial. *Dissertation* **2010**.

173. Al-Musawi, D.; Thompson, J. N., Adhesion prevention: state of the art. *Gynaecological Endoscopy* **2001,** *10* (2), 123-130.

174. Boland, G. M.; Weigel, R. J., Formation and Prevention of Postoperative Abdominal Adhesions. *Journal of Surgical Research* **2006,** *132* (1), 3-12.

175. Ray Ms, N. F.; Denton Rn, M. B. A. W. G.; Thamer PhD, M.; Henderson Ms, S. C.; Perry Md, M. S., Abdominal Adhesiolysis: Inpatient Care and Expenditures in the United States in 1994. *Journal of the American College of Surgeons* **1998,** *186* (1), 1-9.

176. Ellis, H.; Moran, B. J.; Thompson, J. N.; Parker, M. C.; Wilson, M. S.; Menzies, D.; McGuire, A.; Lower, A. M.; Hawthorn, R. J. S.; O'Brien, F.; Buchan, S.; Crowe, A. M., Adhesion-related hospital readmissions after abdominal and pelvic surgery: a retrospective cohort study. *The Lancet* **1999,** *353* (9163), 1476-1480.

177. Orita, A.; Sakamoto, K.; Hamada, Y.; Mitsutome, A.; Otera, J., Mild and practical acylation of alcohols with esters or acetic anhydride under distannoxane catalysis. *Tetrahedron* **1999,** *55* (10), 2899-2910.

178. Xu, S. J.; Held, I.; Kempf, B.; Mayr, H.; Steglich, W.; Zipse, H., The DMAP-catalyzed acetylation of alcohols - A mechanistic study (DMAP=4-(dimethylamino)pyridine). *Chemistry-a European Journal* **2005,** *11* (16), 4751-4757.

179. Rosen, I.; Sturm, C. L., Poly(Chloroaldehydes) .3. Poly(Dichloroacetaldehyde). *Journal of Polymer Science Part a-General Papers* **1965,** *3* (11PA), 3741-3751.

180. Masamoto, J.; Matsuzaki, K.; Iwaisako, T.; Yoshida, K.; Kagawa, K.; Nagahara, H., Development of a new advanced process for manufacturing polyacetal resins. Part III. End-capping during polymerization for manufacturing acetal homopolymer and copolymer. *Journal of Applied Polymer Science* **1993,** *50* (8), 1317-1329.

181. Ho, H. O.; Lin, C. W.; Sheu, M. T., Diffusion characteristics of collagen film. *Journal of Controlled Release* **2001,** *77* (1-2), 97-105.